VOLUME 35, NUMBER 5, OCTOBER 2012

HADRONIC JOURNAL

HADRONIC JOURNAL Volume 35, Number 5, October 2012

Founded in 1978 by Prof. R. M. Santilli at Harvard University. Some of the past Editors include Professors S. L. Adler, A. 0. Barut, L. C. Biedenharn, N. N. Bogoliubov, M. Froissart, J.Lohmus, S. Okubo, Nobel Laureate Ilya Prigogine, M. L. Tomber, J. P.Vigier, J. Wess, Nobel Laureate Chen Ning Yang.

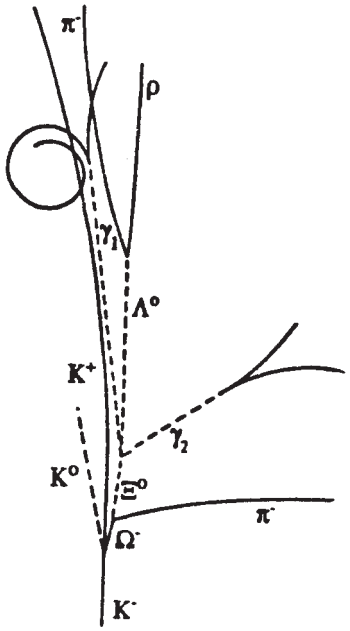

EDITORIAL BOARD
A.O.Animalu
D. P. Bhattacharyya
G.-C. Cavalleri
V. De Sabbata
T. L. Gill
L. P. Horwitz
H. Hurst
S. L. Kalla
S. I. Kruglov
S. S. Moskaliuk
M. Nishioka
R. F. O'Connell
Z. Oziewicz
E. Recami
M. Saleem
D. V. Shirkov
S. Silvestrov
D.S. Sourlas
H. M. Srivastava
A. I. Studenikin
R.I. Tsonchev
QI-Ren Zhang
C.A.Wolf
YI-Zhong Zhuo

FOUNDER:
RUGGERO M. SANTILLI

EDITOR IN CHIEF
CHRISTIAN CORDA

HADRONIC PRESS, INC.

HADRONIC JOURNAL

VOLUME 35, NUMBER 5, OCTOBER 2012

PROOF OF QUARK CONFINEMENT AND BARYON-ANTIBARYON DUALITY: I: GAUGE SYMMETRY BREAKING IN DUAL 4D FRACTIONAL QUANTUM HALL SUPERFLUIDIC SPACE-TIME, 469

ANALYTICAL APPROACH TO GEOMETRIC ERRORS IN RADIOGRAPHY: INVERSE ABEL TRANSFORM FOR A HOMOGENEOUS BALL, 509

RESOLUTION OF KANTOR AND BABCOCK-BERGMAN EMISSION THEORY ANOMALIES, 527

THE COSMOLOGICAL IMPLICATIONS OF NONLOCAL GRAVITY, 557

Andrej E. Inopin
Department of Experimental Nuclear Physics, Karazin National University
Svobody Sq. 4, Kharkiv, 61077 Ukraine
Nathan O. Schmidt
Department of Mathematics, Boise State University
1910 University Drive, Boise, ID 83725

Hanna Makaruk
P-21 Modern Physics, Physics Division
Los Alamos National Laboratory
Los Alamos, NM, 87544, USA
Robert Owczarek
Enfitec Inc. and Department of Mechanical Engineering
University of New Mexico
Albuquerque, NM, 87131, USA

Peter A. Jackson
Orchard House, Whitstable
Canterbury, Kent CT5 3EX, UK
John Minkowski
Baltimore, MD

Peter Rowlands
Department of Physics, University of Liverpool
Oliver Lodge Laboratory, Oxford Street
Liverpool, L69 7ZE, UK

PROOF OF QUARK CONFINEMENT AND BARYON-ANTIBARYON DUALITY: I: GAUGE SYMMETRY BREAKING IN DUAL 4D FRACTIONAL QUANTUM HALL SUPERFLUIDIC SPACE-TIME

Andrej E. Inopin
Department of Experimental Nuclear Physics, Karazin National University
Svobody Sq. 4, Kharkiv, 61077 Ukraine
inopinandrej@yahoo.com
Nathan O. Schmidt
Department of Mathematics, Boise State University
1910 University Drive, Boise, ID 83725
nathanshchmidt@u.boisestate.edu
Received 11-10-2012
Revised 12-15-2012

Abstract

We prove quark (and antiquark) confinement for a baryon-antibaryon pair and design a well-defined, easy-to-visualize, and simplified mathematical framework for particle and astro physics based on experimental data. From scratch, we assemble a dual 4D space-time topology and generalized coordinate system for the Schwarzschild metric. Space-time is equipped with "fractional quantum number order parameter fields" and topological defects for the simultaneous and spontaneous breaking of several symmetries, which are used to construct the baryon wavefunction and its corresponding antisymmetric tensor. The confined baryon-antibaryon pair is directly connected to skyrmions with "massive 'Higgs-like' scalar amplitude-excitations" and "massless Nambu-Goldstone pseudo-scalar phase-excitations". Newton's second law and Einstein's relativity are combined to define a Lagrangian with effective potential and effective kinetic. We prove that our theory upgrades the prediction precision and accuracy of QCD/QED and general relativity, implements 4D versions of string theory and Witten's M-theory, and exemplifies M.C. Escher's duality.

Keywords: Quark confinement proof; Quasiparticles; Fractional statistics; Superfluids; Superconductors; Mott insulator; Monopoles; Goldstone bosons; Higgs-like excitations; Baryon wavefunction; Antisymmetric tensor; Gribov QED/QCD vacuum; Kagome lattice theory; $SU(2)$ gauge theory; Bose-Einstein condensate; Gedanken interferometer; Stereographic gravitational superlensing; High-energy physics; Hadronization; Annihilation; Order parameters; Spontaneous symmetry breaking; String theory; M-theory; Relativity theory; Newtonian mechanics; Quantum gravity; Holographic ring; Riemann surface; Riemannian circle; Space-time duality; Topology; Generalized coordinates; Schwarzschild metric; Superluminal signals.

Copyright © 2012 by Hadronic Press, Inc., Palm Harbor, FL 34682–1577, USA

1 Introduction

Quarks and antiquarks are the fundamental building blocks of baryons and antibaryons, respectively. To date, nature presents an impressive display of mass-energy puzzles in physics, including the creation, annihilation, and confinement of baryons and antibaryons. The mystery of quark confinement is a *colossal* problem in physics; it is the phenomenon that color charged particles (such as quarks) cannot be isolated singularly, and therefore cannot be directly observed [1]. In this first paper of the series, we hunt down this "Great Beast" and prove quark-antiquark confinement for a baryon-antibaryon pair in a 4D space-time, where the dimension of time is circular rather than linear. We attack the problem from multiple perspectives simultaneously to establish a well-defined gauge theory equipped with Legget's superfluid configuration of Landau's order parameter fields [2], Laughlin's quasiparticles [3], a baryon wavefunction, antisymmetric tensors, and more. From scratch, we construct a topological solution and Lagrangian that intertwines Newtonian [4] and Einsteinian concepts [5], improves the predictive capability of quantum chromo-dynamics (QCD) and quantum electro-dynamics (QED) [6], reduces dimensional complexity of string theory and M-theory [7], exhibits M.C. Escher's duality [8], and is directly supported by a diverse experimental array. In short, the *dual* baryon and antibaryon quantum states are encoded with quantum number order parameters of fractional statistics for quasiparticles with baryon wavefunction antisymmetry. We prove quark-antiquark confinement in terms of Laughlin excitations [3] that dynamically arise due to our *fractional quantum Hall superfluidic* (FQHS) space-time and topology inspired by the quasiparticle interferometer experiments of Goldman [9]. We prove that the quarks and antiquarks confined to the holographic ring "cancel out" due to the CPT-Theorem. Spontaneous symmetry breaking (SSB) generates massless "Nambu-Goldstone pseudo-scalar *phase-excitations*" [10, 11, 12, 13] and massive "Higgs-like scalar *amplitude-excitations*" [14] of Laughlin statistics [3]. First, we provide *conceptual* quark confinement proof in Section 2. Second, we provide *mathematical* quark confinement proof in Sections 3, 4, 5, and 6.

In Section 2, we prepare for our quark confinement proof by conceptually aligning the reader to our 4D FQHS space-time scenario. We in-

vestigate the two dynamical scales that arise in the double-confinement, double-stereographic gravitational superlensing, and double-horizons inherent to baryons and antibaryons. We prove that a baryon-antibaryon pair is composed of three distinct quark-antiquark pairs, which form three corresponding "thin color-electric flux tubes" [15] of Laughlin excitations [3] and fractional statistics [16]. We discuss the hadronization process and the modified Gribov QED/QCD vacuum, where all properties in 3D Schwarzschild space can be inferred from the analogue of the 2D gauge field on the six-coloring kagome lattice manifold. Additionally, we venture to the interaction between the boson propagators and gravity by introducing *"gravitational birefringence"*.

In Section 3, we begin mathematically constructing the topology and framework for our quark confinement proof in FQHS. We discuss the surface and generalized Riemann coordinates used to encode our FQHS space-time. We extend the definition of complex numbers and use them to represent locations on the 1D Riemann surface; we prove that the complex numbers are both scalars and Euclidean vectors. We define axis constraints for the vectors, which let us construct a powerful 2D generalized coordinate system on the surface equipped with the Pythagorean identity; the locations may always be expressed in terms of right triangles with real and imaginary components.

In Section 4, we explore the three distinct topological sub-surface zones for a baryon and antibaryon using set and group theory. We formally define the zones using trichotomy and our generalized coordinates for 2D and 3D space. We prove that the time-like region is a holographic ring—a closed curve and simple contour of points, which can be scaled to, for example, the Fermi radius. We formally define space and time as being dual. Additionally, we demonstrate that the time-like region represents the $U(1)$ and $SU(2)$ symmetry groups, which is isomorphic to the $SO(3)$ orthogonal group; all 3D properties are inferred directly from the 2D holographic ring for the $SU(2)$ gauged Bose-Einstein condensate.

In Section 5, we define the *Baryon Wavefunction* (BWF) of fractional quantum number order parameters (OP) for our quark (q) and antiquark ($\bar{q}$) confinement proof. Additionally, we discuss the amplitude-excitations [14] and phase-excitations [10, 11, 12, 13] for Laughlin quasiparticles [3]

experienced by the BWF OPs in our FQHS space-time scenario. For this, we express the full BWF antisymmetries and CPT-transformations.

In Section 6, we express the Lagrangian in terms of *effective potential* and *effective kinetic* for our FQHS space-time scenario. For this, we apply both Newtonian and Einsteinian concepts to the q and $\bar{q}$ confinement proof and thereby incorporate *effective force*, *effective mass*, and *effective acceleration.*

In Section 7, we prepare a concise correspondence to the authors of the Yuan-Mo-Wang (YMW) baryon-antibaryon $SU(3)$ model [17]. In doing so, we relay the importance of the YMW model and report on a number of similarities between it and our confinement scenario. Additionally, we contrast the models by identifying key distinctions and suggest that our model may upgrade the YMW model's state space and accuracy, and thereby extend its prediction horizon. Ultimately, we realize that both constructions exhibit remarkable similarities, and that it may be possible in the near future to consolidate these ideas into a single framework.

In Section 8, we conclude our paper with a brief recapitulation and outlook where we suggest future research trajectories.

To summarize, in this first paper of the series we introduce the topologies, vacuum, generalized coordinates, fractional statistics, quantum number OPs, BWF, gauge symmetry breaking, and Lagrangian for the q and $\bar{q}$ confinement proof in 4D FQHS space-time; for the scenario, we provide a series of colorful depictions and an array of experiments supporting this construction. In the next paper(s) of this series, we will extend our confinement scenario by discussing the anyons, phase locking [18], Hubius helix (HH) [19], attractive and repulsive gravitational effects of quasiparticle signals on the Lagrangian, modified Gullstrand–Painlevé reference frames, and Magnification Effect.

2 Alignment to Confinement: Conceptual Proof

At the Fermi scale, a baryon's event horizon confinement radius $\epsilon_{baryon} = 2M_{baryon}$ strongly depends on it's mass M_{baryon}, which can vary in size in accordance to its quark composition identified by the Standard Model. This is known as *baryon confinement* (for three-quark confinement) and is modeled as a *baryon bag.* Similarly, an antibaryon's event horizon confinement

radius $\epsilon_{antibaryon} = 2M_{antibaryon}$ strongly depends on it's mass $M_{antibaryon}$. This is known as *antibaryon confinement* (for three-antiquark confinement) and is modeled as an *antibaryon bag*. A baryon and its antibaryon merge to reflect three-pair quark-antiquark confinement. For example in a proton-antiproton pair, an antiproton of antimass $M_{antibaryon} = M_{antiproton} = 1$ GeV precisely counterbalances a proton of mass $M_{baryon} = M_{proton} = 1$ GeV due to antiferromagnetic ordering and the CPT-Theorem. On this scale we identify the general mechanism, namely *Baryon-Antibaryon Confinement* (BAC), which is responsible for the dynamics. It is based on the appearance of a critical radius $\epsilon_{2M} = \epsilon_{baryon} = \epsilon_{antibaryon}$ for quark-antiquark confinement at the 1 Fermi scale and the appropriate generalized dynamics—effective gravito-strong interaction. So in gravity plus electromagnetism, there is one interesting mechanism—radiation trapping just on the horizon's surface, that is a coherent particle accumulation structure [18] of fractional statistics and *toroidal vortex* [20]. The toroidal vortex, that stores information as in the holographic hypothesis [15], intertwines the baryon and antibaryon confinement mechanisms, creating BAC. The toroidal vortex forms between the spherical shells defined at the *inner confinement radius* ϵ_{2M} and the *outer confinement radius* $\epsilon_{3M} = 3M$ (based on the effective potential); ϵ_{2M} and ϵ_{3M} correspond to the "horizon" and "imaginary surface", respectively, in Figure 6 of Witten [15]; there are two distinct quantum critical points imposed by an antibaryon or baryon for the *double-stereographic gravitational superlense* with the meta-material, acoustic, double-negative refractive index, and sub-wavelength features of [21, 22, 23, 24]—see Figure 1. These facts are evident from the DIS modeling results of the hadronization process [25]. Quark-hadron duality in jet formation in DIS leads to a two-step process of hadronization, with *two scales* appearing: large $Q_0^2 \gg \Lambda_{QCD}^2$ and small $Q_0^2 \sim 1GeV^2$. An alternative approach in DIS, namely "Local Parton Hadron Duality", also leads to the *two dynamical scales*: $k_\perp = Q_0 \sim \Lambda_{QCD}$ and $k_\perp = Q_0 \sim 1$ GeV [25]. Both models of the hadronization process give us the numbers in accord with our model $\epsilon_{2M} \sim 0.2 - 0.3$ fm and $\epsilon_{3M} \sim 1$ fm. Another fresh perspective can be taken from the "Glue drops" model [26], where the authors gave firm evidence of the existence of a non-perturbative scale, smaller than the usual $\frac{1}{\Lambda_{QCD}} \sim 1$ fm, which is related to gluonic degrees of freedom. The

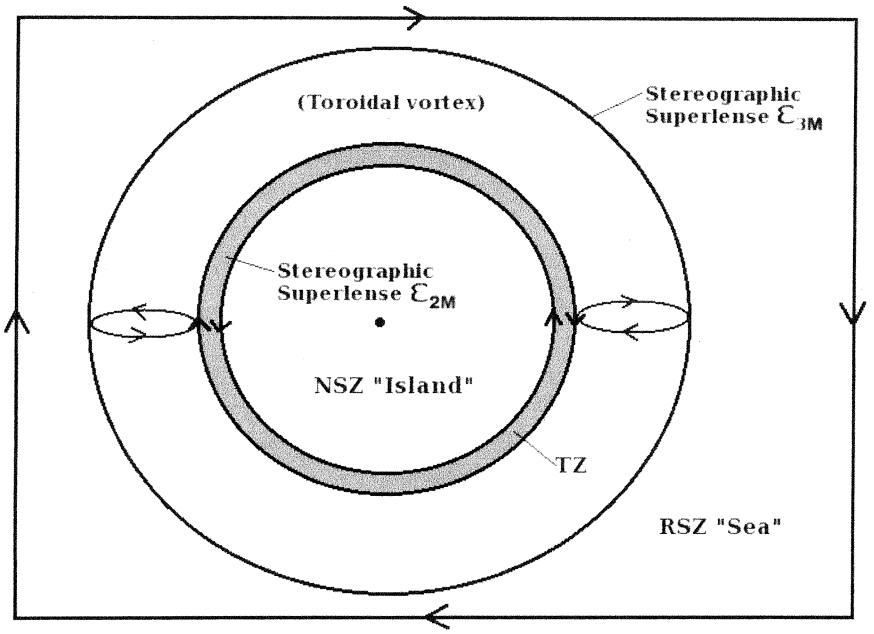

Fig. 1: The Riemannian holographic ring unit circle of two counter-propagating edge channels defines the TZ for quark-antiquark confinement and is isometrically embedded on the 1D Riemann surface. The toroidal vortex between two dynamical scales for a double-stereographic gravitational superlense: the spherical shells located at critical radius $\epsilon_{2M} = 2M$ and $\epsilon_{3M} = 3M$.

evidence for the presence of a *semi-hard* scale in hadronic structure is reviewed from many venues. The most notable effects are: QCD sum rules gives 0.3 fm radius of the corresponding form factor, lattice gives 0.2-0.3 fm for the correlation length, instanton radius peaks approximately at 0.3 fm, diffractive gluon bremsstrahlung in hadronic collisions leads to $k_\perp$ for the gluons in a proton of about 0.7 GeV [27]. At higher scales, chiral symmetry breaking is restored and the vacuum does not feel apparent existence of quark and gluon condensates, which spoil the chiral symmetry from the start—the mechanism for the *spontaneous breaking of chiral symmetry* and *spontaneously emergent behavior* of chaos theory on the Lagrangian.

All together, this brings us to the concept of *Baryon-Antibaryon Du-*

ality (BAD), which is responsible for the stereographic superlensing [23] dynamics. At rest, the massless red, green, and blue quarks are confined to a baryon and circulate *counter-clockwise* along it's event horizon as a *left-handed* HH [19] at the speed of light to generate *effective mass*, such that all observable baryons are *white*; the *visible* colored quarks are *non-Abelian color-electric-magnetic monopoles* [28] which emit red, green, and blue light-rays to render a baryon. Similarly, the resting antired, antigreen, and antiblue antiquarks are confined to a antibaryon and circulate *clockwise* along it's event horizon as a *right-handed* HH [19] to generate *effective antimass*, such that all "observable" antibaryons are *black* (antiwhite); the "visible" anticolored antiquarks are *non-Abelian anticolor-electric-magnetic antimonopoles* [28] which emit antired, antigreen, and antiblue light-rays to render an antibaryon; the relative direction of circulation (with corresponding winding number) distinguishes between mass (i.e. M_{proton}) and antimass (i.e. $M_{antiproton}$). For BAD, the baryon and antibaryon bags are dual, opposite, reverse, and inverse, and are therefore modeled as a *Baryon-Antibaryon Bag* (BAB). The quark and antiquark trajectories follow Wilson loops and form a self-consistent [10] $SU(2)$ gauged Bose-Einstein condensate [29]. The electro-strong duality of the potentials continuously transform in FQHS space-time in accordance with 1D, 2D, and 3D skyrmions [29].

This rich concept of duality enables us to compute observables in time-like regions, given the physics in space-like regions, and vice-versa. Upon considering these dual fields, the idea of *two distance scales* comes up naturally. Our 1D Riemmann surface (2D holographic information structure) is divided into three distinct topological sub-surfaces for quasiparticles:

1. *Non-Relativistic Space Zone* (NSZ) or "Micro" distance scale of *superluminal* signals,

2. *Time Zone* (TZ), and

3. *Relativistic Space Zone* (RSZ) or "Macro" distance scale of *luminal* signals.

The Riemannian holographic ring unit circle represents the TZ and is isometrically embedded on the surface; it bifurcates 3D space to establish the NSZ, such that $0 < x < \epsilon_{2M}$, and the RSZ, where $\epsilon_{2M} < x < \infty$—recall

Figure 1. The gauge field is a 3D analogue of the TZ's Rashba spin-orbit coupling [29]—see Figure 4. The quarks (and leptons) are "split" into three distinct excitation degrees of freedom, namely spinon, holon, and orbitons [3, 30]; the Laughlin excitations of the FQHS 3-branes obey fractional statistics; luminal quasiparticle signals of the RSZ "sea" execute a closed path around the NSZ "island" of superluminal quasiparticle signals and thus acquire statistical phase [9]—see Figure 5.

In QCD, BAC is a difficult strong coupling problem, but a somewhat similar phenomenon in nature is much better understood in QED. The Meissner effect is the fundamental observation that a superconductor expels magnetic flux. Suppose that magnetic monopoles become available for study and that we insert a monopole-antimonopole pair into a superconductor, where the two poles are separated by a large distance x. What will happen? A monopole is inescapably a source of the magnetic flux, but magnetic flux is expelled from a superconductor. So the optimal solution to this problem, energetically, is that a thin, *non-superconducting* tube forms between the monopole and the antimonopole. The magnetic flux is confined to this region, which is known as an *Abrikosov-Gorkov* flux tube (or a *Nielsen-Olesen* flux tube in the context of relativistic field theory). The flux tube has a certain nonzero energy per unit length, so the energy required to separate the monopole and antimonopole by a distance x grows linearly in x, for large x.

As a non-Abelian gauge theory, QCD has fields rather similar to ordinary electric and magnetic fields but obey a *nonlinear* version of Maxwell's equations. Quarks and antiquarks are particles that carry the QCD analog of electric charge and are confined in our QCD vacuum just as ordinary magnetic charges would be in a superconductor. The color-electric-magnetic quark monopoles and anticolor-electric-magnetic antiquark antimonopoles may be separated by a large distance x to form non-Abelian dipoles: red-antired, green-antigreen, and blue-antiblue "thin color-electric flux tubes" [15]. Now from the Aharonov–Casher (AC) effect and Aharonov–Bohm (AB) effect duality [31, 32, 33], it is evident that this analogy immediately leads to the idea that *the QCD vacuum is to a superconductor, just as electricity is to magnetism, and just as the AC effect is to the AB effect*—see Figure 3.

In [34], the author considered a relativistic string model, where a massless quark moves at the speed-of-light in a circular orbit. One can see clearly the $x = x_0 = \epsilon_{2M}$ coordinate represents an event horizon or "impenetrable barrier" and the quark moves in the "half harmonic oscillator" potential. When combined with the phenomenological aspects of [35, 36], a strong QCD/QED string model for the $q\bar{q}$ pairs with the associated quasiparticles [3] emerges in our scenario. So for the $q\bar{q}$ pairs we identify both open-ended ("linear") fermionic strings *and* the closed ("non-linear"/circular) bosonic strings vibrating in our conjugate and dual space-time. All of this is supported by Glue drops [26], where the energy of a QCD string is concentrated in a thin color-electric flux tube [15] of radius $\epsilon_{2M} = 0.3$ fm. All such particles and quasiparticles on the Riemann surface which generate effective mass (and antimass) are projected along the "z-axis" to effective 3D space (recall Figure 4). Here, events are represented on the Lagrangian using generalized coordinates in Schwarzschild space-time on the Riemann surface.

Viewed in certain classes of inertial frames, a superluminal signal travels *backwards* in time. In QED, Feynman diagrams involve a virtual e+e- pair that influences the photon propagator. Here, positrons are replaced with electron-holes. This gives a photon an effective mass (or antimass) on the order of the Compton wavelength for the electron (or electron-hole); leptons are split into quasiparticles [3, 30]. All of this is generalized to QCD, where a virtual $q\bar{q}$ pair influences the gauge boson propagator in FQHS space-time; the propagator is a function which returns a probability amplitude of 1 for the quarks and baryon confined to the TZ. In both QED and QCD, if the space-time curvature has a comparable scale, then an effective boson-gravity interaction is induced; the Higgs-like amplitude excitations [14] for the baryon-antibaryon pair impose effective mass for baryons and quarks, and effective antimass for antibaryons and antiquarks. This depends explicitly on the curvature, in violation of the Strong Equivalence Principle. The boson velocity is changed and light-ray no longer follows the shortest possible path—it bifurcates to both the NSZ and RSZ distance scales. Moreover, if the space-time is anisotropic, this change can depend on the boson's polarization as well as direction. This is the quantum phenomena of "gravitational birefringence". The effective light-cones for boson propagation in gravitational fields *no longer coincide* with the geometrical light-cones fixed

by the local Lorentz invariance of space-time, but depend *explicitly* on the local curvature. This formulation agrees with the von Karman flow and symmetry breaking of [37], the kaleidoscope of exotic quantum phases in the 2D frustrated model of [38], and the deviant Fermi liquid of [39], where the TZ serves a Bose metal as in [40]. All this works in 4D space-time.

The $q\bar{q}$ pairs for a baryon-antibaryon pair are "superbound" to the vacuum [41] as coupled oscillators [42] (see Figure 2) and form red-antired, green-antigreen, and blue-antiblue *Nambu-Goldstone pions*, which are Nambu-Goldstone bosons; the SSB of the three distinct pions generates colored amplitude-excitations [14] and phase-excitations [10, 11, 12, 13]. The $q\bar{q}$ pairs of the three distinct thin color-electric flux tubes are confined to the TZ, which is a *Riemannian holographic ring unit circle* on a 1D Riemann surface equipped with a six-coloring (three coloring plus three anticoloring) kagome lattice manifold generalization of [43] with antiferromagnetic ordering [3]. The ring exhibits the Rashba and fractional quantum Hall effects [44], along with spin-Hall current [45] and chiral magnetic moments [46]. The $q\bar{q}$ pairs are uniformly arranged along the kagome lattice with the triangular chirality of [47] and the self-assembling observables of [18, 48] (recall Figure 3). The quasiparticles of the $SU(2)$ gauged Bose-Einstein condensate are direct 3D analogs of the spontaneously emerging QED and QCD. The kagome lattice hexagonal structure is self-similar to, for example, graphene, which explains the "plasmaron" observations in quasi-freestanding doped graphene [49] and the "soundaron" observations of [50]. The quarks can also be thought as moving along the "caustics" inside the toroidal vortex, where the quark's trajectories are trapped between the dual scale dynamics—they are "gliding" along the surface and are reflected back to the center. The dual confinement boundaries located at ϵ_{2M} and ϵ_{3M} act as reflecting and focusing stereographic superlenses. So baryons and antibaryons become *seashells* closed on ϵ_{3M} [51].

When we come to the vacuum estate, the richness of BAD is shining brightly: Gribov's QED/QCD vacuum [41] resembles a complicated structure of *Unruh-Boulware-Hartle-Hawking*'s black hole vacuum and is fed with solid-state physics along with notions of forbidden zones, Fermi surfaces, particles and holes to encode the BAB on the Riemann surface. But there are some new diagrams that arise with the new zones, and novel types of

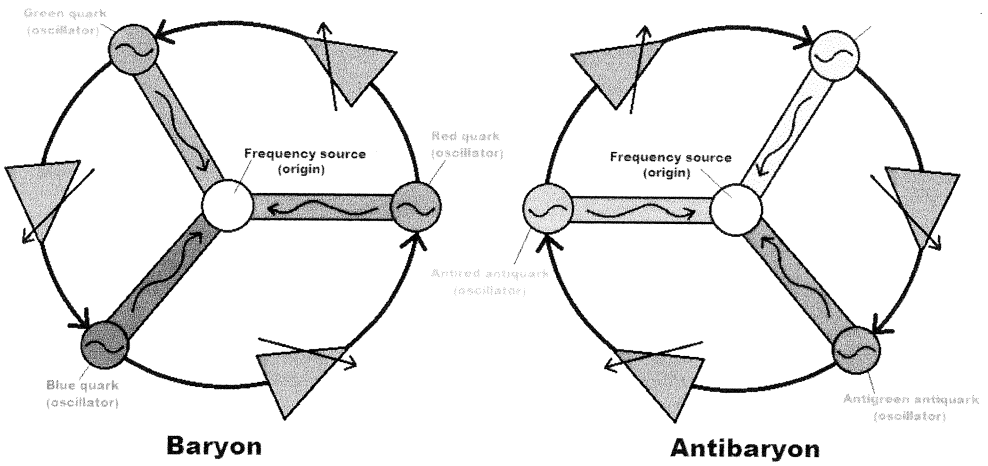

Fig. 2: Schematic of the multiple synchronized quark and antiquark solid-state oscillators (colored and anticolored circles) coupled to generate frequencies for the $SU(2)$ gauged Bose-Einstein condensate with skyrmions [29] in the loop configuration based on the work of Afshari [42]; the coupling circuits (gray triangles) shift the phase of the oscillators.

excitations—enabling us to upgrade Gribov's model. This new vacuum differs drastically from Dirac's vacuum and contains a total of 18 zones for the six-coloring (kagome lattice) manifold on the Riemann surface—Figure 4; these zones are populated with quasiparticles [3, 30] spontaneously generated by the $q\bar{q}$ pairs confined to the TZ with the spin-orbit coupling of [53, 45, 54, 55]. The TZ acquires a geometric phase [56, 31, 32], so the quasiparticles confined to the TZ are dual to those signals propagated across the NSZ and RSZ zones. Laughlin's fractional quantization [16] is axiomatic in this scenario. At proper temperature and pressure, the vacuum is consistent with Chernodub [57]. Clearly, in treating the BAD and superlensing dynamics, it is very convenient to separate the RSZ and NSZ degrees of freedom (Born–Oppenheimer approximation).

The NSZ and RSZ both represent *superconductive, FQHS* 3-*branes* interconnected by the TZ, which serves as a common (2D) surface boundary at ϵ_{2M}. The baryon and antibaryon are spinning objects confined to the TZ so they generate whirlpools on both 3-brane distance scales in ac-

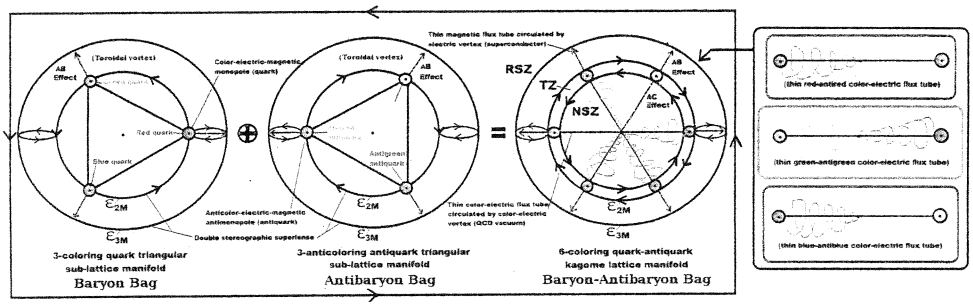

Fig. 3: The loop-induced zero-energy dynamics are described as "gluon dynamics". The 3 distinct $q\bar{q}$ pairs for the baryon-antibaryon pair are "superbound" as coupled oscillators [42] to the Fermi surface in the upgraded Gribov vacuum generalized from [41] and are confined to the kagome lattice antiferromagnet on the six-coloring manifold. The $q\bar{q}$ pairs spontaneously generate *phase-excitations* (massless and pseudo-scalar) [10, 11, 12, 13] and "Higgs-like" *amplitude-excitations* (massive and scalar) [14] Laughlin excitations [3]. The toroidal vortex along the Riemannian holographic ring unit circle for a baryon and/or antibaryon is defined as a toroidal vortex between the spherical shells located at critical radius $\epsilon_{2M} = 2M$ and $\epsilon_{3M} = 3M$; double stereographic superlenses [23] for two dynamical scales [27]. An affinity exists between BAD and M.C. Escher's duality, where the combined baryon event horizon and antibaryon event horizon at ϵ_{2M} exhibit the double horizon phenomena [8]. The $q\bar{q}$ pairs confined to the TZ form thin color-electric flux tubes [15] in the QCD vacuum of the NSZ and exhibit the AC effect, while thin magnetic flux tubes in the RSZ superconductive region exhibit antiferromagnetic ordering and the AB effect; the QCD vacuum is to a superconductor, just as electricity is to magnetism, and just as the AC effect is to the AB effect. This model exhibits vortex-antivortex dancing [52] and confirms the spontaneous appearance of a stable 3D skyrmion in the $SU(2)$ gauged Bose-Einstein condensate of [29] confined to the Riemannian holographic ring unit circle on our 1D Riemann surface.

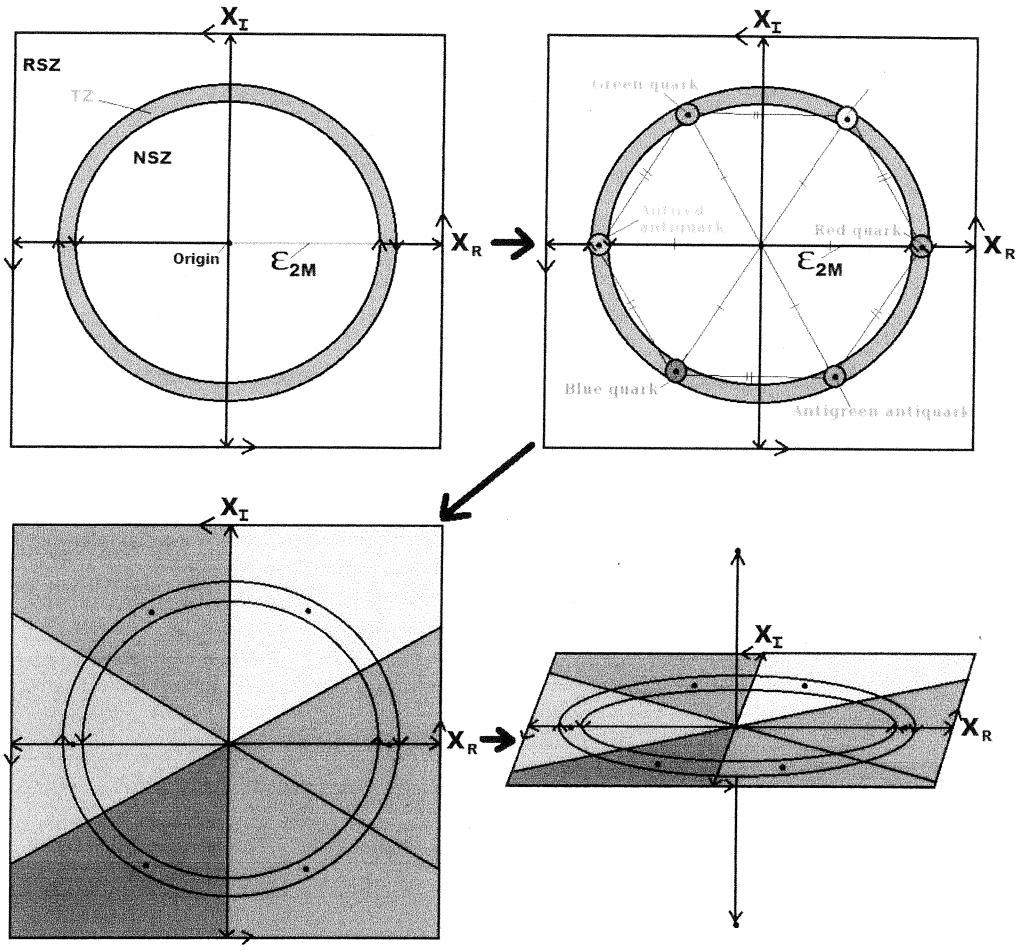

Fig. 4: The gauge-invariant TZ delineates the NSZ and RSZ: a 2-sphere which is dual to *both* 3-branes, where the $SU(2)$ Bose–Einstein condensate and gauge field is a 3D analogue of the Rashba spin-orbit coupling of the TZ, supporting the 1D, 2D, and 3D Skyrmion structures [29] (all). The baryon-antibaryon pair comprises the three distinct $q\bar{q}$ pairs and is modeled as a BAB in the new Gribov vacuum with 18 quasiparticle signal zones (bottom).

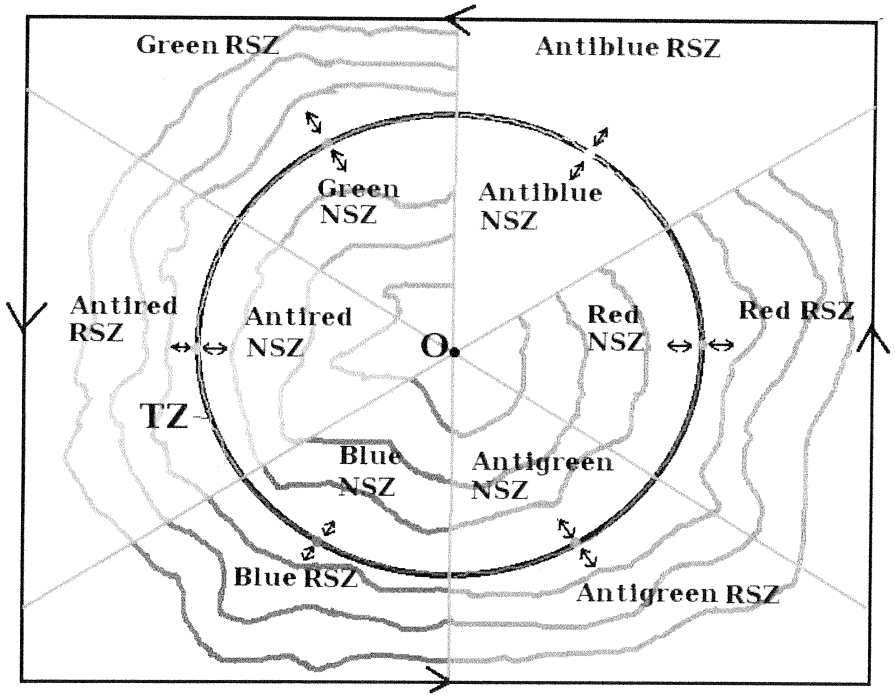

Fig. 5: The upgraded Gribov QCD/QED vacuum with 18 zones for quasiparticle signals pertaining to a BAB on the 1D Riemann surface. The $q\bar{q}$ pairs are confined to the TZ, which is dual to the NSZ and the RSZ. The six-coloring spinon, holon, and orbiton excitations are spontaneously generated and confined to the TZ, which acquires a geometric phase; the TZ excitations are dual to those of the NSZ and RSZ 3-branes.

cordance with seashells closed on ϵ_{3M} [51], thereby exhibiting the Magnus effect [58] and generating a vortex-antivortex dance [52]; these whirlpools are described on the Riemann surface using spirals (i.e. weighted Fibonacci sequence and/or golden spiral). The TZ is a topological Mott insulator for [53, 59, 30, 60], a Fermi surface as in [61], a Goldman-Laughlin quasiparticle interferometer of two counter-propagating edge channels as in [9], a Gedanken interferometer as in [62], a quantum critical point as in [3, 63], and a non-perturbative, self-consistent, $SU(2)$ gauged Bose-Einstein condensate as in [10] that satisfies Novikov's self-consistency principle as in [64]; a picture emerges of the vacuum as a conductor instead of "Dirac's insulator", with a new mass scale that reflects the position of the "Fermi surface" [41]. The six-coloring antiferromagnetic alignment of the $q\bar{q}$ pairs spontaneously generate the physical behavior of the strong interaction as in [3] and thereby triggers parity doubling, CPT violations, and different polarization rotation velocities on *both* the NSZ and RSZ distance scales simultaneously. Here, we identify the Dirac quantization and spin-charge magnetic monopole relations of [65], Fermi liquid deviations of [63], non-linear optics, analogue gravity, and photon emissions analogous to the Hawking radiation as in [66], and Andreev reflections of [67, 68]; the TZ's current continuously undergoes charge-transformation between the NSZ's and RSZ's supercurrent. The $q\bar{q}$ resonances form the exotic meson and broad locking states as in [69]. The $q\bar{q}$ pairs and their waves are phase locked, spontaneously aligning to form dynamical 1D coherent accumulation structures with time-periodic flows [18] and a von Kármán vortex street [20] with impact parameters.

3 The Space-Time Surface and Generalized Riemann Coordinates

Let X be the 1D Riemann surface. We define the complex number $x = x_{\mathbb{R}} + x_{\mathbb{I}}$ as a *position-point and position-vector* on X; $x \in X$ is both a complex scalar *and* Euclidean vector with *amplitude* $|x|$ and *phase* $\langle x \rangle$, which are analogous to *magnitude* and *direction* in conventional notation. The orthogonal components of x, namely $x_{\mathbb{R}} \in \mathbb{R}^1$ and $x_{\mathbb{I}} \in \mathbb{I}^1$ as *axis-constrained* real and imaginary Euclidean vectors, respectively (where in this case $\mathbb{I}$ denotes imaginary rather than irrational); the simple trichotomy

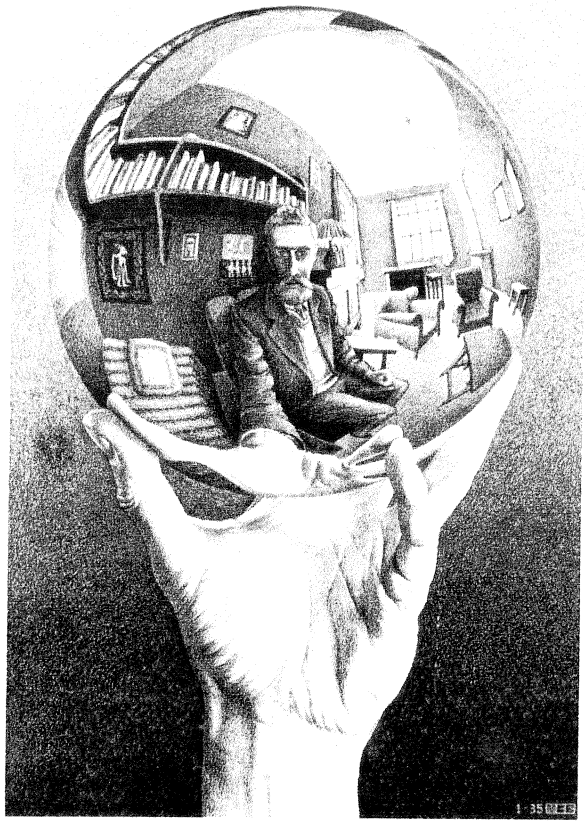

Fig. 6: The TZ is dual to *both* distance scales and imposes the double-confinement and double-lensing of M.C. Escher's duality [8]; it is a stereographic superlense [23] between the two 3-brane distance scales.

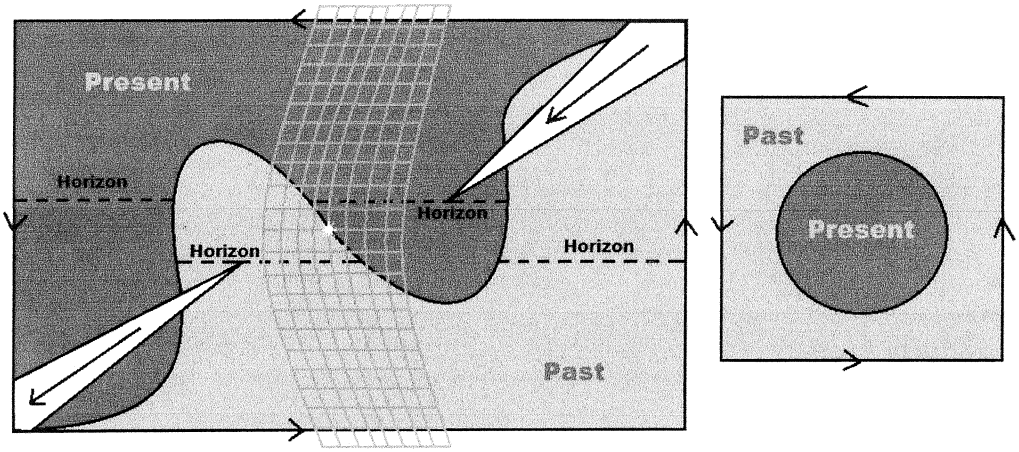

Fig. 7: Inopin's interpretation of M.C. Escher's double-horizons of [8] is directly connected to the $q \to \bar{q}$ transitions, past-present switching, time-reversal operation, and CPT-Theorem on the Riemann surface: time is circular and non-linear, so *the past is the future*. The quarks switch back and forth between the conjugate space-time regions with the appearance and disappearance of 3 quantum critical points in the QCD phase diagram.

axis-constraints for the $\mathbb{R}$-axis are

$$x_{\mathbb{R}} > 0 \Leftrightarrow \langle x_{\mathbb{R}} \rangle = 2\pi = 0, \tag{1}$$
$$x_{\mathbb{R}} = 0 \Leftrightarrow \langle x_{\mathbb{R}} \rangle = \nexists, \tag{2}$$
$$x_{\mathbb{R}} < 0 \Leftrightarrow \langle x_{\mathbb{R}} \rangle = \pi, \tag{3}$$

and for the $\mathbb{I}$-axis are

$$x_{\mathbb{I}} > 0 \Leftrightarrow \langle x_{\mathbb{I}} \rangle = \frac{\pi}{2}, \tag{4}$$
$$x_{\mathbb{I}} = 0 \Leftrightarrow \langle x_{\mathbb{I}} \rangle = \nexists, \tag{5}$$
$$x_{\mathbb{I}} < 0 \Leftrightarrow \langle x_{\mathbb{I}} \rangle = \frac{3\pi}{2}, \tag{6}$$

such that

$$|x_{\mathbb{R}}| = |x| \cos(\langle x \rangle), \tag{7}$$
$$|x_{\mathbb{I}}| = |x| \sin(\langle x \rangle), \tag{8}$$

with Pythagorean form

$$|x|^2 = x_{\mathbb{R}}^2 + x_{\mathbb{I}}^2, \quad \forall x \in X. \tag{9}$$

Thus, we've defined the 2D generalized (Riemann) coordinate system of X as

$$^{2D}X : (x) = (x_{\mathbb{R}} + x_{\mathbb{I}}) = (x_{\mathbb{R}}, x_{\mathbb{I}}) = (|x|, \langle x \rangle), \quad \forall x \in X, \tag{10}$$

with respect to the unique reference origin-point $O \in X$, such that $(O) = (0 + 0i) = (0, 0i) = (0, 0\pi)$; $(x) = (x_{\mathbb{R}} + x_{\mathbb{I}})$ are 1D Riemann coordinates, $(x_{\mathbb{R}}, x_{\mathbb{I}})$ are 2D Cartesian coordinates, and $(|x|, \langle x \rangle)$ are Polar coordinates; a Complex-Cartesian-Polar synchronized and generalized coordinate system. The real and imaginary axis-constraints ensure that the generalized coordinates may always be expressed as a right-triangle with Pythagorean properties.

So how to we extend our 2D generalized coordinates of Definition (10) to 3D Schwarzschild space? Well, for a baryon or antibaryon of scale M (located precisely at the origin position-point $O \in X$) we define the 3D generalized (Schwarzschild) coordinate system of X as

$$^{3D}X : (u_x, |x|, \langle x \rangle) = (\frac{M}{|x|}, |x|, \langle x \rangle), \quad \forall x \in X. \tag{11}$$

4 Zones

We define T as the TZ of X. So T is a topological representation of a Riemannian unit circle, where the critical radius of T is scaled and normalized to precisely $\epsilon_{2M} = 2M = \frac{\pi}{2}\epsilon_{scalar}$. We prove BAC on T. ϵ_{scalar} is the *time unit scale-normalizing constant* and ϵ_{2M} is the inner confinement radius of T. Next, we define the circumference and wavelength of T, namely $T_\lambda = T_{circumference} = T_{wavelength} = 2\pi\epsilon_{scalar}$, as being equivalent to the (normalized) *Mikhail Grimov's area filling conjecture* [70]: $T_{area} = T_\lambda$; $T \subset X$ is a closed curve and simple contour of surface position-points.

We use zone trichotomy to simultaneously define the TZ and SZ regions of X: we define X_- and X_+ as the NSZ and RSZ of X, respectively. The surface T delineates the topological sub-surfaces X_- and X_+ on X; T is a Mott insulator [30] and Fermi surface [41] which delineates two dual superconductors [53, 59, 30, 60, 67, 68]. Thus, $\forall x \in X$ we know that precisely one of the following conditions must be satisfied:

$$|x| < \epsilon_{2M} \Leftrightarrow x \in X_-, \tag{12}$$
$$|x| = \epsilon_{2M} \Leftrightarrow x \in T, \tag{13}$$
$$|x| > \epsilon_{2M} \Leftrightarrow x \in X_+, \tag{14}$$

where clearly $X_- \cap T = T \cap X_+ = X_- \cap X_+ = \emptyset$ and $X_- \cup T \cup X_+ = X$. Hence, T is the multiplicative group of all non-zero complex 1-vectors, such that

$$T = \{t \in X : |t| = \epsilon_{2M}\}, \tag{15}$$

where we define all T position-points as *time-points* and

$$X_- = \{s \in X : |s| < \epsilon_{2M}\}, \tag{16}$$
$$X_+ = \{s \in X : |s| > \epsilon_{2M}\}, \tag{17}$$

where we define all $S = X_- \cup X_+$ position-points as *space-points*. So clearly,

$$\epsilon_{2M}^2 = |t|^2 = |t_{\mathbb{R}}|^2 + |t_{\mathbb{I}}|^2, \quad \forall t \in T, \tag{18}$$
$$|x|^2 = |x_{\mathbb{R}}|^2 + |x_{\mathbb{I}}|^2, \quad \forall x \in X. \tag{19}$$

So T is isometrically embedded in X with the one-to-one holographic mappings $f : T \hookrightarrow X$ and $f : T \to X_- \cup X_+$ with dual simultaneous bijections

$$f_{Time} : X_- \hookleftarrow T \hookrightarrow X_+, \tag{20}$$
$$f_{Space} : X_- \hookrightarrow T \hookleftarrow X_+, \tag{21}$$

for our dual space-time; we've proven that T is dual to X_- and T is also dual to X_+. Interestingly, this formulation may provide a simplification to the Riemann-Hilbert problem as expressed in, for example, [71]. Now because T is a type of Riemannian circle and holographic ring, we know it is a 2-sphere for the $SU(2)$ gauged Bose-Einstein condensate [29]. Thus, for the position-point and position-vector $t \in T$ we apply Definition (10) to express the 2-sphere generalized and synchronized 2D Riemann coordinates

$$^{2D}T : \ (t) = (t_{\mathbb{R}} + t_{\mathbb{I}}) = (t_{\mathbb{R}}, t_{\mathbb{I}}) = (|t|, \langle t \rangle) = (\epsilon, \langle t \rangle), \ \forall t \in T, \tag{22}$$

and in 3D Schwarzschild coordinates

$$^{3D}T : (u_t, |t|, \langle t \rangle) = (\frac{M}{|t|}, |t|, \langle t \rangle), \quad \forall t \in T. \tag{23}$$

Now because $\forall t \in T$ we have the uniform radius $|t| = \epsilon_{2M}$, we can alternatively drop the $|t|$ amplitude coordinate and just use the $\langle t \rangle$ phase coordinate to *directly* specify position-points on the 1D non-linear surface. Therefore, T is

- the *1D circular Abelian group* $U(1)$;
- the *2D spherical non-Abelian group* $SU(2)$; and
- isomorphic to the *3D orthogonal non-Abelian group* $SO(3)$,

which directly supports 1D, 2D, and 3D skyrmions [29]. So parity doubling [27] is synonymous of the term degeneracy, and Escher gave an example of how one can establish 2D - 3D correspondence [8]. We see here again the road to the t'Hooft and Maldacena holographic model for high-energy physics—all the 3D properties are inferred directly from the 2D (Riemannian holographic ring) domain [72].

We define T as a "fermiwire," which is nothing more than a "nanowire" [55, 73] with Rashba spin-orbit coupling [30, 32, 44] on the Fermi scale. The spin geometric phase for electrons in [32] is applied directly to the spin Hall effect [44], effective spin-dependent flux, and Andreev reflections [67, 68] of the quarks and antiquarks confined to the universal curve T (the holographic ring with uniform radius $|t| = \epsilon_{2M}$) embedded in X; the duality derivation between the AAS effect and the AC effect of [32] is written for T as $\frac{\Phi_{mag}}{\Phi_0/2} \Longleftrightarrow \sqrt{1 + \left(\frac{2m_t\langle t\rangle|t|}{\hbar^2}\right)^2}, \quad \forall t \in T$, where Φ_{mag} is the magnetic flux, $\Phi_0 = h/e$ is the one flux quantum period, $\langle t\rangle = \alpha$ is the amplitude and strength of the Rashba spin-orbit interaction, and m_t is the effective mass; the left term is the AAS effect flux and the right term is the time-reversal AC effect oscillation unit with effective spin-dependent flux for the conductance modulation and voltage dependence observations of the AAS amplitude at zero magnetic field [32]. This formulation is crucial to our six-coloring quark-antiquark configuration for the BAC scenario because the magneto-resistance oscillations of [32, 74] along T are attributed to the AAS effect.

5 The Wavefunction Definition of Fractional Quantum Number Order Parameters

Landau introduced the concept of OPs [2], which we define as complex scalar fields [10] on X. Here, we construct the BWF using OPs and Laughlin statistics [3] in our non-Abelian $SU(2)$ gauge theory. In the theory of superfluidity the OP measures the existence of Bose condensed particles (Cooper pairs) and is given by the probability amplitude of such particles. The inter-particle forces between quarks and antiquarks, and between ^{4}He and between ^{3}He atoms, are *rotationally invariant in spin and orbital space* and, of course, conserve quantum number [27]. The latter symmetry gives rise to gauge symmetry, which is *broken* in any superfluid. First, for the theory of *isotropic* superfluids like a BCS superconductor or superfluid ^{4}He, we define the *global* OP $\psi = \psi_{\mathbb{R}} + \psi_{\mathbb{I}}$ as a complex number (which inherits the notation similar to x as defined in Section 3 without loss of generality); ψ is both a complex scalar *and* Euclidean vector with the *amplitude* $|\psi|$ [14] and *phase* $\langle\psi\rangle$ components [10]. Then for *local* gauge SSB, we define the

OP $\psi[x]$ as the complex scalar field

$$\psi[x] = \psi[x]_{\mathbb{R}} + \psi[x]_{\mathbb{I}}, \quad \forall x \in X, \tag{24}$$

where $|\psi[x]|$ and $\langle\psi[x]\rangle$ are the "gauge" amplitude and phase components local to $x \in X$, respectively, in accordance to Englert [10]. Furthermore, we define $\Delta|\psi[x]|$ and $\Delta\langle\psi[x]\rangle$ as the *change of* the OP's amplitude and phase due to a "massive Higgs-like *amplitude-excitation*" and "massless Nambu-Goldstone *phase-excitation*" components, respectively—see Figures 8 and 9. Since the Mott insulator and stereographic superlense T is dual to both $X-$ and X_+, we express Equation (24) specifically for time-points as the *parametric* function

$$\psi(t) = \psi(t)_{\mathbb{R}} + \psi(t)_{\mathbb{I}}, \quad \forall t \in T, \tag{25}$$

where the $SU(2)$ gauge-invariant T acquires a Berry–Aharonov–Anandan geometric phase as in [56]; T is an *ordered medium* equipped with an OP space for topological defects. The classical energy density distribution along T is a function of the OP $\psi(t)$; within the ordered (superfluid) phase, Nambu-Goldstone and Higgs modes arise from the $\langle\psi(t)\rangle$ and $|\psi(t)|$, respectively, where the energy density transforms into a function for T with a minimum at $|\psi(t)| = 0$ [14]. So $|\psi(t)|$ is excited with a periodic modulation of the spin-orbit coupling, which amounts to a "shaking" of the energy density (effective) potential for topological deformations along T in accordance with [14]. Furthermore, because the baryon-antibaryon pair is confined to T on the kagome lattice of antiferromagnetic ordering [43], we define the BWF for the six-coloring position-points $\{r, g, b\}$ $subset T$ and $\{\bar{r}, \bar{g}, \bar{b}\} \subset T$ of three colored quarks and three anticolored antiquarks in the vacuum, respectively (recall Figures 3 and 4).

Above the critical temperature the system is invariant under an arbitrary change of the phase $\langle\psi[x]\rangle \to \langle\psi[x]\rangle'$, i.e. under a gauge transformation. Below the critical temperature a particular value of $\langle\psi\rangle$ is *spontaneously* preferred. In anisotropic superfluids, additional symmetries can be spontaneously broken, corresponding to *multiple* OP components of the BWF. In ^{3}He—the best studied example with multiple OP components—the pairs are in a spin-triplet state, meaning that rotational symmetry in spin space

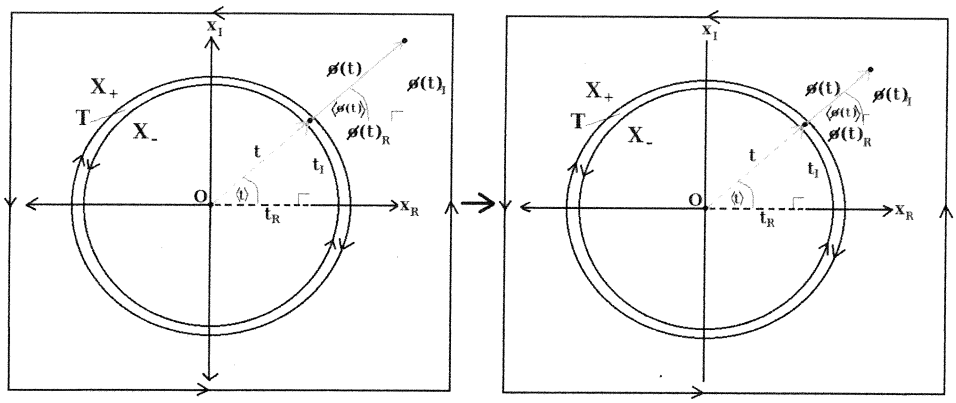

Fig. 8: A complex scalar field $\psi(t)$ experiences a massive "Higgs-like" *amplitude-excitation* [14] (right), which is characteristic of the Nambu-Goldstone *scalar* boson SSB order parameter fluctuations discussed by [10]; a classical wave imposes volume effects and stretches the vacuum field.

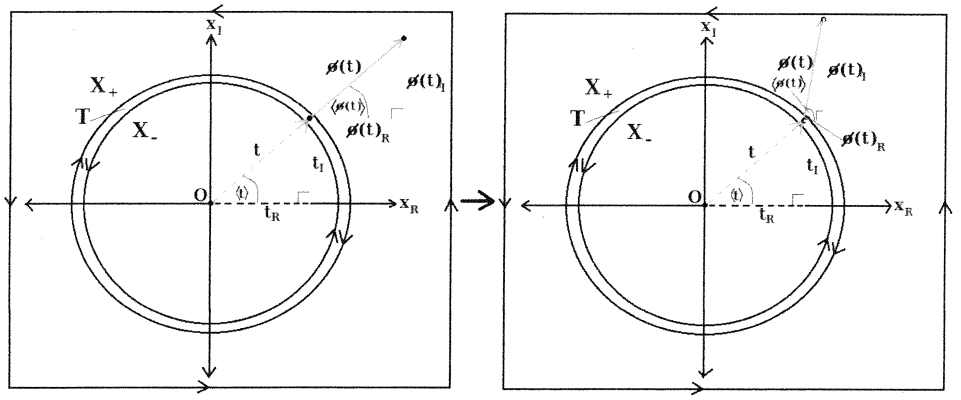

Fig. 9: A complex scalar field $\psi(t)$ experiences a *phase-excitation* (right), which is characteristic of the Nambu-Goldstone *pseudo-scalar* SSB order parameter fluctuations discussed by [10]; a classical wave imposes rotational effects on the vacuum field in accordance with vacuum degeneracy.

is broken, just as in a magnet. At the same time, the anisotropy of the Cooper-pair wavefunction in orbital space calls for a spontaneous breakdown of orbital rotation symmetry, as in *liquid crystals* [27]. Including the gauge symmetry, three symmetries are therefore broken in superfluid ^{3}He. The theoretical discovery that *several simultaneously broken symmetries* can appear in condensed matter was made by Antony Leggett, and represented a breakthrough in the theory of anisotropic superfluids, ^{3}He [2]. This leads to *superfluid phases* whose properties cannot be understood by simply adding the properties of systems in which each symmetry is *broken individually.* Such phases may have *long range* order in *combined*, rather than individual degrees of freedom. So to construct a strong BWF constraint for BAC to T, we "Cooper pair" the OP set of strongly conserved quantum numbers

$$\Phi_{OP} = \{\psi_C, \psi_I, \psi_J\}, \tag{26}$$

which is listed in Table 1; the spin-orbit coupling of [44, 45, 65] applies directly to T, where $\psi_J(t)$ is identical to the "B_{SO}-vector" of [73], such that

$$\psi_J(t) = \psi_S(t) + \psi_L(t), \quad \forall t \in T. \tag{27}$$

The $q\bar{q}$ pairs confined to T on the six-coloring kagome lattice manifold are located at position-points $r, g, b, \bar{r}, \bar{g}, \bar{c} \in T$; they adhere to the uniformly-arranged position-point constraints

$$\langle r \rangle = \langle \bar{r} \rangle \pm \pi, \quad \langle g \rangle = \langle \bar{g} \rangle \pm \pi, \quad \text{and} \quad \langle b \rangle = \langle \bar{b} \rangle \pm \pi, \tag{28}$$

with uniform amplitudes $|r| = |g| = |b| = |\bar{r}| = |\bar{g}| = |\bar{b}| = \epsilon_{2M}$, and antiferromagnetic ordering

$$\langle \psi_J(r) \rangle = \langle \psi_J(\bar{r}) \rangle \pm \pi, \tag{29}$$

$$\langle \psi_J(g) \rangle = \langle \psi_J(\bar{g}) \rangle \pm \pi, \quad \text{and} \tag{30}$$

$$\langle \psi_J(b) \rangle = \langle \psi_J(\bar{b}) \rangle \pm \pi, \tag{31}$$

(recall Figure 3). A little flight of imagination lead us to this new approach, where the OPs $\forall t \in T$ are "Cooper paired" to form a Leggett *superfluid B phase* of [2] with azimuthal "alpha" phase angle $\langle t \rangle$; the OPs $\forall \psi \in \Phi_{OP}$ rotate freely in 2D and 3D space, while the superfluid B phase angle $\langle t \rangle \in$

Table 1: The quantum number order parameters for the BWF states on the 1D Riemann surface X. Here, $\psi_J = \psi_S + \psi_L$ and $\psi_J(t) = \psi_S(t) + \psi_L(t)$ for the spin-orbit coupling of the holographic confinement ring $T \subset X$.

Order Parameter	**Symbol**	**Global**	**Local**
Color Charge	C	$\psi_C = \psi_{C_{\mathbb{R}}} + \psi_{C_{\mathbb{I}}}$	$\psi_C[x] = \psi_C[x]_{\mathbb{R}} + \psi_C[x]_{\mathbb{I}}$
Isospin	I	$\psi_I = \psi_{I_{\mathbb{R}}} + \psi_{I_{\mathbb{I}}}$	$\psi_I[x] = \psi_I[x]_{\mathbb{R}} + \psi_I[x]_{\mathbb{I}}$
Orbital Angular Momentum	L	$\psi_L = \psi_{L_{\mathbb{R}}} + \psi_{L_{\mathbb{I}}}$	$\psi_L[x] = \psi_L[x]_{\mathbb{R}} + \psi_L[x]_{\mathbb{I}}$
Spin Angular Momentum	S	$\psi_S = \psi_{S_{\mathbb{R}}} + \psi_{S_{\mathbb{I}}}$	$\psi_S[x] = \psi_S[x]_{\mathbb{R}} + \psi_S[x]_{\mathbb{I}}$
Total Angular Momentum	J	$\psi_J = \psi_{J_{\mathbb{R}}} + \psi_{J_{\mathbb{I}}}$	$\psi_J[x] = \psi_J[x]_{\mathbb{R}} + \psi_J[x]_{\mathbb{I}}$

$\{\langle r\rangle, \langle g\rangle, \langle b\rangle, \langle \bar{r}\rangle, \langle \bar{g}\rangle, \langle \bar{b}\rangle\}$ between them remains *constant*. Such phases form correlated helices along T, serving as constraints for the BWF—see Figure 10.

Next, we construct our BWF for the BAB states. For a baryon and antibaryon centered on the origin-point $O \in X$ and confined to T we define the *full* baryon and antibaryon states as

$$\Psi_{total}(r, g, b) = \Psi(r) \times \Psi(g) \times \Psi(b) \quad \text{and} \tag{32}$$

$$\Psi_{total}(\bar{r}, \bar{g}, \bar{b}) = \Psi(\bar{r}) \times \Psi(\bar{g}) \times \Psi(\bar{b}), \tag{33}$$

respectively, for the BAC and BAD; the *red*, *green*, and *blue* quark wavefunctions respectively located at time-points $r, g, b \in T$ on the three-coloring triangular sub-lattice are

$$\Psi(r) = \psi_C(r) \times \psi_J(r) \times \psi_I(r) \times r, \quad \Psi(r) \stackrel{def}{=} \langle r|\Psi\rangle, \tag{34}$$

$$\Psi(g) = \psi_C(g) \times \psi_J(g) \times \psi_I(g) \times g, \quad \Psi(g) \stackrel{def}{=} \langle g|\Psi\rangle, \tag{35}$$

$$\Psi(b) = \psi_C(b) \times \psi_J(b) \times \psi_I(b) \times b, \quad \Psi(b) \stackrel{def}{=} \langle b|\Psi\rangle, \tag{36}$$

and the *antired*, *antigreen*, and *antiblue* antiquark wavefunctions respectively located at time-points $\bar{r}, \bar{g}, \bar{b} \in T$ on the three-anticoloring triangular sub-lattice are

$$\Psi(\bar{r}) = \psi_C(\bar{r}) \times \psi_J(\bar{r}) \times \psi_I(\bar{r}) \times \bar{r}, \quad \Psi(\bar{r}) \stackrel{def}{=} \langle \bar{r}|\Psi\rangle, \tag{37}$$

$$\Psi(\bar{g}) = \psi_C(\bar{g}) \times \psi_J(\bar{g}) \times \psi_I(\bar{g}) \times \bar{g}, \quad \Psi(\bar{g}) \stackrel{def}{=} \langle \bar{g}|\Psi\rangle, \tag{38}$$

$$\Psi(\bar{b}) = \psi_C(\bar{b}) \times \psi_J(\bar{b}) \times \psi_I(\bar{b}) \times \bar{b}, \quad \Psi(\bar{b}) \stackrel{def}{=} \langle \bar{b}|\Psi\rangle; \tag{39}$$

the BWF for the three distinct $q\bar{q}$ pairs that are confined to T along the six-coloring kagome lattice manifold (recall Figure 3). So the antisymmetric BWF is described with the six-coloring components

$$\Psi(r,\bar{r}) = -\Psi(\bar{r},r), \tag{40}$$
$$\Psi(g,\bar{g}) = -\Psi(\bar{g},g), \quad \text{and} \tag{41}$$
$$\Psi(b,\bar{b}) = -\Psi(\bar{b},b), \tag{42}$$

for the confined quark and antiquark (two-particle) cases.

So for Definition (32) and the related six-coloring Definitions (31–37), we define the full BWF antisymmetrization via the covariant antisymmetric metric tensor: the 2D antisymmetric BWF matrix

$$\begin{pmatrix} 0 & \Psi_{total}(r,g,b) \\ \Psi_{total}(\bar{r},\bar{g},\bar{b}) & 0 \end{pmatrix} \tag{43}$$

and the expanded 3D antisymmetric BWF matrix

$$\begin{pmatrix} 0 & \Psi(r) & \Psi(g) \\ \Psi(\bar{r}) & 0 & \Psi(b) \\ \Psi(\bar{g}) & \Psi(\bar{b}) & 0 \end{pmatrix} \tag{44}$$

for T. So given complex tangent vectors μ and ν we define

$$g_x(\mu,\nu) = -g_x(\nu,\mu) \in \mathbb{C}, \quad \forall x \in X; \tag{45}$$

the tensor describes the X curvature ("vector phase") $\langle g_x(\mu,\nu)\rangle$ and the field strength ("vector amplitude") $|g_x(\mu,\nu)|$ at a position-point $x \in X$. The Levi-Civita symbol for the color singlet function is

$$\zeta_{rgb} = \zeta^{rgb} = \begin{cases} +1 \text{ if } (r,g,b) \text{ is } (1,2,3),\ (2,3,1),\ \text{or } (3,1,2) \\ \ \ 0 \text{ if } r=g \text{ or } g=b \text{ or } b=r \\ -1 \text{ if } (r,g,b) \text{ is } (3,2,1),\ (2,1,3),\ \text{or } (1,3,2) \end{cases} \tag{46}$$

The CPT-Theorem is a fundamental property of T. Hence, for a baryon or antibaryon of scale M we have the OP *charge transformation(s)*, $\forall\psi \in$

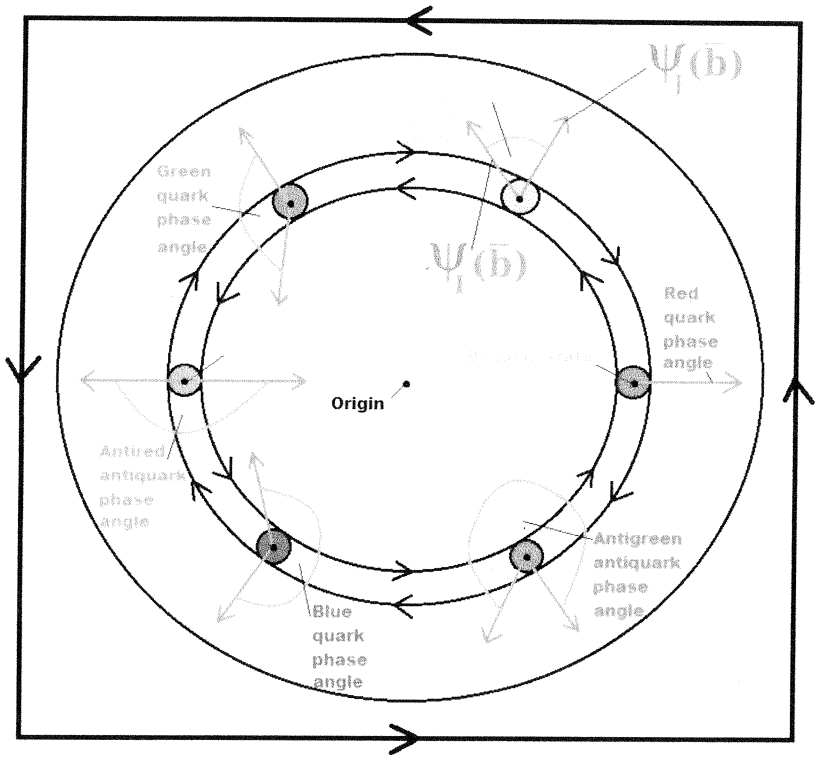

Fig. 10: Leggett's [2] six distinct superfluid B phase angles for the three $q\bar{q}$ pairs confined to T along the six-coloring kagome lattice of antiferromagnetic ordering [3, 43]. The superfluid B phase angles $\langle r\rangle, \langle g\rangle, \langle b\rangle, \langle \bar{r}\rangle, \langle \bar{g}\rangle, \langle \bar{b}\rangle$ remain *constant* and correlate the OPs as they rotate freely in 2D and 3D space; this *long range order* applies $\forall t \in T$, $\forall \psi \in \Phi_{OP}$, to form correlated helices along T; this concept serves as a strong BWF constraint and applies to all OPs for a given time-point. In this diagram, only $\psi_J(t)$ and $\psi_I(t)$ are shown, but $\psi_C(t)$ is also correlated with $\langle t\rangle$.

Φ_{OP},

$$C : \begin{cases} \psi(t) & \mapsto -\psi(t), \\ \begin{pmatrix} \psi(t)_{\mathbb{R}} \\ \psi(t)_{\mathbb{I}} \end{pmatrix} & \mapsto \begin{pmatrix} -\psi(t)_{\mathbb{R}} \\ -\psi(t)_{\mathbb{I}} \end{pmatrix}, \\ \begin{pmatrix} |\psi(t)| \\ \langle \psi(t) \rangle \end{pmatrix} & \mapsto \begin{pmatrix} |\psi(t)| \\ \langle \psi(t) \rangle \pm \pi \end{pmatrix}, \end{cases} \tag{47}$$

the *parity transformation(s)* (in generalized 2D Riemann coordinates for 3D Schwarzschild space) is the flip in the sign of the one coordinate

$$P : \begin{cases} \begin{pmatrix} t_{\mathbb{R}} \\ t_{\mathbb{I}} \\ \frac{M}{|t|} \end{pmatrix} & \mapsto \begin{pmatrix} -t_{\mathbb{R}} \\ -t_{\mathbb{I}} \\ -\frac{M}{|t|} \end{pmatrix}, \\ \begin{pmatrix} |t| \\ \langle t \rangle \\ \frac{M}{|t|} \end{pmatrix} & \mapsto \begin{pmatrix} |t| \\ \langle t \rangle \pm \pi \\ -\frac{M}{|t|} \end{pmatrix}, \end{cases} \tag{48}$$

and *time reversal transformation(s)*

$$T : \begin{cases} t & \mapsto -t, \\ \begin{pmatrix} t_{\mathbb{R}} \\ t_{\mathbb{I}} \end{pmatrix} & \mapsto \begin{pmatrix} -t_{\mathbb{R}} \\ -t_{\mathbb{I}} \end{pmatrix}, \\ \begin{pmatrix} |t| \\ \langle t \rangle \end{pmatrix} & \mapsto \begin{pmatrix} |t| \\ \langle t \rangle \pm \pi \end{pmatrix}, \end{cases} \tag{49}$$

which comprise a CPT-transformation, $\forall t \in T$. We see that for Definitions (47), (48), and (49) there are multiple equivalent transformations for each case because the generalized Riemann coordinates of Definition (10) and the OP Definition (24) use synchronized Complex-Cartesian-Polar values (where the magnitude and direction of the Polar components are replaced with amplitude and phase, respectively).

6 The Lagrangian: Effective Potential and Effective Kinetic

Here, we express the gauged SSB in our FQHS space-time scenario on X, which is applicable to both 2D and 3D space; the Lagrangian is defined as

$$\mathcal{L}[x] = E_K[x] - E_P[x], \quad \forall x \in X, \tag{50}$$

using our generalized coordinates, where $E_K[x]$ and $E_P[x]$ are the *effective kinetic* and *effective potential*, respectively, for a position-point x. From [75] the gauge boson's E_P is defined as

$$E_P[x] = \frac{\sqrt{1-2u_x}}{|x|}, \quad \forall x \in X. \tag{51}$$

The E_P depends on the Schwarzschild geometry but not on the choice of orbit. Only one E_P is required to analyze the motion of all radiation (including radio waves, radar pulses, gamma rays, etc.). It is important to stress E_P differences and similarities between a massive particle and its massless limit: radiation-rays. Next, the E_K is defined as

$$E_K[x] = \frac{1}{2} m_x v_x^2 = \frac{1}{2} \frac{F_x}{a_x} v_x^2, \quad \forall x \in X, \tag{52}$$

where F_x is the *effective force*, where m_x is the *effective mass*, a_x is the *effective acceleration*, and v_x is the *effective velocity* of the particle at x in the FQHS space-time. Einstein's F_x, the E_P *per unit of particle effective mass* m_x, is defined as

$$F_x = m_x a_x = \frac{E_P[x]}{m_x} = \sqrt{(1-2u_x)\left[1 + \frac{(\frac{J}{m_x})^2}{|x|^2}\right]}, \quad \forall x \in X, \tag{53}$$

where the a_x along coordinate phase $\langle x \rangle$ is

$$a_x = \frac{1}{\hbar^2} \sum_{m_x} \frac{\partial^2 \varepsilon(k_x)}{\partial k_{\langle x \rangle} \partial k_{m_x}} e_x E_{m_x}, \quad \forall x \in X, \tag{54}$$

where k_x is the wave vector, $\varepsilon(k_x)$ is the dispersion relation, and e_x is the point charge in an external electric field E.

7 A Brief Correspondence to Yuan, Mo, and Wang

So now that we've presented our model, we realize that it inherits exceptional components from the YMW baryon-antibaryon $SU(3)$ model [17]; in particular, it is evident that their ideas and applied methodology strongly support our BAC proof. Here, we compare and contrast our model with the YMW model and provide a brief correspondence aimed at unifying the conceptual and mathematical components of both schemes. We've identified the YMW model as a well-defined framework that provides crucial insight into the nature of (theoretical and experimental) particle physics. Moreover, we've found that the construction of our BAC proof has inevitably led us to assemble a theory and framework that effectively replicates core expressions of the YMW paradigm, bringing us along similar paths of exploration.

To summarize, the YMW model is a nonet scheme which predicts many new baryon-antibaryon bound states and their possible productions in quarkonium decays and B decays [17]. It is designed to classify the increased number of experimentally observed enhancements near the baryon-antibaryon threshold. It is largely based on the Fermi-Yang-Sakata (FYS) model [76, 77], in which mesons were interpreted as baryon-antibaryon bound states [17]. The discovery of the increased number of baryon-antibaryon enhancements near thresholds reminds the YMW authors of the era prior to the development of the $SU(3)$ quark model over half a century ago, when the so-called elementary particles emerged one-by-one [17]. So YMW return to the FYS model and extend various aspects of it.

First, we identify a few key *similarities* between our model and the YMW model [17]. In short, both schemes:

- Share the core hexagon structure equipped with a baryon-antibaryon pair.
- Intertwine a hexagon and circle(s) to encode certain fundamental aspects of the baryon-antibaryon state space.
- Predict many new baryon-antibaryon bound states.
- Accommodate the enhancements near the baryon-antibaryon mass thresholds.

- Predict the increase and decrease of masses for the dual three-quark system (the baryon and the antibaryon) with respect the baryon-antibaryon mass threshold.

- Organize quark-antiquark pairs into flavorless mesons.

- Account for pseudo-scalar meson states.

- Support the possible charmonium and B decay modes as listed by YMW.

Second, we identify a few key *dissimilarities* between our model and the YMW model [17]. In doing so, we clarify that our model is not only consistent with the YMW model, but upgrades many of its components by simplifying the nonet representation from $SU(3)$ to $SU(2)$ and extending its state space, accuracy, and predictive capability. In short, the schemes differ in that:

- The hexagon structure of the YMW model does not incorporate the six-coloring kagome lattice antiferromagnet, whereas our model does; but the YMW model can be equipped with this powerful lattice structure to fundamentally enhance its representational capability.

- The YMW model does not model the quarks as coupled oscillators which generate effective mass, whereas our model does; but the YMW model can be equipped with quark coupled oscillators to attribute its mass increases and decreases to the effective mass generated by the interconnected oscillators.

- The YMW model employs classic *quantum numbers* (for total angular momentum, isospin, strangeness, and charge) to encode the system state, whereas our model employs *quantum number OPs* (for total angular momentum, isospin, and color charge) to encode the system state with additional precision; but the YMW model can be equipped with quantum number OPs of fractional statistics to construct a well-defined (baryon and antibaryon) wavefunction in state space, where the OPs are correlated with superfluid B phases [2].

- The YMW model only accounts for pseudo-scalar mesons, whereas our model accounts for pseudo-scalar *and* scalar mesons, while directly associating these components to massless Nambu-Goldstone phase-excitations [11, 12, 13] and massive Higgs-like amplitude-excitations [14], respectively; but the YMW model can be equipped with scalar mesons, phase-excitations, and amplitude-excitations that correspond to a "Goldstone Family" of gauge bosons for SSB.

- The YMW model does not define a Lagrangian that is consistent with Newtonian *and* Einsteinian paradigms in 4D space-time, whereas ours does; but the YMW model can be simplified and formulated as such to highlight these additional space-time and dynamical system relationships.

- The circular structures of the YMW model do not consider a well-defined circular dimension of time that is modeled as a Riemannian holographic ring unit circle, stereographic gravitational superlense [23], Gedanken interferometer [62], and Mott insulator [30] that is dual to both superconducting 3-branes which simultaneously triggers CPT-violations on the dual distance scales, whereas ours model does employ these notions; but the YMW model can be equipped with this paradigm so it is consistent with, for example, M.C. Escher's duality [8].

- The YMW model is not based upon a dual space-time topology equipped with topological deformations of intertwined superluminal (non-relativistic) signals and luminal (relativistic) signals, whereas our model does incorporate this arrangement; but the YMW model can be equipped with such energy deformations, signal classifications, and topological structure.

At this point we've provided a brief report that compares and contrasts some high-level aspects between the two models. For the future, this suggests that we may clarify a plethora of new ideas and fundamental relationships through an objective consolidation of both frameworks.

8 Conclusion and Outlook

In this first paper of the series, we introduced the topologies, vacuum, generalized coordinates, fractional statistics, BWF quantum number OPs, gauge symmetry breaking, and Lagrangian for our BAC proof and BAD in 4D FQHS space-time that complies with Newtonian and Einsteinian mechanics, and low-dimensional implementations of string theory and M-theory. In the next paper(s) of this series, we will extend our quark-antiquark confinement scenario by discussing the anyons, phase locking, HH, attractive and repulsive gravitational effects of quasiparticle signals on the Lagrangian, modified Gullstrand–Painlevé reference frames, and Magnification Effect.

In our opinion, this proof of quark-antiquark confinement with the amplitude–excitations and phase–excitations begins to reveal additional fundamental mechanisms and relationships inherent to our universe. In doing so, we've been able to shed more light on a number of mysterious concepts in nature, including antibaryons, baryons, baryon asymmetry, creation, annihilation, double horizons, and FQHS space-time. We suspect that these formulations, which are inspired by a plethora of experimental data, can be used to construct a unified field theory in the near future, thereby advancing physics to the "next level." Through global cooperation, competition, hard work, and creativity, these powerful concepts can be further scrutinized, extended, and applied to virtually all areas of mathematics, science, medicine, and engineering.

References

[1] V. Barger and R. Phillips. *Collider physics.* Addison-Wesley publishing company, 1997.

[2] A. Reading. Leggett, aj: A theoretical description of the new phases of liquid he. *Rev. Mod. Phys*, 47:331, 1975.

[3] RB Laughlin. Parallels between quantum antiferromagnetism and the strong interactions. *Arxiv preprint cond-mat/9802180*, 1998.

[4] P.N. Principia. Philosophiæ naturalis principia mathematica. *Isaac Newton*, page 154.

[5] K.S. Thome. *Black Holes and Time Warps: Einstein's outrageous legacy.* New York: WW Norton&Company, 1994.

[6] T.P. Cheng, L.F. Li, and T.P. Cheng. *Gauge theory of elementary particle physics*. Clarendon Press Oxford, 1984.

[7] K. Becker, M. Becker, and J.H. Schwarz. *String theory and M-theory: A modern introduction*. Cambridge University Press, 2006.

[8] MC Escher, B. Ernst, and J.E. Brigham. *The magic mirror of MC Escher*. Random House, 2007.

[9] FE Camino, W. Zhou, and VJ Goldman. Realization of a Laughlin quasiparticle interferometer: observation of fractional statistics. *Physical Review B*, 72(7):075342, 2005.

[10] F. Englert. Symmetry breaking and the scalar boson - evolving perspectives. *Arxiv preprint hep-th/1204.5382v1*, 2012.

[11] J. Goldstone. Broken symmetries. *Selected papers of Abdus Salam:(with commentary)*, 5:204, 1994.

[12] Y. Nambu. Axial vector current conservation in weak interactions. *Physical Review Letters*, 4(7):380–382, 1960.

[13] Y. Nambu and G. Jona-Lasinio. Dynamical model of elementary particles based on an analogy with superconductivity. i. *Physical Review*, 122(1):345, 1961.

[14] M. Endres, T. Fukuhara, D. Pekker, M. Cheneau, P. Schauβ, C. Gross, E. Demler, S. Kuhr, and I. Bloch. The 'Higgs' amplitude mode at the two-dimensional superfluid/Mott insulator transition. *Nature*, 487(7408):454–458, 2012.

[15] E. Witten. Black holes and quark confinement. *Current Science-Bangalore-*, 81(12):1576–1581, 2001.

[16] R.B. Laughlin. Fractional quantization. *Nobel lectures, physics, 1996-2000*, page 264, 2002.

[17] CZ Yuan, XH Mo, and P. Wang. Baryon–antibaryon nonets. *Physics Letters B*, 626(1):95–100, 2005.

[18] DO Pushkin, DE Melnikov, and VM Shevtsova. Ordering of small particles in one-dimensional coherent structures by time-periodic flows. *Physical Review Letters*, 106(23):234501, 2011.

[19] Q.H. Hu. The nature of the electron. *Arxiv preprint physics/0512265*, 2005.

[20] Marie-Jean Thoraval, Kohsei Takehara, Takeharu Goji Etoh, and et al. Popinet, Stéphane. von Kármán vortex street within an impacting

drop. *Phys. Rev. Lett.*, 108:264506, Jun 2012.

[21] RA Shelby, DR Smith, SC Nemat-Nasser, and S. Schultz. Microwave transmission through a two-dimensional, isotropic, left-handed metamaterial. *Applied Physics Letters*, 78:489, 2001.

[22] J. Li and CT Chan. Double-negative acoustic metamaterial. *Physical Review E*, 70(5):055602, 2004.

[23] U. Leonhardt. Perfect imaging without negative refraction. *New Journal of Physics*, 11:093040, 2009.

[24] VG Veselago and EE Narimanov. The left hand of brightness: past, present and future of negative index materials. *Nature materials*, 5(10):759–762, 2006.

[25] W. Melnitchouk, R. Ent, and CE Keppel. Quark–hadron duality in electron scattering. *Physics reports*, 406(3):127–301, 2005.

[26] B.Z. Kopeliovich, B. Povh, and Ivan Schmidt. Glue drops inside hadrons. *arXiv:hep-ph/0607337v1 [hep-ph]*, 2006.

[27] A. Inopin. Parity doublers and topology twists in hadrons. In *AIP Conference Proceedings*, volume 1030, page 298, 2008.

[28] P. Zhang, P. Horvathy, and J. Rawnsley. Topology, and (in)stability of non-Abelian monopoles. *Annals of Physics*, 327:118–165, 2012.

[29] Takuto Kawakami, Takeshi Mizushima, Muneto Nitta, and Kazushige Machida. Stable skyrmions in SU(2) gauged Bose-Einstein condensates. *Phys. Rev. Lett.*, 109:015301, Jul 2012.

[30] J. Schlappa, K. K. Wohlfeld, and M. et al. Zhou J., Mourigal. Spinorbital separation in the quasi-one-dimensional mott insulator Sr2CuO3. *Nature*, 2012.

[31] Y. Aharonov and J. Anandan. Phase change during a cyclic quantum evolution. *Physical Review Letters*, 58(16):1593–1596, 1987.

[32] F. Nagasawa, J. Takagi, Y. Kunihashi, and et al. Kohda. Experimental demonstration of spin geometric phase: Radius dependence of time-reversal Aharonov-Casher oscillations. *Physical Review Letters*, 108(12):086801, 2012.

[33] K. Richter. The ABC of Aharonov effects. *Physics*, 5:22, Feb 2012.

[34] M.G. Olsson. *arXiv:hep-ph/0001227*, 2000.

[35] S. Todorova. About the helix structure of the Lund string. *Arxiv preprint arXiv:1101.2407*, 2011.

[36] S. Todorova. Study of the helix structure of QCD string. *arXiv:1204.2655v1 [hep-ph]*, 2012.

[37] P.P. Cortet, A. Chiffaudel, F. Daviaud, and B. Dubrulle. Experimental evidence of a phase transition in a closed turbulent flow. *Physical review letters*, 105(21):214501, 2010.

[38] C.N. Varney, K. Sun, V. Galitski, and M. Rigol. Kaleidoscope of exotic quantum phases in a frustrated xy model. *Physical Review Letters*, 107(7):77201, 2011.

[39] D.A. Siegel, C.H. Park, C. Hwang, and et al. Deslippe, J. Many-body interactions in quasi-freestanding graphene. *Proceedings of the National Academy of Sciences*, 108(28):11365, 2011.

[40] A. Paramekanti, L. Balents, and M. Fisher. Ring exchange, the bose metal, and bosonization in two dimensions. *Arxiv preprint cond-mat/0203171*, 2002.

[41] F.E. Close, Y.L. Dokshitzer, V.N. Gribov, and et al. Khoze, V.A. Eye-witnesses of confinement. *Physics Letters B*, 319(1):291–299, 1993.

[42] Y.M. Tousi, V. Pourahmad, and E. Afshari. Delay coupled oscillators for frequency tuning of solid-state terahertz sources. *Physical Review Letters*, 108(23):234101, 2012.

[43] O. Cépas and A. Ralko. Resonating color state and emergent chromodynamics in the kagome antiferromagnet. *Physical Review B*, 84(2):020413, 2011.

[44] S. Souma and B.K. Nikolić. Spin hall current driven by quantum interferences in mesoscopic rashba rings. *Physical review letters*, 94(10):106602, 2005.

[45] T.W. Chen and G.Y. Guo. Torque and conventional spin Hall currents in two-dimensional spin-orbit coupled systems: Universal relation and hyperselection rule. *Physical Review B*, 79(12):125301, 2009.

[46] Catherine Pappas. New twist in chiral magnets. *Physics*, 5:28, Mar 2012.

[47] K. Marty, V. Simonet, E. Ressouche, and et al. Ballou, R. Single domain magnetic helicity and triangular chirality in structurally enantiopure Ba3NbFe3Si2o14. *Arxiv preprint arXiv:0809.3067*, 2008.

[48] E. Edlund, O. Lindgren, and M. Nilsson Jacobi. Chiral surfaces self-assembling in one-component systems with isotropic interactions. *Phys.*

Rev. Lett., 108:165502, Apr 2012.

[49] A. Bostwick, F. Speck, T. Seyller, and et al. Horn, K. Observation of plasmarons in quasi-freestanding doped graphene. *Science*, 328(5981):999–1002, 2010.

[50] A. Principi, R. Asgari, and M. Polini. Acoustic plasmons and composite hole-acoustic plasmon satellite bands in graphene on a metal gate. *Solid State Communications*, 2011.

[51] A.E. Inopin. Comment to the review by L. Glozman, hep-ph/0701081. *arXiv:hep-ph/0702257v1 [hep-ph]*, 2007.

[52] P. Engels. Observing the dance of a vortex- antivortex pair, step by step. *Physics*, 3:33, 2010.

[53] D. Sticlet, C. Bena, and P. Simon. Spin and Majorana polarization in topological superconducting wires. *Physical Review Letters*, 108(9):096802, 2012.

[54] CHL Quay, TL Hughes, JA Sulpizio, and LN et al. Pfeiffer. Observation of a one-dimensional spin–orbit gap in a quantum wire. *Nature Physics*, 6(5):336–339, 2010.

[55] S. Nadj-Perge, VS Pribiag, JWG Berg, and et al. Zuo. Spectroscopy of spin-orbit quantum bits in indium antimonide nanowires. *Physical Review Letters*, 2012.

[56] P. Bruno. Quantum geometric phase in Majoranas stellar representation: Mapping onto a many-body Aharonov-Bohm phase. *Phys. Rev. Lett*, 108:240402, 2012.

[57] MN Chernodub. Superconductivity of qcd vacuum in strong magnetic field. *Physical Review D*, 82(8):085011, 2010.

[58] EB Sonin. Magnus force in superfluids and superconductors. *Physical Review B*, 55(1):485, 1997.

[59] L. Fu and C.L. Kane. Superconducting proximity effect and Majorana fermions at the surface of a topological insulator. *Physical review letters*, 100(9):96407, 2008.

[60] J.D. Sau, R.M. Lutchyn, S. Tewari, and S. Das Sarma. Generic new platform for topological quantum computation using semiconductor heterostructures. *Physical review letters*, 104(4):40502, 2010.

[61] V. N. Gribov. *Eur. Phys. J. C 10*, pages 91–105, 1999.

[62] V. Jacques, F. Grosshans, F. Treussart, and P. Grangier. Experimental

realization of Wheeler's delayed-choice gedanken experiment. *Science Magazine*, 315(5814):966–968, 2007.

[63] H. Pfau, S. Hartmann, U. Stockert, and et al. Sun, P. Thermal and electrical transport across a magnetic quantum critical point. *Nature*, 484(7395):493–497, 2012.

[64] J. Friedman, M.S. Morris, I.D. Novikov, and F. et al. Echeverria. Cauchy problem in spacetimes with closed timelike curves. *Physical Review D*, 42(6):1915, 1990.

[65] F. Wilczek. Magnetic flux, angular momentum, and statistics. *Physical Review Letters*, 48(17):1144–1146, 1982.

[66] D. Faccio. Laser pulse analogues for gravity and analogue Hawking radiation. 2011.

[67] X. Du, I. Skachko, and E.Y. Andrei. Josephson current and multiple Andreev reflections in graphene sns junctions. *Physical Review B*, 77(18):184507, 2008.

[68] H. Nilsson, P. Samuelsson, P. Caroff, and H. Xu. Supercurrent and multiple Andreev reflections in an insb nanowire Josephson junction. *Nano Letters*, 2012.

[69] VV Anisovich, DV Bugg, and AV Sarantsev. Exotic mesons, locking states, and their role in the formation of the confinement barrier. *Physical Review D*, 58(11):111503, 1998.

[70] V. Bangert, C. Croke, S. Ivanov, and M. Katz. Filling area conjecture and ovalless real hyperelliptic surfaces. *Geometric and Functional Analysis*, 15(3):577–597, 2005.

[71] A. Its. The Riemann-Hilbert problem and integrable systems. *Notices of the AMS*, 50(11):1389–1400, 2003.

[72] J. Maldacena. The illusion of gravity. *Scientific American*, 11:57–63, 2005.

[73] V. Mourik, K. Zuo, SM Frolov, and et al. Plissard, SR. Signatures of Majorana fermions in hybrid superconductor-semiconductor nanowire devices. *Arxiv preprint arXiv:1204.2792*, 2012.

[74] B. Pannetier, J. Chaussy, R. Rammal, and P. Gandit. First observation of Altshuler-Aronov-Spivak effect in gold and copper. *Phys. Rev. B*, 31:3209–3211, Mar 1985.

[75] E.F. Taylor and J.A. Wheeler. Exploring black holes: introduction to

general relativity. *Recherche*, 67:02, 2000.

[76] E. Fermi and C.N. Yang. Are mesons elementary particles? *Physical Review*, 76:1739–1743, 1949.

[77] S. Sakata. On a composite model for the new particles. *Progress of theoretical physics*, 16(6):686–688, 1956.

ANALYTICAL APPROACH TO GEOMETRIC ERRORS IN RADIOGRAPHY: INVERSE ABEL TRANSFORM FOR A HOMOGENEOUS BALL

Hanna Makaruk
P-21 Modern Physics
Physics Division
Los Alamos National Laboratory
Los Alamos, NM, 87544, USA

Robert Owczarek
Enfitec Inc. and Department of Mechanical Engineering
University of New Mexico
Albuquerque, NM, 87131, USA

Received 9-3-2012
Revised 11-15-2012

Abstract

Inverse Abel transform is the main tool in reconstruction of objects with cylindrical symmetry from their radiographic images. The procedure is ill-posed, which results in amplification of noise in the data and of numerical errors, usually removed with the help of regularization procedures. In the paper we study the errors caused by deviations of the axis of reconstruction from the axis of symmetry of the reconstructed object. We study these errors in the framework of unregularized inverse Abel transform. In general, two kinds of such errors (and their combination) are possible, the shift of the axis of the axially-symmetric body from the axis about which we do the reconstruction, and the tilt of the axis. The object we deal with in this paper is a homogeneous ball. In this case the tilt of the axis does not influence the reconstruction, so that we discuss only the shift error. We study the effect analytically; the inverse Abel transform is in this case expressible in terms of the elliptic integrals. We give detailed formulas in the paper, and their derivations in the Appendices. We also give numerical results based on the formulas.

Copyright © 2012 by Hadronic Press, Inc., Palm Harbor, FL 34682–1577, USA

I Introduction

Radiography for axially symmetric objects essentially boils down to application of the inverse Abel transform. Numerical instabilities connected with singular character of the inverse Abel transform can be fought with various regularizations. For example, total variation regularization is applied when the object consists of homogeneous layers [1], [2].

Existence of problems in which non-axially symmetric distributions of matter were present caused interest in generalizations of the Abel transform method. For example, Gueron and Deutsch [3] introduced a generalization of the Abel transform to the case in which instead of circular symmetry of the cross-sections was considered a situation, in which all contours of equal density were self-similar, and could be in principle of any convex shapes. The cases of elliptic symmetry, and polygonal symmetry were discussed there. In another work, Tomassini and Giulietti [4] considered a generalization of the Abel transform method to the case when axially symmetric density distribution is perturbed in such a way that the density distribution is expressible in terms of truncated Legendre polynomial expansion in the azimuthal angle. Another approach to the problem of non-axisymmetric density reconstructions was presented by Schwierz-Iosefzon, Notea and Deutsch [5]. The method in [5] develops further the methods from [3] and assumes only mirror symmetry of the object with respect to the plane of the radiogram.

The paper by Dribinski et al. [6] rather than trying to generalize the Abel inversion discusses a proper numerical implementation of the method, using the Gaussian basis-set. In the paper is discussed the relationship of the Gaussian-basis based method to more standard Fourier-Henkel method and it is pointed out that the Gaussian basis based method seems to be better suited for obtaining high quality reconstructions.

The approach from the paper by Cristoforetti et al. [7] borrows from the ideas of perturbing the axially symmetric density distributions with truncated Legendre polynomials, like [4], but it applies a kind of onion-peeling algorithm as well.

Onion-peeling kind of ideas is also applied in the paper by Roberts et al. [8], while different functional bases are used for Abel type of reconstructions in papers by Chattopadhyay [9], and by Ma, Gao and Wu [10].

In this paper we focus on errors in the geometry of the system. What kind of errors do we have in mind? In applying the inverse Abel transform we assume the position of the axis, with respect to which the inversion is performed, coincides with the axis of the axially-symmetric body that is reconstructed. Different deviations from this position result in different geometric errors treated in this paper, and in papers to follow. One kind of geometric errors appears if the real axis of the object is under a certain angle with respect to the presumed axis. It is the tilt error. Tilt errors were discussed in numerical papers by Beery [11], [12], but the role of the inverse Abel transform was only marginally mentioned there. Another kind of geometric errors appears when the axis of the object has been shifted from the position we assumed in the reconstruction. It is the shift error. Of course one can have both kinds of errors simultaneously, but we will focus on one of them at a time.

In this paper we study the errors in the case of a homogeneous ball. It is clear, however, that due to the rotational symmetry of a ball, the tilt error does not result in an erratic reconstruction. This is an exceptional situation, and in future papers we will study other objects, for which the tilt error will influence reconstruction. In the case of a homogeneous sphere, though, we study just the shift error.

In the second section we briefly review the standard inverse Abel transform. In the third section we present the geometry for the shifted ball case. In the fourth section we derive the form of the integrals to be calculated. In the fifth section we present analytical results. In the sixth section we present some numerical results based on analytical formulas from the fifth section.

The detailed derivation of one of the integrals is given in the Appendix A, while formulas

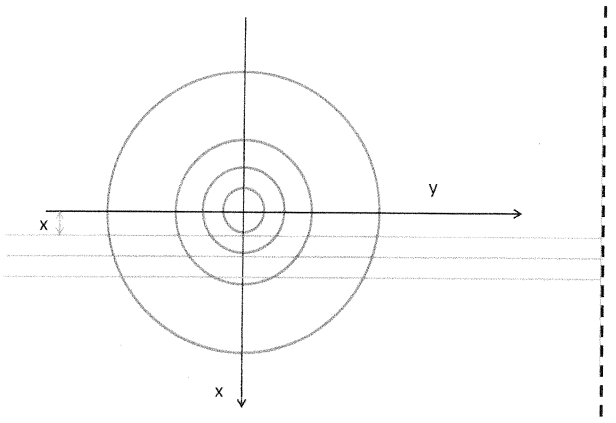

Figure II.1: Schematics of the radiography

on which the calculations (for all cases) are based are given in the Appendix B.

II Inverse Abel transform

The Abel transform appears in radiography thanks to the empirical law of exponential attenuation. Let us consider a parallel beam in the direction of the y axis of a Cartesian system, with intensity I_0, passing through a body, registered with intensity I in the screen, II.1

Suppose $\mu(r)$ denotes the attenuation function, assumed to be either radially symmetric, or axially symmetric, in which case the radial symmetry concerns a slice at height z (so that the function should be actually denoted $\mu(r,z)$). Then, the following is true

$$F(x) := ln\Big(\frac{I_0}{I(x)}\Big) = \int_{-\infty}^{+\infty} \mu(\sqrt{x^2+y^2})\,dy = 2\int_x^{+\infty} \frac{\mu(r)\,r\,dr}{\sqrt{r^2-x^2}} \tag{1}$$

because, for fixed x, $y = \sqrt{r^2-x^2}$, and thus $dy = \frac{r\,dr}{\sqrt{r^2-x^2}}$.

Generally, for a function of one variable r, its Abel transform is defined as

$$F(x) = 2\int_x^{+\infty} \frac{f(r)\,r\,dr}{\sqrt{r^2-x^2}} \tag{2}$$

Therefore, the function $F(x)$ defined above as a logarithm of the ratio of initial intensity of the beam to the measured intensity, is just the (forward) Abel transform of the attenuation coefficient function. If the function $F(x)$ satisfies certain functional analytic conditions, which as a rule are satisfied, the Abel transform can be inverted, and thus the attenuation function in the case of radiography can be found. The inverse Abel transform is given by

$$f(r) = -\frac{1}{\pi}\int_r^{+\infty} \frac{dF}{dx}\frac{dx}{\sqrt{x^2 - r^2}} \tag{3}$$

It is clear that the subintegral function is in general singular in the lower limit, which causes problems with numerical calculations, since the data always contain noise, and the noise will be amplified in that region. However, the singularity is integrable, so that theoretical considerations do not lead to any problems. The presence of geometric errors like tilt or shift complicate the analytical computations, as will be shown below. Even if geometric errors are not present, one has to use some regularization in numerical calculations in order to avoid noise amplification, but this is not of our interest in this paper. An interesting potential outcome of the inverse Abel transform reconstruction under conditions where the axial symmetry is perturbed is the existence of locally negative attenuation.

III Geometry

Let us consider a homogeneous ball whose attenuation is normalized to unity. Let the ball's axis be located at a distance d along the x-axis, in its positive direction (we will also consider the case of the shift in the opposite direction, which is actually easier). The geometry is illustrated in figure III.1 for the case $d < R$, which we discuss first.

The ball is bounded by the sphere, which in this system of coordinates is described as

$$(x - d)^2 + y^2 + z^2 = R^2 \tag{4}$$

where R is the radius of the ball. The ball is penetrated by rays parallel to y axis, characterized by coordinates (x, z). The length of the path of each ray through the ball is found from y coordinates of the entrance and exit of the ray, provided they exist.

In the case of a ball, the coordinates are easy to find, and are given by

$$y = \pm\sqrt{R^2 - (x - d)^2 - z^2} \tag{5}$$

Therefore, if both the entrance and the exit exist, the length of the path is given by

$$l(x) = 2\sqrt{R^2 - (x - d)^2 - z^2} \tag{6}$$

and then its derivative with respect to x, which is a part of the inverse Abel transform formula is

$$\frac{dl}{dx} = -2\frac{x - d}{\sqrt{R^2 - (x - d)^2 - z^2}} \tag{7}$$

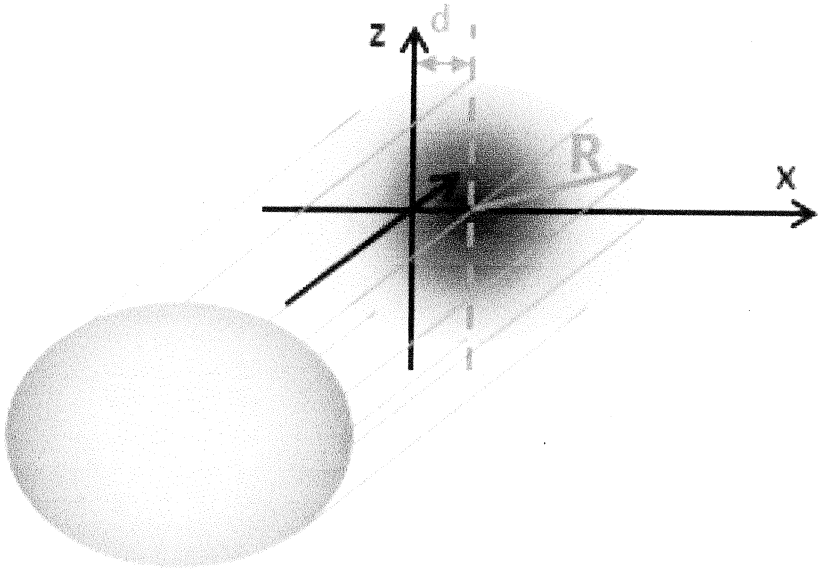

Figure III.1: Shifted ball geometry

One can, due to symmetry, limit oneself to consideration of a quarter-plane (r, z), such that $r \geq 0$, $z \geq 0$. The consideration of existence of intersections in the case $d < R$ leads to the following split of the (r, z) quarter-plane into subareas of interest (see corresponding figures for cases, for which there are intersections).

- $0 \leq z \leq \sqrt{R^2 - d^2}$, $r > d + \sqrt{R^2 - z^2}$. In this region there are no intersections, and thus $l = 0$
- $0 \leq z \leq \sqrt{R^2 - d^2}$, $0 \leq r \leq d + \sqrt{R^2 - z^2}$ (see figure III.2). In this region there are intersections, and thus $l = 2\sqrt{R^2 - (x - d)^2 - z^2}$
- $\sqrt{R^2 - d^2} \leq z \leq R$, $r > d + \sqrt{R^2 - z^2}$. In this region there are no intersections, and thus $l = 0$
- $\sqrt{R^2 - d^2} \leq z \leq R$, $0 < d - \sqrt{R^2 - z^2} \leq r \leq d + \sqrt{R^2 - z^2}$ (see figure III.3). In this region there are intersections, and thus $l = 2\sqrt{R^2 - (x - d)^2 - z^2}$
- $\sqrt{R^2 - d^2} \leq z \leq R$, $0 \leq r < d - \sqrt{R^2 - z^2}$ (see figure III.4). In this region there are intersections, and thus $l = 2\sqrt{R^2 - (x - d)^2 - z^2}$
- $z > R$, any r. In this region there are also no intersections, and thus $l = 0$

The analogous split in the case $d \geq R$ is simpler and looks as follows

- $0 \leq z \leq R$, $r > d + \sqrt{R^2 - z^2}$. In this region there are no intersections, and thus $l = 0$
- $0 \leq z \leq R$, $0 < d - \sqrt{R^2 - z^2} < r < d + \sqrt{R^2 - z^2}$. In this region there are intersections, and thus $l = 2\sqrt{R^2 - (x - d)^2 - z^2}$
- $0 \leq z \leq R$, $0 \leq r \leq d - \sqrt{R^2 - z^2}$. In this region there are intersections, and thus $l = 2\sqrt{R^2 - (x - d)^2 - z^2}$
- $z > R$, any r. In this region there are no intersections, and thus $l = 0$

Now let us discuss the case of the shift in negative direction of the x axis. The only interesting case is $|d| < R$. The equation of the sphere bounding the ball in this system of coordinates reads

$$(x + d)^2 + y^2 + z^2 = R^2 \tag{8}$$

In this case the length of the path of each ray through the ball is found from y coordinates of the entrance and exit of the ray, provided they exist.

In the case of a ball, the coordinates are easy to find, and are given by

$$y = \pm\sqrt{R^2 - (x + d)^2 - z^2} \tag{9}$$

Therefore, if the entrance and the exit exist, the length of the path is given by

$$l(x) = 2\sqrt{R^2 - (x + d)^2 - z^2} \tag{10}$$

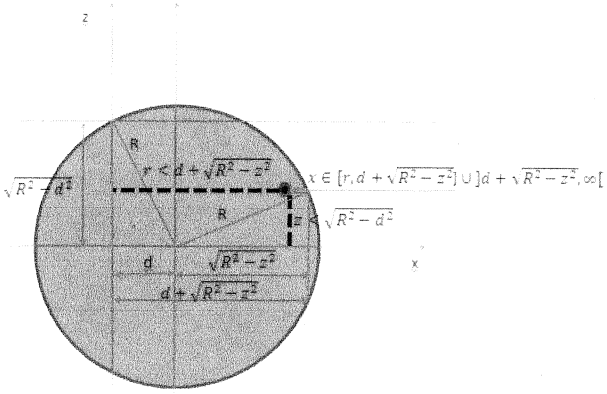

Figure III.2: The case of $0 \leq z \leq \sqrt{R^2 - d^2}$, $r < d + \sqrt{R^2 - z^2}$

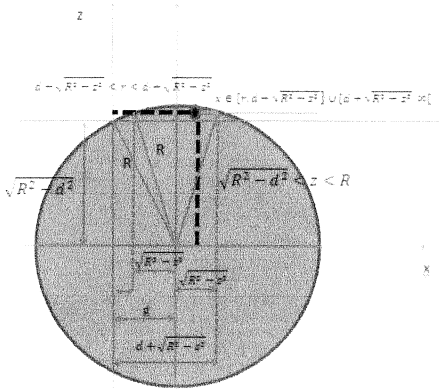
z
$d - \sqrt{R^2 - z^2} < r < d - \sqrt{R^2 - z^2}$
$x \in [r, d - \sqrt{R^2 - z^2}[\cup]d - \sqrt{R^2 - z^2}, \infty[$
R
R
$\sqrt{R^2 - R^2}$
$\sqrt{R^2 - d^2} \leq z < R$
$\sqrt{R^2 - r^2}$
$\sqrt{R^2 - z^2}$
d
$d + \sqrt{R^2 - z^2}$
x

Figure III.3: The case of $\sqrt{R^2 - d^2} \leq z \leq R$, $d - \sqrt{R^2 - z^2} < r < d + \sqrt{R^2 - z^2}$

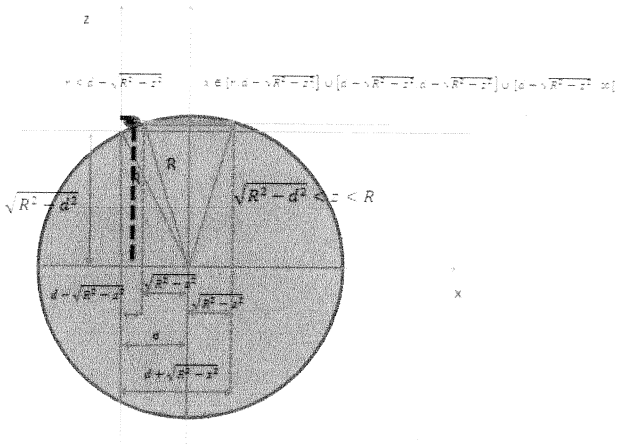

Figure III.4: The case of $\sqrt{R^2-d^2} \le z \le R$, $0 < r < d - \sqrt{R^2-z^2}$

so that its derivative with respect to x is

$$\frac{dl}{dx} = -2\frac{x+d}{\sqrt{R^2-(x+d)^2-z^2}} \tag{11}$$

Finally, we have in the case of negative shift.

- $0 \le z \le \sqrt{R^2-d^2}$, $r > \sqrt{R^2-z^2} - d$. In this case there are no intersections and $l = 0$
- $0 \le z \le \sqrt{R^2-d^2}$, $0 \le r < \sqrt{R^2-z^2} - d$. In this case there are intersections and $l = 2\sqrt{R^2-(x+d)^2-z^2}$
- $z > \sqrt{R^2-d^2}$, any r. In this case there are no intersections and $l = 0$

IV The integrals to be calculated

In each of the cases we have to calculate (or just state it is zero) certain integrals to recover attenuation μ. In the case $d < R$ these are as follows

- $0 \le z \le \sqrt{R^2-d^2}$, $r > d + \sqrt{R^2-z^2}$. In this case $\mu(r,z) = 0$.
- $0 \le z \le \sqrt{R^2-d^2}$, $0 \le r \le d + \sqrt{R^2-z^2}$. In this region there are intersections (see figure III.2), and thus $l = 2\sqrt{R^2-(x-d)^2-z^2}$ and

$$\mu(r,z) = \frac{2}{\pi}\int_r^{d+\sqrt{R^2-z^2}} \frac{(x-d)\,dx}{\sqrt{R^2-z^2-(x-d)^2}\sqrt{x^2-r^2}}$$

- $\sqrt{R^2-d^2} \le z \le R$, $r > d + \sqrt{R^2-z^2}$. In this case $\mu(r,z) = 0$
- $\sqrt{R^2-d^2} \le z \le R$, $0 < d - \sqrt{R^2-z^2} \le r \le d + \sqrt{R^2-z^2}$. In this region there are intersections (see figure III.3), and thus $l = 2\sqrt{R^2-(x-d)^2-z^2}$ and

$$\mu(r,z) = \frac{2}{\pi}\int_r^{d+\sqrt{R^2-z^2}} \frac{(x-d)\,dx}{\sqrt{R^2-z^2-(x-d)^2}\sqrt{x^2-r^2}}$$

- $\sqrt{R^2-d^2} \le z \le R$, $0 \le r < d - \sqrt{R^2-z^2}$. In this region there are intersections (see figure III.4), and thus $l = 2\sqrt{R^2-(x-d)^2-z^2}$ and

$$\mu(r,z) = \frac{2}{\pi}\int_{d-\sqrt{R^2-z^2}}^{d+\sqrt{R^2-z^2}} \frac{(x-d)\,dx}{\sqrt{R^2-z^2-(x-d)^2}\sqrt{x^2-r^2}}$$

- $z > R$, any r. In this case $\mu(r,z) = 0$

The case $d \ge R$ gives the following formulas

- $0 \le z \le R$, $r > d + \sqrt{R^2 - z^2}$. In this case $\mu(r, z) = 0$
- $0 \le z \le R$, $0 < d - \sqrt{R^2 - z^2} < r < d + \sqrt{R^2 - z^2}$.
  In this case $l = 2\sqrt{R^2 - (x-d)^2 - z^2}$ and

$$\mu(r,z) = \frac{2}{\pi} \int_r^{d+\sqrt{R^2-z^2}} \frac{(x-d)\,dx}{\sqrt{R^2 - z^2 - (x-d)^2}\sqrt{x^2 - r^2}}$$

- $0 \le z \le R$, $0 \le r \le d - \sqrt{R^2 - z^2}$. In this case $l = 2\sqrt{R^2 - (x-d)^2 - z^2}$ and

$$\mu(r,z) = \frac{2}{\pi} \int_{d-\sqrt{R^2-z^2}}^{d+\sqrt{R^2-z^2}} \frac{(x-d)\,dx}{\sqrt{R^2 - z^2 - (x-d)^2}\sqrt{x^2 - r^2}}$$

- $z > R$, any r. In this case $\mu(r, z) = 0$

Finally, we have in the case of negative shift.

- $0 \le z \le \sqrt{R^2 - d^2}$, $r > \sqrt{R^2 - z^2} - d$. In this case $\mu(r, z) = 0$
- $0 \le z \le \sqrt{R^2 - d^2}$, $0 \le r < \sqrt{R^2 - z^2} - d$. In this case $l = 2\sqrt{R^2 - (x+d)^2 - z^2}$ and

$$\mu(r,z) = \frac{2}{\pi} \int_r^{\sqrt{R^2-z^2}-d} \frac{(x+d)\,dx}{\sqrt{R^2 - z^2 - (x+d)^2}\sqrt{x^2 - r^2}}$$

- $z > \sqrt{R^2 - d^2}$, any r. In this case $\mu(r, z) = 0$

V Analytical results

Calculation of the integrals gives the following expressions for attenuation μ, first for the case $d < R$ (in the process of calculating the integrals the case $0 \le z \le \sqrt{R^2 - d^2}$, $0 \le r \le d + \sqrt{R^2 - z^2}$ splits into two subcases $0 \le z \le \sqrt{R^2 - d^2}$, $\sqrt{R^2 - z^2} - d \le r \le d + \sqrt{R^2 - z^2}$, and $0 \le z \le \sqrt{R^2 - d^2}$, $0 \le r < \sqrt{R^2 - z^2} - d$.)

- $0 \le z \le \sqrt{R^2 - d^2}$, $r > d + \sqrt{R^2 - z^2}$. In this case $\mu(r, z) = 0$
- $0 \le z \le \sqrt{R^2 - d^2}$, $\sqrt{R^2 - z^2} - d \le r \le d + \sqrt{R^2 - z^2}$. In this case

$$\begin{aligned}
&\mu(r,z) = \\
&= \frac{2}{\pi} \frac{d + r + \sqrt{R^2 - z^2}}{\sqrt{r\sqrt{R^2 - z^2}}} \times \\
&\times \Pi\left(-\frac{d - r + \sqrt{R^2 - z^2}}{2r}, \frac{1}{2}\sqrt{\frac{d^2 - (\sqrt{R^2 - z^2} - r)^2}{r\sqrt{R^2 - z^2}}} \right) + \\
&-\frac{2}{\pi} \frac{d + r}{\sqrt{r\sqrt{R^2 - z^2}}} K\left(\frac{1}{2}\sqrt{\frac{d^2 - (\sqrt{R^2 - z^2} - r)^2}{r\sqrt{R^2 - z^2}}} \right)
\end{aligned}$$

- $0 \leq z \leq \sqrt{R^2 - d^2}$, $0 \leq r < \sqrt{R^2 - z^2} - d$. In this case

$$\begin{aligned}
&\mu(r,z) = \\
&= \frac{8}{\pi} \frac{\sqrt{R^2 - z^2}}{\sqrt{(\sqrt{R^2 - z^2} + r)^2 - d^2}} \times \\
&\times \Pi\left(- \frac{d - r + \sqrt{R^2 - z^2}}{r - d + \sqrt{R^2 - z^2}}, \sqrt{\frac{(\sqrt{R^2 - z^2} - r)^2 - d^2}{(\sqrt{R^2 - z^2} + r)^2 - d^2}} \right) + \\
&- \frac{4}{\pi} \frac{\sqrt{R^2 - z^2}}{\sqrt{(\sqrt{R^2 - z^2} + r)^2 - d^2}} K\left(\sqrt{\frac{(\sqrt{R^2 - z^2} - r)^2 - d^2}{(\sqrt{R^2 - z^2} + r)^2 - d^2}} \right)
\end{aligned}$$

- $\sqrt{R^2 - d^2} \leq z \leq R$, $r > d + \sqrt{R^2 - z^2}$. In this case $\mu(r,z) = 0$
- $\sqrt{R^2 - d^2} \leq z \leq R$, $0 < d - \sqrt{R^2 - z^2} \leq r \leq d + \sqrt{R^2 - z^2}$. In this case

$$\begin{aligned}
&\mu(r,z) = \\
&= \frac{2}{\pi} \frac{d + r + \sqrt{R^2 - z^2}}{\sqrt{r\sqrt{R^2 - z^2}}} \times \\
&\times \Pi\left(- \frac{d - r + \sqrt{R^2 - z^2}}{2r}, \frac{1}{2} \sqrt{\frac{d^2 - (\sqrt{R^2 - z^2} - r)^2}{r\sqrt{R^2 - z^2}}} \right) + \\
&- \frac{2}{\pi} \frac{d + r}{\sqrt{r\sqrt{R^2 - z^2}}} K\left(\frac{1}{2} \sqrt{\frac{d^2 - (\sqrt{R^2 - z^2} - r)^2}{r\sqrt{R^2 - z^2}}} \right)
\end{aligned}$$

- $\sqrt{R^2 - d^2} \leq z \leq R$, $0 \leq r < d - \sqrt{R^2 - z^2}$. In this case

$$\begin{aligned}
&\mu(r,z) = \\
&= \frac{4}{\pi} \frac{d + r + \sqrt{R^2 - z^2}}{\sqrt{d^2 - (\sqrt{R^2 - z^2} - r)^2}} \times \\
&\times \Pi\left(- \frac{2\sqrt{R^2 - z^2}}{d + r - \sqrt{R^2 - z^2}}, 2\sqrt{\frac{r\sqrt{R^2 - z^2}}{d^2 - (\sqrt{R^2 - z^2} - r)^2}} \right) + \\
&- \frac{4}{\pi} \frac{r + d}{\sqrt{d^2 - (\sqrt{R^2 - z^2} - r)^2}} K\left(2\sqrt{\frac{r\sqrt{R^2 - z^2}}{d^2 - (\sqrt{R^2 - z^2} - r)^2}} \right)
\end{aligned}$$

- $z > R$, any r. In this case $\mu(r,z) = 0$

Then, the analogous results in the case of $d > R$ are

- $0 \le z \le R$, $r > d + \sqrt{R^2 - z^2}$. In this case $\mu(r, z) = 0$
- $0 \le z \le R$, $0 \le r \le d - \sqrt{R^2 - z^2}$. In this case

$$\mu(r,z) =$$
$$= \frac{4}{\pi} \frac{d + r + \sqrt{R^2 - z^2}}{\sqrt{d^2 - (\sqrt{R^2 - z^2} - r)^2}} \times$$
$$\times \Pi\left(- \frac{2\sqrt{R^2 - z^2}}{d + r - \sqrt{R^2 - z^2}}, 2\sqrt{\frac{r\sqrt{R^2 - z^2}}{d^2 - (\sqrt{R^2 - z^2} - r)^2}} \right) +$$
$$- \frac{4}{\pi} \frac{r + d}{\sqrt{d^2 - (\sqrt{R^2 - z^2} - r)^2}} K\left(2\sqrt{\frac{r\sqrt{R^2 - z^2}}{d^2 - (\sqrt{R^2 - z^2} - r)^2}} \right)$$

- $0 \le z \le R$, $0 \le d - \sqrt{R^2 - z^2} < r \le d + \sqrt{R^2 - z^2}$. In this case

$$\mu(r,z) =$$
$$= \frac{2}{\pi} \frac{d + r + \sqrt{R^2 - z^2}}{\sqrt{r\sqrt{R^2 - z^2}}} \times$$
$$\times \Pi\left(- \frac{d + \sqrt{R^2 - z^2} - r}{2r}, \frac{1}{2}\sqrt{\frac{d^2 - (\sqrt{R^2 - z^2} - r)^2}{r\sqrt{R^2 - z^2}}} \right) +$$
$$- \frac{2}{\pi} \frac{r + d}{\sqrt{r\sqrt{R^2 - z^2}}} K\left(\frac{1}{2}\sqrt{\frac{d^2 - (\sqrt{R^2 - z^2} - r)^2}{r\sqrt{R^2 - z^2}}} \right)$$

- $z > R$, any r. In this case $\mu(r, z) = 0$

Finally, in the case of negative shift

- $0 \le z \le \sqrt{R^2 - d^2}$, $r > \sqrt{R^2 - z^2} - d$. In this case $\mu(r, z) = 0$
- $0 \le z \le \sqrt{R^2 - d^2}$, $0 \le r < \sqrt{R^2 - z^2} - d$. In this case

$$\mu(r,z) =$$
$$= \frac{8\sqrt{R^2 - z^2}}{\pi\sqrt{(\sqrt{R^2 - z^2} + r)^2 - d^2}} \times$$
$$\times \Pi\left(- \frac{\sqrt{R^2 - z^2} - d - r}{\sqrt{R^2 - z^2} + d + r}, \sqrt{\frac{(\sqrt{R^2 - z^2} - r)^2 - d^2}{(\sqrt{R^2 - z^2} + r)^2 - d^2}} \right) +$$
$$- \frac{4\sqrt{R^2 - z^2}}{\pi\sqrt{(\sqrt{R^2 - z^2} + r)^2 - d^2}} K\left(\sqrt{\frac{(\sqrt{R^2 - z^2} - r)^2 - d^2}{(\sqrt{R^2 - z^2} + r)^2 - d^2}} \right)$$

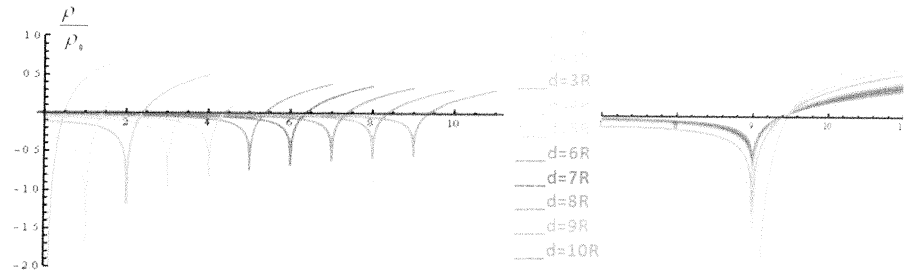

Figure VI.1: Plots of analytical results in cases of $d > R$

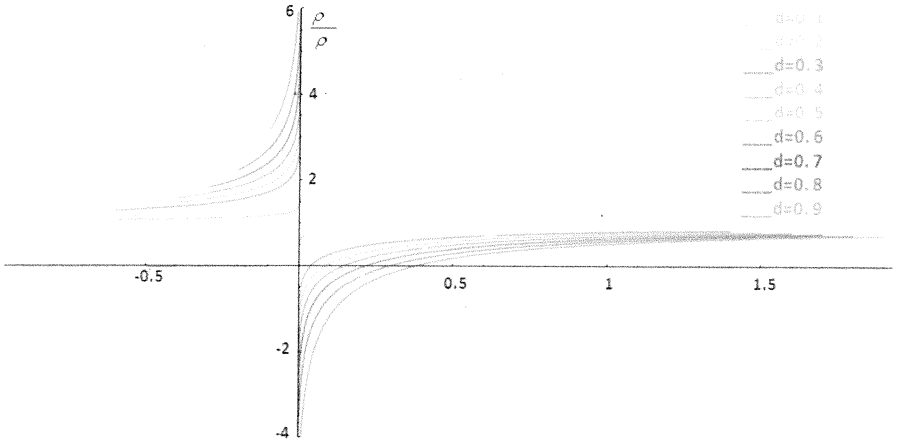

Figure VI.2: Plots of analytical results in cases $d < R$

- $z > \sqrt{R^2 - d^2}$, any r. In this case $\mu(r, z) = 0$

The detailed calculations of one of the integrals are given in Appendix A, while the formulas we used to calculate all integrals are listed in Appendix B.

VI Plots of analytical results

In the figures are shown numerical results for reconstructions of the attenuation when different shifts are present. The reconstructions were done for $z = 0$ cross sections. The first picture shows ratios of reconstructed attenuations $\mu(r)$ to the one with no shift (actually, we assumed proportionality of attenuation and density of materials, which is not exact, and the density ρ is used instead). We show separately results for $d > R$ and for $d < R$, and in the latter case both positive and negative values of d are included.

VII Conclusions

In the paper we studied the geometric errors in Abel inversion reconstruction of objects with axial symmetry. The errors originate from deviations of the position of the axis of reconstruction from the axis of symmetry of the body. They are in general of two kinds, tilt and shift. We considered in the paper reconstruction of the homogeneous ball. In this case, due to symmetry of the ball, the tilt error does not appear, but the shift error does. We gave the general analytical formulas for inverse Abel inversion of the ball in cases of different shifts. The formulas in this case are expressible in terms of elliptic integrals of the first and third kind. The deviations from correct values (no shift) are rather significant. In particular, the deviations of a few percent appear already at as small shifts as 0.02 of the radius of the ball, and may give, e.g., locally negative values of attenuation when shift is as small as 0.3 of the radius of the ball. We considered besides small shifts (smaller than the radius) also large shifts, since in some experiments may appear extra objects, breaking the axial symmetry, on the background distribution of matter, which remains axially symmetric. Such an object, when modeled by a homogeneous ball, may disturb proper reconstruction, especially in the areas of small density, as is visible from plots of the derived analytical formulas.

Our methods using the elliptic integrals can be applied also to found shift and tilt effects in the other reconstructions, which we plan to pursue later.

VIII Acknowledgments

The authors would like to thank Chris Tomkins for posing the problem and helpful discussions. RO would like to thank Dr. Albert Engelhardt from Enfitec, Inc. for his help and possibility to pursue this research.

APPENDIX

A Calculation of the integrals

We give calculation of one of the integrals introduced in the main text. Other integrals are calculated along basically the same lines.

Namely, we calculate

$$\frac{2}{\pi}\int_r^{d+\sqrt{R^2-z^2}} \frac{(x-d)\,dx}{\sqrt{R^2-z^2-(x-d)^2}\sqrt{x^2-r^2}} \tag{A-1}$$

in the regions $\sqrt{R^2-d^2} \le z \le R$, $d-\sqrt{R^2-z^2} \le r \le d+\sqrt{R^2-z^2}$, as well as in the region $0 \le z \le \sqrt{R^2-d^2}$, $0 \le r \le d+\sqrt{R^2-z^2}$

We have

$$\frac{2}{\pi}\int_r^{d+\sqrt{R^2-z^2}} \frac{(x-d)\,dx}{\sqrt{R^2-z^2-(x-d)^2}\sqrt{x^2-r^2}} = \tag{A-2}$$

$$= \frac{2}{\pi}\left[\int_r^{d+\sqrt{R^2-z^2}} \frac{x\,dx}{\sqrt{(d+\sqrt{R^2-z^2}-x)(x-r)(x-(d-\sqrt{R^2-z^2}))(x-(-r))}} + \right.$$

$$\left. -d\int_r^{d+\sqrt{R^2-z^2}} \frac{dx}{\sqrt{(d+\sqrt{R^2-z^2}-x)(x-r)(x-(d-\sqrt{R^2-z^2}))(x-(-r))}}\right]$$

where, due to the definitions of the regions, $d+\sqrt{R^2-z^2} \geq r \geq d-\sqrt{R^2-z^2} > -r$, so, identifying $\alpha = d+\sqrt{R^2-z^2}$, $\beta = r$, $\gamma = d-\sqrt{R^2-z^2}$, $\delta = -r$, we reduce the integrals to

the forms given in Appendix B. Therefore, accordingly to the formulas for these integrals

$$\frac{2}{\pi}\int_r^{d+\sqrt{R^2-z^2}} \frac{(x-d)\,dx}{\sqrt{R^2-z^2-(x-d)^2}\sqrt{x^2-r^2}} = \tag{A-3}$$

$$= \frac{2}{\pi}\Bigg\{\Bigg[\frac{2(-r)}{\sqrt{(d+\sqrt{R^2-z^2}-d+\sqrt{R^2-z^2})(r+r)}}\times$$

$$\times F\Bigg(arcsin\sqrt{\frac{(r+r)(d+\sqrt{R^2-z^2}-r)}{(d+\sqrt{R^2-z^2}-r)(r+r)}},\dots$$

$$\dots\sqrt{\frac{(d+\sqrt{R^2-z^2}-r)(d-\sqrt{R^2-z^2}+r)}{(d+\sqrt{R^2-z^2}-d+\sqrt{R^2-z^2})(r+r)}}\Bigg)+$$

$$+\frac{2(d+\sqrt{R^2-z^2}+r)}{\sqrt{(d+\sqrt{R^2-z^2}-d+\sqrt{R^2-z^2})(r+r)}}\times$$

$$\times\Pi\Bigg(arcsin\sqrt{\frac{(r+r)(d+\sqrt{R^2-z^2}-r)}{(d+\sqrt{R^2-z^2}-r)(r+r)}},\dots$$

$$\dots-\frac{d+\sqrt{R^2-z^2}-r}{r+r},\dots$$

$$\dots\sqrt{\frac{(d+\sqrt{R^2-z^2}-r)(d-\sqrt{R^2-z^2}+r)}{(d+\sqrt{R^2-z^2}-d+\sqrt{R^2-z^2})(r+r)}}\Bigg)\Bigg]+$$

$$-d\frac{2}{\sqrt{(d+\sqrt{R^2-z^2}-d+\sqrt{R^2-z^2})(r+r)}}\times$$

$$\times F\Bigg(arcsin\sqrt{\frac{(r+r)(d+\sqrt{R^2-z^2}-r)}{(d+\sqrt{R^2-z^2}-r)(r+r)}},\dots$$

$$\dots\sqrt{\frac{(d+\sqrt{R^2-z^2}-r)(d-\sqrt{R^2-z^2}+r)}{(d+\sqrt{R^2-z^2}-d+\sqrt{R^2-z^2})(r+r)}}\Bigg)\Bigg\}=$$

$$= -\frac{2}{\pi}\frac{d+r}{\sqrt{r\sqrt{R^2-z^2}}}F\left(\frac{\pi}{2},\frac{1}{2}\sqrt{\frac{d^2-(\sqrt{R^2-z^2}-r)^2}{r\sqrt{R^2-z^2}}}\right)+$$

$$+\frac{2}{\pi}\frac{d+\sqrt{R^2-z^2}+r}{\sqrt{r\sqrt{R^2-z^2}}}\Pi\left(\frac{\pi}{2},-\frac{d+\sqrt{R^2-z^2}-r}{2r},\frac{1}{2}\sqrt{\frac{d^2-(\sqrt{R^2-z^2}-r)^2}{r\sqrt{R^2-z^2}}}\right)=$$

$$= -\frac{2}{\pi}\frac{d+r}{\sqrt{r\sqrt{R^2-z^2}}}K\left(\frac{1}{2}\sqrt{\frac{d^2-(\sqrt{R^2-z^2}-r)^2}{r\sqrt{R^2-z^2}}}\right)+$$

$$+\frac{2}{\pi}\frac{d+r+\sqrt{R^2-z^2}}{\sqrt{r\sqrt{R^2-z^2}}}\Pi\left(-\frac{d-r+\sqrt{R^2-z^2}}{2r},\frac{1}{2}\sqrt{\frac{d^2-(\sqrt{R^2-z^2}-r)^2}{r\sqrt{R^2-z^2}}}\right)$$

This ends the calculation of this integral.

B The formulas used in calculating the integrals

Here we give the formulas we used in calculation of all the integrals, which are straight out of the Gradshteyn and Ryzhik book [13].

First, let us give the formulas we used that are from Gradshteyn and Ryzhik book, under the numbers 3.147 7. and 6, with a, b, c, d parameters replaced with parameters names α, β, γ, δ, respectively

$$\int_u^\alpha \frac{dx}{\sqrt{(\alpha-x)(x-\beta)(x-\gamma)(x-\delta)}} = \tag{B-1}$$

$$= \frac{2}{\sqrt{(\alpha-\gamma)(\beta-\delta)}} F\left(arcsin\sqrt{\frac{(\beta-\delta)(\alpha-u)}{(\alpha-\beta)(u-\delta)}}, \sqrt{\frac{(\alpha-\beta)(\gamma-\delta)}{(\alpha-\gamma)(\beta-\delta)}} \right)$$

where $\alpha > u \geq \beta > \gamma > \delta$

$$\int_\beta^u \frac{dx}{\sqrt{(\alpha-x)(x-\beta)(x-\gamma)(x-\delta)}} = \tag{B-2}$$

$$= \frac{2}{\sqrt{(\alpha-\gamma)(\beta-\delta)}} F\left(arcsin\sqrt{\frac{(\alpha-\gamma)(u-\beta)}{(\alpha-\beta)(u-\gamma)}}, \sqrt{\frac{(\alpha-\beta)(\gamma-\delta)}{(\alpha-\gamma)(\beta-\delta)}} \right) \tag{B-3}$$

where $\alpha > u \geq \beta > \gamma > \delta$. In both cases F is the elliptic integral of the first kind.

Then, we use also formulas 3.148 7 and 6 from Gradshteyn and Ryzhik book [13].

$$\int_u^\alpha \frac{x\,dx}{\sqrt{(\alpha-x)(x-\beta)(x-\gamma)(x-\delta)}} = \tag{B-4}$$

$$= \frac{2\delta}{\sqrt{(\alpha-\gamma)(\beta-\delta)}} F\left(arcsin\sqrt{\frac{(\beta-\delta)(\alpha-u)}{(\alpha-\beta)(u-\delta)}}, \sqrt{\frac{(\alpha-\beta)(\gamma-\delta)}{(\alpha-\gamma)(\beta-\delta)}} \right) +$$

$$+ \frac{2(\alpha-\delta)}{\sqrt{(\alpha-\gamma)(\beta-\delta)}} \Pi\left(arcsin\sqrt{\frac{(\beta-\delta)(\alpha-u)}{(\alpha-\beta)(u-\delta)}}, -\frac{\alpha-\beta}{\beta-\delta}, \sqrt{\frac{(\alpha-\beta)(\gamma-\delta)}{(\alpha-\gamma)(\beta-\delta)}} \right)$$

where $\alpha > u \geq \beta > \gamma > \delta$

$$\int_\beta^u \frac{x\,dx}{\sqrt{(\alpha-x)(x-\beta)(x-\gamma)(x-\delta)}} = \tag{B-5}$$

$$= \frac{2\gamma}{\sqrt{(\alpha-\gamma)(\beta-\delta)}} F\left(arcsin\sqrt{\frac{(\alpha-\gamma)(u-\beta)}{(\alpha-\beta)(u-\gamma)}}, \sqrt{\frac{(\alpha-\beta)(\gamma-\delta)}{(\alpha-\gamma)(\beta-\delta)}} \right) + \tag{B-6}$$

$$+ \frac{2(\beta-\gamma)}{\sqrt{(\alpha-\gamma)(\beta-\delta)}} \Pi\left(arcsin\sqrt{\frac{(\alpha-\gamma)(u-\beta)}{(\alpha-\beta)(u-\gamma)}}, \frac{\alpha-\beta}{\alpha-\gamma}, \sqrt{\frac{(\alpha-\beta)(\gamma-\delta)}{(\alpha-\gamma)(\beta-\delta)}} \right)$$

where $\alpha \geq u > \beta > \gamma > \delta$. In both cases F is the elliptic integral of the first kind, and Π is the elliptic integral of the third kind. However, as we checked the formulas, the second argument of the Π function has to have opposite sign if the definition of the Π function 8.111 4 from [13] is accepted.

References

[1] T.J. Asaki, et al. *Abel inversion using total-variation regularization*, Inverse Problems, **21**, 2005, 1895-1903

[2] T.J. Asaki, et al. *Abel inversion using total variation regularization: applications*, Inverse Problems in Science and Engineering, **14**, 2006, 873-885

[3] S. Gueron, M. Deutsch, *Single-projection radiography for noncircular symmetries: Generalization of the Abel transform method*, J. Appl. Phys., **79**, 1996, 8879-8885

[4] P. Tomassini, A. Giulietti, *A generalization of Abel inversion to non-axisymmetric density distribution*, Optics Communications, **199**, 2001, 143-148

[5] T. Schwierz-Iosefzon, A. Notea, M. Deutsch, *Radiography of nonaxisymmetric objects: An onion-peeling inversion method*, Applied Physics Letters, **81**, 2002, 2121-2123

[6] V. Dribinski, A. Ossadtchi, V.A. Mandelshtam, H. Reisler, *Reconstruction of Abel-transformable images: The Gaussian basis-set expansion Abel transform method*, Review of Scientific Instruments, **73**, 2002, 2634-2642

[7] G. Cristoforetti, S. Legnaioli, V. Palleschi, A. Salvetti, E. Tognoni, P. Tomassini, *Reconstruction of laser-induced plasma spectral emissivity in non-axisymmetric conditions*, Spectrochimica Acta Part B, **60**, 2005, 888-896

[8] G.M. Roberts, J.L. Nixon, J. Lecointre, E. Wrede, J.R.R. Verlet, *Toward real-time charged-particle image reconstruction using polar onion-peeling*, Review of Scientific Instruments, **80**, 2009, 053104-1- 053104-7

[9] A.K. Chattopadhyay, *Abel inversion using Bessel function as a radial basis function for sparse spectroscopic data*, Plasma Devices and Operations, **16**, 2008, 115-126

[10] S. Ma, H. Gao, L. Wu, *Modified Fourier-Hankel method based on analysis of errors in Abel inversion using Fourier transformation techniques*, Applied Optics, **47**, 2008, 1350-1357

[11] T. Beery, *Memory Conservation Methods Essential for Operation of the BIE*, internal Los Alamos National Laboratory report, Feb. 2009

[12] T. Beery, *Ambiguous Reconstructions of Tilted Axis-Symmetric Objects*, internal Los Alamos National Laboratory report, June 2009

[13] Gradshteyn, Ryzhik, *Table of Integrals, Series, and Products*, Seventh Edition, Elsevier, (2007)

HADRONIC JOURNAL 35, 527-555 (2012)

RESOLUTION OF KANTOR AND BABCOCK-BERGMAN EMISSION THEORY ANOMALIES

Peter A. Jackson
Orchard House, Whitstable
Canterbury Kent CT5 3EX, UK
Peter.jackson53@ymail.com
John S. Minkowski
Baltimore, MD
jminkowl@jhmi.edu

Received 9-9-2012
Revised 1-24-2013

Abstract

Kantor's 1962 interferometer result supporting the emission theory of light was tested by Babcock and Bergman (B&B) in 1964, but with rotating glass plates placed in a vacuum. The result was different and consistent with Einstein's Special Theory of Relativity (STR). Two *"not fully understood"* anomalies remained; A 0.02 fringe shift was still found (Kantor found 2.9), and the kinetic fringe shift with rotating plates was far *smaller* than the shift with the plates static. The results falsified the theory that light passing out of the glass continued at c+v in the lab frame, but the anomalies were not resolved. We review these alongside related and poorly understood effects including kinetic reverse refraction and non-linear optics. We also consider advances in science and astrophysics and find and describe a theoretical resolution. We find that Kantor's finding may also be *'apparent'* without violating the postulates of the STR or invoking an absolute 'ether' frame. Relationships between Maxwell's near field transition zone, photo-ionization, non-linear optics and the surface electro/magneto-optic Kerr effects emerge, building an ontological construction which we describe and quantify. Proper Time is found as required for Proper speed. A relativistic theoretical model is built from a diffractive mechanism, as used by the US Naval Observatory for accuracy in the AA2010 aberration declination model, but now with a *"consistent relativistic theory"* to support it. We show how the inconsistency between Michelson's 1924 experiment supporting ether and his famous null result may arise from systemic errors of symmetry in 1924. The quantum mechanisms of Raman (and coherent forward) scattering, optical axis rotation and CMB frames last scattered are shown to directly derive the STR postulates. Some further experiments are suggested.

Copyright © 2012 by Hadronic Press, Inc., Palm Harbor, FL 34682–1577, USA

1. Introduction

Wallace Kantor (1962) reported experimental findings that *"the relative speed of light is dependent on the uniform motion of the source."* which contradicted the postulates of the STR. Plates of glass on a rotating arm were placed between the static mirrors of a modified Michelson-Morley (M&M) interferometer moving in free air in the lab frame. Kantor found that light passing through the glass was re-emitted at c with respect to the glass and continued through the medium at c in the frame of the re-emitting glass surface. In 1964 Babcock and Bergman (B&B) repeated the experiment with four times greater sensitivity, using a reversible motor, and measuring; *"the speed of light which has passed through moving glass plates by the observation of the shift of interference fringes"* in a vacuum, and *"with the fringes observed at infinity."* Where Kantor's emission theory predicted 2.9 fringes B&B found *"less than 0.02 fringe."* The B&B result was consistent with the propagation speed of c/n in the inertial frame of the glass plates, and c = d/t while passing through the vacuum, consistent with the postulates of the STR. The result was also in accord with the proof of the first STR postulate using binary stars, where the light travels at c irrespective of the approach of recession of the star as first found by Comstock (1910) and de Sitter (1913).

J.G. Fox suggested (1965) Ewald-Oseen extinction at change of propagation velocity after emission from the ions and electrons of a mirror at $c + v$ in the laboratory frame. The velocity of radiation *"received by the air molecules as a frequency of* $\nu(1+\beta)(1+\beta) \approx \nu(1+2\beta)$... *is quickly localized by them to* c [$\lambda/(n-1) = 0.3$ *mm* (in air) at NTP]," (Fox 1965), where $v \equiv \beta c$ is the velocity of the glass and ν the frequency of the light source. Kantor considered experiments inconclusive, extinction unproven and said; *"Rather than confirming the absolute speed of light, these null result experiments can also be regarded as merely showing the obliteration of the relative speed of light as it propagates through various media."* (Kantor 1971). Of course Kantor had a logical point, but any implication that c + v would then occur in a vacuum was still contrary to de Sitter's proof of the first STR postulate, consistently confirmed by spectroscopy including by Brecher (1977) who reasoned that extinction could not apply over short vacuum distances. So the problem then remained; ***How could extinction occur in a vacuum? Or what else was happening?***

Speed, as distance over time d/t, requires a datum; two frames, an emitter frame and background reference frame, or two reference points (a known distance) to be assignable. The background 'ether' frame had to be removed to allow the STR to explain constancy of c (CSL) for all moving *receivers.* But this then allowed only relative velocity between bodies. Einstein's tried (Leiden 1921<) to reinstate an ether frame to defeat emission theory, (c always with respect to emitter) which confounded c = d/t. But such a background or 'absolute' frame then confounded any explanation of CSL for *observers* moving through the ether. Length contraction had been invoked to escape that apparent paradox, but has so far still never been proven so theories of speed c in vacua with respect to the original emitter have endured. The B&B experiment might have been conclusive but the "*not fully understood*" fringe shifts and full theoretical basis remained unexplained. To explain these we invoke related effects and phenomena, some not fully understood and some not currently considered related. These include among others Maxwell's near and far field transition zone, non-linear optics, the fine structure constant, magnetohydrodynamics, Raman scattering, aberration, birefringence, surface charge, plasmons and the Surface Magneto Optic Kerr effect (SMOKE). Light as waves overcomes the problem of photon momentum in media, avoiding the Minkowski/Abraham tensor issue and even suggesting the Einstein-Loeb model may be locally valid.

2. Birefringence and Extinction

First found in calcite in 1669 birefringence is considered as decomposition of a 'ray' of light into two rays. It may be more properly considered in terms of plane waves and the 'optical axis'. Raman found birefringence (1921) in diffuse gas in his 1930 Noble prize winning work on scattering, and free electron/ proton plasma of highly birefringent with a refractive index n =~1. We know that the quantum vacuum is also birefringent. We suggest that kinetic effects related to twin 'light paths' (refracted axis) are evidence of gradual extinction of emissions due to coupling interaction in a diffuse particle medium over vast distances. Laplace considered 'intensity' in r = (mass) *M sin z.* But consistent with Raman's findings in diffuse media we predict that the two optical axes also represent different *velocities* of propagation, as c in both the 'arrival' and re-scattered frames. We propose a series of experiments to confirm this theory

including *[Exp.1]* with a plasma particle chamber and varying emission rates in an interferometer to compare arrival times of the two (birefringent) components of light, which we propose arises from a relative rotation of optical signal axis.

Enders (2011) suggests that wave extinction at the surface of a new medium contradicts the Huygens-Fresnel Principle (HFP) which says that the incident wave is absent after excitement of the secondary wave source. We suggest that extinction will be progressive and subject to particle density so both waves will exist during the process. Neither Birefringence nor extinction conflict with the HFP, but neither do they provide additional clarification. Some confusion exists between the axis of polarity and the optical axis. The former relates to Faraday rotation of polarity *around* the optical axis or axial vector, the optical axis giving the apparent source position, normally considered as the 'light path vector' in geometrical optics. In a solid such as calcite the optical axis is considered as a function of the medium particles. In plasma the change in optical axis is considered here as having two components. The first is the normal charge/scattering dispersion delay giving refraction, which is itself still not fully understood. We propose that a second change is kinetic, due to the axis of the arriving signal waves being rotated on re-emission by charge asymmetry due to lateral motion of the particles, or bulk plasma flow during the non zero charge time. This rotation of re-emission due to *asymmetry of charge* is additional to the more fundamental effect arising from the first STR postulate, where the signal is 'carried' by the new medium if in relative motion.

Recent findings from the *SAURON* survey (Davis, 2001) and the ensuing ATLAS^{3D} results (Emsellem, et al. 2011) include spectroscopic red and blue shift derived halo rotation velocities. These findings are consistent with the well known kinetic Sunyaev-Zeldovich (kSZ) effect but are troublesome without invoking refraction of light in 'space', *apparently* contradicting the STR. We find a consistent explanation by including scattering, birefringence and gradual extinction in diffuse media, as found with radio signals (Sukamar 1987). The vacuum itself is considered as a medium, but an exceptionally diffuse medium, implementing change very gradually across exceptional distances measured in kilo-parsecs. Vacuum extinction cannot then be detected in a laboratory, except by using partial vacua. We propose a partially evacuated

chamber at varying density as the basis for further experimentation *[Exp.2]* but more thought is still required. An important experiment is R. Wang's linear 'Sagnac' interferometer (Wang 2006). When using a fully evacuated wave-guide tube, whatever the frame of the emitter, a glass sealing plate or the walls of a tightly wound tube will re-emit the light at c in the frame of the tube. This may explain why propagation in this case remains at c in the wave-guide frame.

3. B&B Accommodation.

There does now seem to be a quantum based solution possible for the outstanding anomalies of the Babcock and Bergman findings. The speed, total thickness and refractive index of the glass and Fresnel drag co-efficient were applied, and no systemic errors were apparent (see Babcock-Bergman 1964). We must first remind ourselves the Fresnel's refractive index 'n' may only be found by experimentation, but is well known for glass, although only approximated by B&B at n~1.5. When determining refractive index, however, it is common to just consider a single piece of glass of a given thickness. This procedure does not allow for surface absorption and emission delays, which are not yet well understood, but which we predict will be found approximately equivalent to the surface losses to transmission of heat. In the case of heat the transmission loss (k value) is an additional ~0.18k 'per surface' in addition to the transmission loss from the glass itself, making a significant contribution to total loss. Two separate glass plates each 0.35cm will then have greater transmission loss than one sheet 0.7cm thick. Experiments with light passing through small apertures have shown transmission delays due to surface oscillator interactions (Dogariu et al. 2001). We suggest an experiment *[Exp.3]* comparing varying numbers of surfaces for a given glass thickness to quantify the effect. We predict that the result will be found to give in the order of the additional 0.01fringe shift which B&B found as the unexplained fringe shift with the two glass plates stationary so with no Fresnel flow.

The question of the absorption and emission processes at the surface is again raised, and we must consider the additional time delay as well as the changes in transmission velocity between the media. Firstly however we must consider the interesting additional anomaly of the low magnitude fringe shift derived solely from the velocity of the glass plates. The relative speed of rotation (allowing

for changing glass vector due to rotation) was an average of ~90 rps. The additional fringe shift change in this case over the static case was ave ~ 0.004 fringes. We suggest a kinetic solution based on the phenomena considered in section 2 above. B&B gave; v(glass) /c = 1.27 x 10^{-7} a very small percentage of the speed of light. We clarify that the refractive index of a medium is a constant irrespective of any relative motion of the medium (representing an inertial frame) and its surroundings. The effect of the n value of glass of ~n = 1.55 will then give a reduction to speed of propagation in the mirror frame of ~1/1.55 = ~200,000 km/sec. This change applies to both the static and rotating case, and will be significantly greater than just the kinetic effect of the moving glass. The latter gives only the 0.004 fringe shift, or ~$1/5^{th}$ of the total static shift including any 'surface transmission' losses.

It is apparent that the 0.004 kinetic shift is slightly higher than might be expected rather than anomalously low. Even a good vacuum on Earth contains a significant particle density, as does the Intra Galactic Medium, but at entirely insignificant densities. B&B reported fringe instability due to air turbulence prior to evacuation, and ran the tests at a medium vacuum of ~0.02 Torr where a significant particle density of ~1.5kPa remains. Particle kinetics will then be likely to have an effect on the result and a lower figure should be achievable in a higher vacuum. Whether or not this is the case we are now able to explain the B&B results. The Kantor result, if found in a significant depth of air circulated by the rotating glass plates, would certainly also be possible if the kinetic shift effect were thus increased by a factor of 7 from ~ 0.04 to ~ 0.29. We have, in any case, now identified three separate but related causes of the speed change of light passing through the glass when observed from the laboratory frame, all apparently consistent with the STR and also giving results consistent with the STR. None of these are fully understood or applied within current science;

1. *Kinetic.* Due to the change in position of the glass during the time taken by the light to pass through it.
2. *Medium.* By c/n due to the thickness and refractive index n of the glass, only found experimentally.
3. *Surface*. Absorption and transmission losses at speed change interfaces, normally included in 2 above.

The first two are the more familiar, though often not properly considered independently. We will theoretically consider the third as it is not normally identified as the independent effect witnessed by the B&B results. First we discuss reverse refraction, a kinetic optical effect also poorly understood, rarely considered and not yet assimilated into theory. We now allow assimilation.

4. Kinetic Reverse Refraction

This well known geometrical optical effect is found experimentally between co-moving media and apparently violates Snell's Law of Refraction (Ko, Chuang 1977, Mackay, Lakhtakia 2006). When observed from an incident frame, light at near normal incidence passing into a co-moving medium appears to be 'dragged' by the medium (Grzegorczyk 2006). However, when observed from the frame of the second medium it is found that the optical axis has actually reversed, and the 'light path' is refracted back towards the normal. When considered in terms of quantum optics this reversal highlights the important fact that the optical axis of light is *rotated* at the interface of a co-moving medium. We are also reminded that 'vectors' within another inertial frame are not 'real' but are an *effect* which is subject to the observer's frame and the rules of 'Proper Time'. Speed and direction are only valid using Proper Time, which is time in the frame of the observer, giving *propagation speed*. '*Co-ordinate time*' only gives '*apparent*' speed. Detecting by direct interaction is a different case to 'observing' via secondary emissions, with different results. A 'Ray' and its 'light path' are then inadequate concepts. For consistency we must consider plane wave propagation and the local 'optical axis' of scattered light. The rotation then informs us as to the mechanism at the medium interface.

Stellar aberration has also remained problematic because the phenomena of kinetic reverse refraction was not known by Lodge in 1893 when interpreting the effects of light entering a spinning glass disc. Observed correctly from the *disc* frame (Lodge wrongly used his Lab to represent the Geocentric frame) the optical axis is rotated *towards* the normal, as found, but now explained using only EM waves and without invoking ballistic photons or ether. A full relativistic theory for aberration then emerges consistent with observation and the empirical diffraction addition currently required for precise predictions. The

troublesome Aberration 'Constant' was abandoned by the IAU in 2000 due to inconsistencies. The US Naval Observatory developed the SAM13 Ionospheric model but have to add refraction empirically to NOVAS algorithms for accurate Astronomical Almanac (AA2010) declination aberration data. USNO circular 179 (Kaplan 2005) admits that *"a consistent relativistic theory of Earth rotation is still some years away."* At 60^{o}-90^{o} zenith the significant corrections 'by hand' to algorithmic predictions are <34 arc minutes (λ ~0.5 microns). We now offer a consistent theoretical solution. Magnetohydrodynamic turbulence and incomplete extinction ensure that a <5% inaccuracy (Heymens et al. 2005) of aberration remains (see Part 8). The atmosphere's rotation within the ***non***-rotating ECI frame is part of the solution, giving turbulence, ducts and 'green flashes' from temperature inversions. An intuitive cause of red shift of evening sunlight emerges 'scattered' from protons and dust receding from the sun and ECI shock frame with planetary rotation. A fluid dynamic coupling effect at the shock, where ions both sides re-emit at the local c, resolves the balance.

In finding consistency with STR's postulates we then imply that the light speed reverts to c with respect to the 'vacuum' on passing from glass to vacuum both by the factor c/n *and* the kinetic factor v of the relative media motion. The latter may logically imply a vacuum inertial frame, or 'ether', so the apparent paradox of the STR is so far unresolved at the quantum level. A possible solution emerges from the medium interface mechanism, consistent with the reference frame by which the speed of a proton bunch through an accelerator vacuum tube is measured. This is considered as the frame of the static electromagnetic (EM) field of the magnets used to accelerate the bunch in the tube. It is also the frame of the static part of the 'virtual electron' cloud which builds in the tube with increasing bunch velocity, consistent with the Unruh effect (Crispino et al 2008). In invoking this effect for 'glass plate' shaped particle bunches moving through vacua we next consider less familiar aspects of Maxwell's equations.

5. Maxwell's Near and Far Field Transition Zone.

The behaviour of EM waves at the near and far field transition zone (TZ) of an emitter has poor and widely varying understandings. Six radio engineers familiar with antenna science, when asked for the equation for the TZ position, might all feel they know the precise answer. Yet each of their answers could be

different. For wavelength λ answers may range from $\lambda/2\pi$ to $5\lambda/2\pi$ or 50D to $2/\lambda$ to $2D^2/\lambda$ where D is the radius of the transmitter (dish, or antenna length). For visible light this (Fraunhofer) transition distance from the surface of a small mass at rest is ~1 micron<1mm. Surface phenomena normally considered unrelated include surface charge, static electricity, fine structure electrons, atomic coupling, plasmons, the outer limit of Fresnel (and inner limit of Fraunhofer) diffraction, and the domain of the laws of geometrical optics. The near field is referred to as the quasi-stationary, 'static', reactive and extinction zone, where "*scattering intensity hot spots*" (and) "*striking differences in the phase functions*" (Quinten 2007) can occur. The TZ, also termed the induction field, is turbulent and dynamic with high plasma energies. HFP has been found valid within it (Depasse et al. 1995) implying extinction. The far field coupling regime at $>10^{-6}$m is also termed the radiative field or radiation zone (Lamothe et al. 2007). At radio frequencies the far field is where stable reception starts.

We need to find a conceptual ontology to derive the observed classical effects before applying the normal mathematical tests, so we first consider logic and phenomenological aspects. We find we must reconsider our limited knowledge of the quantum processes at the zone where light propagation speed increases from ~200,000 to 300,000kps on entering air from glass. Light achieves this *speed change* even before we consider the *additional* 'kinetic' speed change due to relative motion of the media (see part 1). The Dynamic Casimir effect shows electron production at moving surfaces, but then gives c in the *medium* frame not the emitter's supporting the hypothesis of fluid dynamic coupling at the TZ. 'Coherent forward scattering' in plasma is invoked as the key TZ mechanism.

Our knowledge is limited and we still have incomplete understanding of kinetic and refractive index derived speed change processes at nanoscale level. There are obvious practical difficulties in carrying out experiments at fast moving media interfaces, but a number of interesting and incidental effects have been found. We identify some relevant effects and consider their implications. In particular we review knowledge of the population of the near field and transition zones, some strange behaviours and effects on EM waves. We thus briefly consider the Kerr effects, including the surface magneto optic Kerr effect (SMOKE), surface plasmons and the strange world of non-linear optics.

6. Surface Plasmon Resonance (SPR) and SMOKE.

A plasmon is considered as a nanoscale quanta of plasma oscillation, as free electrons on the surface of a solid charged by light (Hecht et al. 1996). SPR is collective oscillation, resonant with the wavelength λ. Plasmons are considered to exist as a 'quasiparticle', at media interfaces (they are most commonly studied at metal and dielectric interfaces). Plasmons interact strongly with light, holding high energies and electric fields at the surface. Plasmons are closely associated with the bizarre effects of 'non linear optics' (NLO) at high light intensities, quantum cavity opto-mechanics and plasma Surface Enhanced Raman Scattering (SERS) (Kneipp 1997). NLO includes many poorly understood phenomena such as the second, third and higher harmonic generation, creating frequencies from twice the original to ~<1000 times greater. X-ray frequencies may be produced from visible light in this way.

Superposition of waves also fails in the domain of NLO, and 'self phase modulation' (SPM) is caused by temporal intensity variations which give temporal variation of the refractive index n. *Spatial* variation of the refractive index also arises from the electric and complex Surface Magneto-Optic Kerr Effect (SMOKE) where the optical and polarisation axes are rotated, which also produces birefringence. As has been pointed out by Qui and Bader (2000) the Kerr effects are far from understood macroscopically or theoretically complete. In the 'DC Kerr' effect the index value n is changed by the square of a changing electric field. The Kerr constant for a medium K may vary between ~10^{-22} and 10^{-14} $m^2/_V{}^2$. Where the electric field strength is E; $\Delta n = \lambda K E^2$. SERS is attributed to Surface Plasmon Resonance but transmission enhancements of >7 as well as suppression have been more specifically shown to be modulated by wave diffraction from 'sub-wavelength surface features' (Lazec, Thio 2004), which would be consistent with a transition zone velocity change. We propose that all these effects may be rationally explained by a better understanding of propagation kinetics. In the AC or Optical Kerr effect the light itself produces the electric field and Δn giving unstable self-focussing/phase modulation. The result is an *intensity dependent refractive index* (IDRI) limited only by high 'multiphoton ionization' or the more familiar *photo-ionisation,* effectively ion production from light energy.

Plasma spatial distribution near surfaces is complex and dynamic. At a density limit of ~10^{20}-10^{22} electrons/cm^3 optical breakdown (OB) mode is reached causing shock waves, explosive heat release and thermal damage. At the lowest thermal energy limit light may be 'frozen' and re-released as demonstrated by Harvard's Hau Lab in Bose-Einstein condensate. With increasing light intensity and 'quantization' into plasmons, the ionization rate and the electric field also increase. It is in this spatial zone that the wavelength dependant and poorly understood dynamic 'non-linear' optical effects found. It is clear that many of these non-linear effects, or violations, are closely equivalent to those of Maxwell's transition zone (TZ) at the Fraunhofer distance including the breakdown of geometric optics, Fresnel Refraction and also of Snell's Law where media co-motion exists. We suggest the same solution applicable to kinetic reverse refraction, which is an observer acceleration to a new frame, recovering c and the laws of geometrical optics in the new frame. TZ positions for emitter diameter D are commonly considered as $2D^2/\lambda$. We must, however, remember that the distance from 'surface' to TZ and from emitting TZ *particles* to the Fresnel limit may prove to differ. As all signal wavelengths dictating Fresnel limits 'exist' at once, then TZ positions will also vary widely.

The STR and B&B result are consistent with the apparently anomalous effect of light reflected from a mirror moving in a vacuum reflecting at c reciprocal to the incident velocity, not c with respect to the mirror. This counter intuitive result was as found by Michelson in his 1913 experiments with rotating mirrors. The effect may now, however, be logically explained via the proposed scattering mechanism. Whether considering a polished metal surface or silvered glass, the TZ would implement the absorption and kinetic change by re-emission. The incident (outer layer) photo-ionised particles are the new reference for the emitted speed c. We suggest that this effect alone is adequately compelling to justify significant experimental falsification.

7. Lateral Motion.

How does relative lateral motion of the media give Kinetic Reverse Refraction? If coupling with particles at rest gives symmetrical charge then we suggest that lateral relative motion results in asymmetry of charge. The change of apparent

'light path' termed KRR can then be more consistently characterised as rotation of the optical axis (apparent source position) when re-emitted, accompanying Faraday rotation of polarity. In the case of an asymmetric charge, a mechanism producing ellipticity and elliptical polarity also emerges. The effect is a small angular deflection of the re-emission axis of light from the 'moving' scattering particle. This optical axis rotation due to charging asymmetry now allows KRR to be assimilated into theory, including as the source of wave based stellar aberration. Faraday rotation of polarity and ellipticity are the natural results (see Fig.1). The role of Huygens construction is confirmed by the self focussing and 'regenerative' quality of a Bessel beam when its 'path' has been blocked.

Unlike the ballistic model, the mechanism invoking optical axis rotation consistently applies to waves, and also preserves the *integrity of the causal wavefront.* The translation effect across the whole refractive plane derives the departure of the optical axis from the wavefront normal. Circular polarity then becomes elliptical. Bi/multirefringence in plasma then naturally emerges from this 'progressive' interaction process. The non-zero interaction time giving rise to the axial rotation was recognised by Max Planck in his 'New radiation hypothesis' (1911). The energy structure of his thesis was not adopted, so the implications of the non-zero charge time were not studied or the consequences analysed. Figure 1 shows some of the effects of a circularly polarised emission or re-emission (or 'a photon') translating downwards via interactions with the

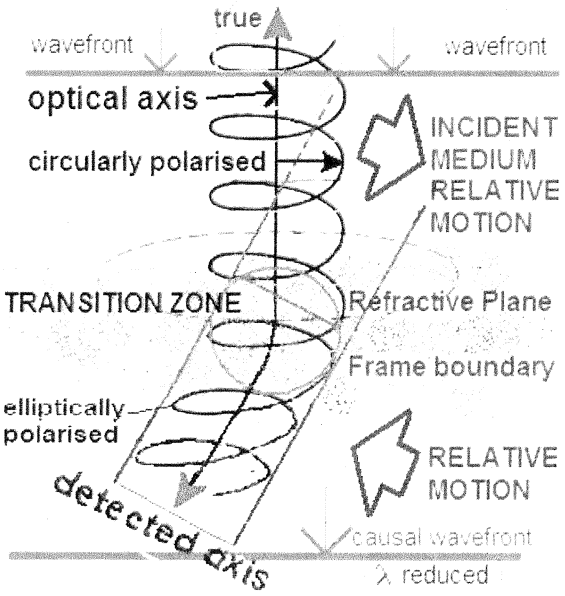

Figure 1. Transition Zone scattering, giving non-linear optics effects at electron shocks. The 'Optical axis' rotates, wavelength changes (due to relative v) and polarity is ellipticised. The causal wavefront is conserved as the optical axis is NOT perpendicular.

particles of the new refractive plane dielectric medium *with lateral media co-motion*. Note the ellipticity, axis change, and conservation of the causal plane.

We suggest that Fresnel refraction may be recovered beyond the Fraunhofer distance and the TZ and in the same way that Snell's Law is recoverable in kinetic reverse refraction. This is by an *observer* acceleration into the new inertial frame, so only when using *Proper Time*. We're also therefore suggesting that non-linear optical effects may then be recovered, which *recovers c and the laws of physics* in the new inertial frame. The quantum mechanism invoked, based on Raman atomic scattering will then be consistent with the postulates of the STR. We also point out that the mechanism is reciprocal so is also fully symmetrical. If this proposed ontological construction of phenomenological relationships is experimentally verified then a *direct causal relation* between quantum mechanisms and Relativity will have been be identified. Altewischer et al. (2002) have already discussed the compatible quantum and macroscopic nature of surface plasmons; "*in the sense that they involve some 10^{10} electrons*" (and) "*because they can act as intermediates in transmitting entangled photons to yield the expected fourth-order interference*". We point out that the mechanisms identified lead to a more consistent kinetic derivation of relativity and classical physics direct from the quantum mechanisms. Figure 2 shows the observed effects from the evolution of interaction through the TZ of a mirror in motion in a medium.

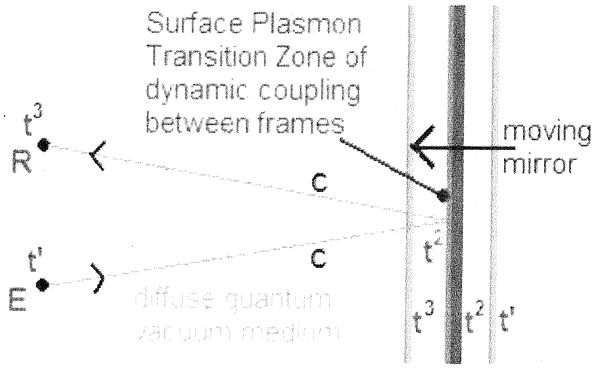

Figure 1: Mirror in motion during crossing of Transition Zone (TZ). Light propagates at c with respect to the 'far field' medium outside the TZ's two-part 'dynamic coupling' region. PJ 2012.

8. Incidental effects

The limited understanding of non-linear optical effects may be improved by the consideration of a change in wave propagation speed consummate with $\Delta\lambda$. Such 'dispersive' effects are of course found in refraction, and we postulate are

modulated at the transition zone (TZ). For instance it is found (Bloembergen 1965 [1977]) that the speed of light in a non-linear medium depends on light *intensity*. We briefly identify other effects which may bear some relation when looked upon from this new perspective. As the intensity of incident light also dictates TZ particle density, then a laser beam might simulate the effects of co-motion between media in a vacuum. Lasers are indeed the normal and an effective means of promoting plasmons. We thus propose an experiment similar to that of B&B in a vacuum *[Exp.4]* but using laser light of varying intensity to find and assess the kinetic effects on activity. The less simple task of moving the emitter and/or the surface plane in the vacuum should allow more to be learned. We predict that electron densities increase along with frequency in proportion to the incident plane velocity in a vacuum, increasing the kinetic optical effects. This may support the notion that the most diffuse vacuum medium, or at least any vacuum containing an em field, may nonetheless be considered a medium, with optical effects ~proportional to particle density.

In considering the optical breakdown limit of electron density we find an analogy with meteors and spacecraft re-entries where the peak plasma density is set well off the surface itself, and also blacks out em transmission. The shock frequencies exceed 10^9cps at >100km altitude (NASA) in the planetary ionosphere, driven by ion collision intensity. The International Standard Plasmasphere-Ionosphere model (SPIM) uses effective altitudes of <20,000km and <1,000km and maximum vertical total electron content (TEC) electron density may be ~ $<40 \times 10^{16} m^{-2}$, with flux in the lower bands peaking at over three times the density at 850 km. (NWRA). The heliosheath is estimated, from *Voyager* and *SOHO* data (Czechowski 2006) at a flux of ~$1.13 \times 10^{14} cm^{-2}$ at the termination shock of the solar winds against the ISM. Pair production from the vacuum field and increased particle density and frequency with velocity are consistent with the propagation of virtual electrons in accelerators, also the kinetic astrophysical effects identified in part 2, and findings of peak propagation at relative velocity peaks in galaxies (Wozniac, 2007, Dobbs, Pringle 2010). The localisation of velocity suggested by Fox from extinction via coupling and scattering emission at local c does have a philosophical kinetic equivalence to the 'local reality' of inertial frames which Einstein described long before space exploration. We explore the ontology of this equivalence and

find Ewald-Oseen Extinction consistent as a concentrated boundary condition effect from Maxwell's equations, which is as found by Dialetis (1978).

9. Magnetohydrodynamics

We invoke particle magnetohydrodynamics at the transmission zone (TZ) which gives a kinetic relationship with the Navier-Stokes fluid dynamic mixing process familiar at the ionospheric bow shocks of planets and stars. The vacuum particle densities at bow shocks are measured at $<10^{14}cm^3$. The particles on the near field side of the zone or shock are in the inertial frames of the moving body, and those photo-ionised at the incident (far field) side are in the incident frame. The severe turbulence arises from the constant hydrodynamic particle mixing process. In atomic scattering Raman (1921) found that electrons in a 'turbid medium' re-emitted light at c with respect to the state of motion (frame) of the local bulk plasma. This seems unsurprising, however, when we consider the greater implications we find that we are then discussing two separate local speeds c, or rather c with respect to two particle scattering surfaces in different states of motion. This change in relative speed is indeed what is found between the Earth centred inertial (ECI) frame and Barycentric frame, it is also consistent with the local cosmic microwave background (CMB) 'frames last scattered', and derives the effects postulated in the STR. Our ontological construction is again consistent, as it is with the finding from laser interferometry (Wise, Chhabildas 1985) that, in dynamic compression, refractive index data can '*exhibit a pronounced deviation*' from all predictions including the Lorentz-Lorentz and Drude relations. Kinetically, in the case of a mirror moving in a vacuum, the light arriving is transformed to c with respect to the mirror, and the light leaving the surface would be transformed back to the c of incident light, all within some $\sim 10^{-6}$m.

The Navier-Stokes hydrodynamic equations cannot be solved to within ~25% so precise maths gives way to small scale uncertainties. The kinetic relationship between each side of the 'collisionless' shock is then closely equivalent to the Fox (1965) view of velocity being localised to c by absorption and re-scattering via extinction and birefringence within the nanoscale shock. Doppler shift then initially arises from the ***real*** quantity of *wavelength* λ, modulating the time based derivation of frequency and conserving the constant $c = f\lambda$.

We must remember that to find any Doppler shift an observer must always ***detect,*** and use a different frame to the emitter. Being in a different frame **contravenes Proper Time rules**, so valid measurement of c and wavelength in the *emitter* frame cannot be made. Crossing the TZ boundary causes emitted wavelengths to contract or dilate, so ***wavelength λ is not co-variant.*** The TZ is then the spatial limit to the local inertial frame. Magnetohydrodynamics and re-emissions then create the boundary of a system's background 'state of motion', which may be termed the physical 'field limits' of the local inertial frame. $\Delta\lambda$ on transform then consistently derives *contraction and dilation of an event period.* What is more, shock ion state is uncountable, yet a 'group' motion is assignable. In this case *uncertainty* is only complexity and ***remains entirely deterministic.*** We suggest that perhaps the most compelling part of this dynamic hypothesis is that neither the component mechanisms or effects are unfalsifiable predictions but are already well known as atomic scattering and the co-variance of light speed. Both have strong experimental support, but the latter, as described in the second postulate of the STR, is as yet unexplained in quantum terms. No algorithmic basis has yet emerged to describe the physical position of a shock or TZ with respect to a massive body or system. We propose that the effects of influencing factors should be explored including, mass, relative motion in a local background, relevant wavelength and dominant em field. Ionospheric limit positions may initially only be established by observation, in an the same way as refractive index n. Spectroscopy and kinetic analysis of astronomical observation will become even more important tools at macroscopic scales. The transformation between inertial frames itself can, however, be described mathematically. The terms below are for an interacting observer, (detector), medium or plasma shock (n = 1) in relative motion v approaching the source.

Wavelength will be; $\lambda_c = \lambda_{c+v} (1 + {}^{v}/_{c})^{-1}$ (1)

or for a receding observer; $\lambda_c = \lambda_{c-v} (1 - {}^{v}/_{c})^{-1}$ (2)

The shifted wavelength is then; $\lambda' = \lambda_O (1 + {}^{v}/_{c})^{-1}$ (3)

The shifted frequency; $f' = f_O (1 + {}^{v}/_{c})$. (4)

Incident wave (not observable), at c is; $\psi = \psi_O \sin 2\pi(f t + {}^{1}/_{\lambda} x)$ (5)

The wave equation remains invariant on transformation in Euclidean space, so the scattered wave is;

$$\psi' = \psi'_O \sin 2\pi(f't' + {}^{1}/_{\lambda'}x') \qquad (6)$$

Observed light speed, observer approaching source;

$$f'\lambda' = \{f(1 + {}^{v}/c)\}\{\lambda(1 + {}^{v}/c)^{-1}\} = f\lambda = c \qquad (7)$$

Observed light speed, observer receding from source;

$$f'\lambda' = \{f(1 - {}^{v}/c)\}\{\lambda(1 - {}^{v}/c)^{-1}\} = f\lambda = c \qquad (8)$$

The constant speed of light for observers in any state of motion interacting with all light signals is thus derived due to the fact that although c is co-variant, neither wavelength λ, or therefore its derivative frequency (f) are co-variant on transformation. The importance of considering observers 'class' and frame is highlighted: An observer *not* changing frame (so measuring indirectly) will *not* find *apparent* co-variant c as he is *not* then interacting with the original emission, but *will* find derivative f co-variant, so no Doppler shift.

10. Dynamic and Kinetic Logic

In the case of the B&B moving glass surface, the two kinetic systems of electrons mixed at the TZ would represent the inertial frames of the glass and of the quantum vacuum. If the velocity change is indeed at the TZ then a logical explanation exists for the change from the laws of geometrical optics to the unexplained non-linear effects and from Fresnel to Fraunhofer refraction at that zone. The same mechanism then resolves our central problem, namely the acceleration of the light leaving the glass plate to c with respect to the vacuum. The 'kinetic frame' of the vacuum emissions appears able to be defined by the incident light speed itself because photo-ionised electron flux in that frame increases with intensity and λ decreases with increased incident velocity, thereby increasing frequency. The speed differential between the outer electron layer and the arriving light would need to be precisely c for any reciprocal emissions into the vacuum to also be at c. The *relative electron velocity across the TZ* would then be the co-variant frame speed v. The photoelectric effect on the outer electrons also emerges as incident photon and electron energy

correlate. If one medium n value is above unity, normal non-kinetic refractive effects (2 and 3 in Part 3) may be implemented independently of the TZ.

We apply the modality principles of propositional dynamic logic (PDL) developed for computing but with broader relevance. At a quantum level (Baltag, Smets 2010) systems may be 'interleaved' but are kinetically separated. An acceleration is therefore required between leaves. We find this discrete 'planar' approach analogous to Einstein's concept of Cartesian co-ordinates as 'planes' *"rigidly attached"* to bodies. Motion is an invalid concept in geometry, and so limits or boundaries between geometries are implied, where one space time geometry is not valid in a different geometry. We suggest that Cartesian co-ordinates must then exist as 3D interleaved or 'nested' kinetic planes or bodies which do not co-exist spatially. If Einstein's smaller space s moves within S, it becomes bounded. The fundamental structure of truth function logic (TFL) is that a compound proposition may be part of another compound proposition, which may be part of another compound proposition ad infinitum. This precise nested hierarchical structure emerges, simply substituting kinetic states (frames) for propositions, showing the logical consistency of the model. The ontology implies that the similar spatial positions of Earth's shock and the *limits* of Earth's non rotating frame are **not** co-incidental. We propose a detailed analysis and possibly another experiment *[Exp.5]* involving orbiter or probe telemetry to investigate the relationship between the non-linear effects found in the region of the TZ and the effects of our planetary bow shock.

Invoking kinetic logic, and postulating that all detector lenses are equivalent to new media, we find that an approaching signal of any wavelength cannot hold any information as to the existence or motion of the ***new*** field or medium ***prior to interaction***. Logic then dictates that if signal velocity is altered **after** the initial interaction, then any quantum process involved would occur ***at*** that initial interaction point. Science may have assumed that a quantum mechanism is not needed, but Einstein was searching for just such mechanism to unify QM with the STR. The importance of direct ***interaction*** of observer with observed is confirmed, and consistent with ***the observer as part of*** the system. The proposed TZ mechanism may then also be considered as providing the Lorentz transformation (LT) by producing co-variance to the limit of gamma at OB

electron density. The LT curve profile may prove to require a slight adjustment to align more closely with the 'input' power curve of LHC acceleration and the synchrotronic emission frequency curve approaching c. The Unruh effect (Crispino et al. 2008) would give similar photoelectrons, from speed not its Δ.

11. Michelson-Gale-Pearson (1925) Falsification.

Our hypothesis is kinetically similar to the Fresnel/Stokes/Heaviside 'dragged ether' theory, but with *particle interactions* modulating c. Planck dismissed the doubts Lorentz expressed about 'varying ether density' but the logical basis of Stokes thesis was unfalsified when the conception was forgotten with the rise of the STR. The suggestion of experimental falsification of 'ether drag' only really came with the Michelson-Gale-Pearson experiment (1924) with a 1.9km perimeter fixed mirror interferometer in a low vacuum. The result contradicted the original Michelson Morley 1887 (M&M) 'null' result, and was reported as fringe shifts due to ether flow with respect to the Earth's rotation in; "***stationary ether*** *as well as* ***in accordance with relativity.***"! The mixing of ether and the SRT was highly problematic. The interpretation that 'ether drag' was 'disproved' is also logically inconsistent. The assumed basis of consistency with relativity is that rotation is a special case in the STR. The explanation of rotation within a 'fixed ether' refers to a fixed Earth centred local inertial (ECI) coordinate system, a concept similar to the surface ECRF but non rotating. The ECI frame then represents a 'dragged ether' frame. As the Earth's ionospheric shock does not rotate with the planet yet the atmosphere does, that ECI frame is consistent with our re-emission model at and beyond a planetary scale. The ECI is also the frame used by GPS, and both this frame and the ionosphere are 'at rest' only locally with Earth as we orbit the sun. Similarly the barycentric (Solar system) frame which each planet moves through is only at rest with respect to our own sun, extending only to the heliospheric bow shock and heliosheath at ~100 AU's. The group 'galactic arm' state of motion (frame) then applies. But where extinction distance is greater than shock thickness we will still find birefringence, scintillation and the non-zero results of Michelson, also those consistently reported by Dayton Miller always found greater at higher altitudes.

The arrangement of inertial frames in relative motion which emerges is precisely equivalent to Minkowski (1908) and Einstein's (1952) conception of;

"endlessly many spaces in motion relatively." Their boundary is kinetic, or a 'change of assignable state of motion', and physically implemented by coupling and scattering in the diffuse medium in the same way that two moving bodies of water particles will always change light speed to the *local* c/n of the water. The kinetic interface of the moving bodies of water particles is analogous to local CMB scattering surfaces, explaining the CMB anisotropic velocities of various systems, and the frames last scattered of Scott & Smoot (2004). The process may be seen as '*continuous spontaneous localisation*' of c giving CSL.

Despite the above logical consistency, however, if the reported fringe shifts of the MGP experiment did occur due to Earth's rotation in an ether frame, then our local scattering basis may still be falsified at an atomic scale unless ether is invoked. This is because the mirrors are at rest in the incident frame, so light scattered at the surface of the mirror after reflection would then travel at c with respect to the mirror. A problem then exists. LIGO long baseline interferometry has not confirmed the 1924 MGP findings, and GPS one-way measurement (four orders more sensitive than the MGP experiment) also gives null ether flow results in the ECI system. We identify some possible systemic errors in the MGP experiment which may have caused the apparently anomalous result. Any asymmetry in a reciprocating beam system will produce a fringe shift. For instance any differences in the ***number*** of TZ shock crossings, surface encounters (of two TZ crossings each), reflections, passages through glass, or changes of media will affect the overall, so the relative, propagation time, so change the phase, negating the result.

The MGP set-up contained at least one of the above asymmetries, but the mirror construction is not described apart from being lightly (50% reflection) or heavily silvered (or gold). We cannot then identify the actual asymmetry present but the configuration cannot avoid at least one. The diagrammatic set up (MGP Fig.1) indicates four passages through mirror glass in each case, but also partly with 'incident surface' reflection and partly silvered back surface reflection (mirror A). If the diagram is correct in terms of reflective surface detail, the (delayed) counter clockwise beam has **eight** *changes* of medium (two each at *A,C,B* and *A*) and the clockwise beam only **six**, explaining it's earlier arrival. Reflection can polarise light and causes polarisation mode

dispersion (PMD) propagation delays. If we then consider just shock crossings and reflections, the counter clockwise beam has one *additional* internal reflection (absorption and re-emission) requiring to be negotiated at mirror A.

If MGP's Fig. 1 simple 'surface' reflection was purely diagrammatic and more conventional back silvered mirrors were actually used, then subject to the set up of mirror *A* the counter clockwise beam may have encountered up to two additional glass transits. It is even conceivable that because some asymmetries are repeated in the shorter 'datum' path the fringes may have been misidentified on the initial *'correction'* of the *'apparent displacement,'* and the shift between each long and short path measured, although this might seem quite unlikely. The reason for the contradiction with the M&M null result is not discussed, but no other experiment has repeated the MGP finding. Our model is consistent with the M&M result and logical analysis by Christov (2006). If all systemic errors in the MGP experiment were eliminated, then ether would be required for our atomic scattering model, but otherwise the ontological foundation of our model is consistent with or without any 'sub-particle' medium.

12. Ontological Construction

We now propose and logically establish that there are ***two*** theoretical cases of observation and measurement of light speed which are allowed to give different results. We will term the first case *'direct'*; via the evidence of wavelength λ of directly received light, calculated from frequency f and assumed velocity using the constant $c = f \lambda$ and energy conservation law $e = f \lambda$. We term the second case, *'indirect'*; via the evidence of light scattered from particles of a medium *charged by* the original pulse. Our proposed experiment [1] considers the medium as diffuse plasma in a cloud chamber. An observer ***at rest*** with the chamber may record a propagation speed c. But if he then passes by in a frame accelerated to v and records the apparent speed he may of course find ***apparent*** $c + v$, (or c - v) *because the rules of Proper Time do not then apply.* If he is 'at rest' and the chamber passes by him, the result is the same. This is clearly because the light then observed is *only the light,* ***scattered*** *by the particles.* This light of course travels, locally, at c, but interpretation up to now has been that the original signal must violate the STR even if we measure *apparent* c + v!

Current mainstream interpretation commonly assumed that the 'light speed' derived from this scattering information cannot apparently exceed c from any observer frame. ***This assumption is incorrect*** and, we suggest is the cause of much confusion and questioning of the logic of the STR. We can only actually observe ***indirect*** light or em energy via atomic scattering however diffuse the medium particles. By definition then even the quantum vacuum is equivalent to a medium. *Apparent* c + v is then allowable in the case of *secondary* detection of *indirect* emissions but actual c remains constant ***within*** any frame and co-variant *between* frames, exposing the true intuitive logic of the STR postulates.

The concept of 'apparent' c+v turns out to be merely a re-interpretation of space-time consistent with the comment that; "*...cases with a velocity greater than that of light will henceforth play only some such part as that of figures with imaginary co-ordinates in geometry.*" (H. Minkowski 1908). We now consider a Minkowski space time 'event' (constituting any non-zero 'period' of time), negotiating a TZ. We find that the period of the event in the emitter frame is *changed* by the re-scattering mechanism at the TZ. The change in apparent 'period length' is entirely due to the wavelength change but co-variant propagation velocity c is derived. The apparent length of events will then not be co-variant but will be contracted or extended subject to v. Identical clocks will then run at the *same speed in all frames* but, quite intuitively, clocks in relative motion to any observer will simply appear to him to run at different speeds. A clock approaching an observer at 0.1c will then simply appear to run 10 per cent faster. Both SR and QM then use the same absolute time, but time period evidence, once emitted, does not commute between frames.

Photo-ionisation already tells us that incident light itself can produce the ions, and at rates subject to relative 'arrival' velocity so no 'ether' needs to be invoked for the process of light re-emission. This removes the apparent inconsistency of the concept of CMB 'frames last scattered' (Scott, Smoot 2004) with the SR postulates. The varying CMB anisotropic flows found are real, with real ion shock 'scattering surface' boundaries between them. The quantum vacuum and interstellar medium are endowed by this 'discrete fields' model (DFM) with the qualities of a very diffuse medium, condensing to a local modulating plasma medium with any motion of mass within it. Local dynamic background inertial

frames result, with speed always limited only by the local background defined by arriving light speed. A scale invariant process implies that infinitely many such 'nested' states of motion would exist. The speed of Earth would then bear no direct relationship to the speed of a distant star, because Proper Time ***does not apply***. Logical equivalence is found with the Minkowski (1908) and Einstein (1952) conception of; *"endlessly many spaces in motion relatively."* The fine structure constant of $1/137^{th}$ may perhaps also be considered as a TZ 'ground state', at rest. The proposed experiment under varying laser light intensities and in a dynamic mode would falsify this suggestion with regard to kinetic variation. An additional laser experiment is proposed where a secondary signal beam is harmonically merged with and carried by an intense principal beam *[Exp.6]*. Signal arrival times are predicted to vary at certain harmonics, somewhat similar to the effects termed quantum tunnelling, and the apparent superluminal pulses in quasar jets such as those of M87.

13. Theoretical constraints

We have found that all 'Proper' speed is **propagation speed.** Solutions based on deterministic Local Reality have been constrained by Bell's, Haag's and Currie-Jordan-Sudarshan (CJS) theorems. Haag disallowed any field theory requiring 'invariance'. As λ is indeed not 'co-variant' on transformation between frames the terms are met. CJS states that two relative frames cannot interact or exchange energy for the LT to be used. But the LT does not apply to the '*direct*' case of observation involving interaction. At relativistic velocities plasma density becomes critical and the optical breakdown limit discussed above is reached. In the *indirect* case 'proper time' *does not apply* so apparent c+v is allowed. Bell's theorem similarly is not valid in the case of a Local Reality contextual to *detectors* in proper time and with no other variables. In this locally deterministic case analogies with virial 'inertial systems' and 'quantum mixing' may also apply ('t Hooft 2009). The field based ontology invoked in the cycle then avoids the previous constraints on Local Reality in the unified field solution as sought by Einstein. The function of the hyperbole of 'rapidity' in constraining apparent c+v is no longer required, so it's additive qualities can be returned as the '*imaginary*' c+v of Minkowski. 'Rapidity' may then become a more useful word, to distinguish real local ('proper') propagation velocity (<c) from apparent 'velocities' derived only via sequential scattering evidence.

14. Conclusions

We have found and described a consistent resolution to the B&B anomalies via an ontological construction of known quantum mechanisms and in accordance with the postulates of Einstein's Special Theory of Relativity. We have also, however, shown that the conflicting result of Kantor's experiment may have been due to the air flow along the beam paths caused by the rotating plates. We find similarity with Fox's (1965) localisation of c via extinction, and *apparently* successful refutations of that thesis for vacua, including by Brecher (1977). We have further theoretically investigated mechanisms at the emitter surface, more consistently explaining Maxwell's near field transition zone, plasmons and non-linear optics. We refer to apparently anomalous and related astrophysical findings, and also identify and discuss a connection with the kinetic reverse refraction effect of geometrical optics, equivalent to the breakdown of linear optics and Fresnel refraction at the Fraunhofer distance. The rotation of optical axis giving refraction alongside Faraday rotation of polarity is found to derive elliptical polarity and stellar aberration while conserving causal wavefronts by showing the optical axis is ***not*** tied to the wavefront normal (as Calcite crystals reveal). This significant stellar aberration component is as added by hand by the US Naval Observatory to get the accurate predictions of the AA2010 data. The missing underlying relativistic theoretical basis for kinetic refraction in frame transition is identified in the ontology as arising from charge asymmetry.

We propose a possible new set of consistent kinetic relationships and quantum mechanisms arising from photo-ionization, Raman scattering, extinction and many other familiar phenomena at the refractive plane of co-moving media. Previously assumed interpretations of classical theories are falsified with the application of the modality of propositional dynamic logic as developed for computing. We find the conceptual 'interleaved' basis of modal logic applies perfectly to Einstein's and Minkowski's conceptions. Cartesian co-ordinate systems as within space-time geometries are not required to move, but each geometric system itself may move and has a discrete domain limited by acceleration. Speed is only then relevant to the local background, yet is set by atomic scattering from matter, constantly modulating light propagation at the near field limit. Two distinct 'speed change' components are then identified; the

first caused by refractive index n from interaction time, the second kinetic caused by the relative motion of the re-emitting particle compared to the previous emitter. Both contribute to wavelength change so also derived Doppler shift of observed frequency. The effects of lateral motion are aberration and birefringence found as rotation of re-emitted optical axis due to the asymmetry of charge the motion brings, giving the kinetic reverse refraction.

We have identified that constraints such as Bells inequality, CJS and Haag's theorem are overcome in our proposed ontology by the 'detection' change $\Delta\lambda$. We have discussed the 1924 Michelson-Gale-Pearson (MGP) interferometer experiment, which conflicts with the 1887 M&M null result, and has not been confirmed. The MGP result is the only cited falsification of the 'ether drag' theory, kinetically similar to our discrete field model. We have logically analysed the MGP experiment and shown how the result would be consistent with the non-rotating ECI frame, but not with an 'ether flow' caused by our orbital path. In this case the result, though proving little, does not disprove our ontology of kinetic 'nesting'. We do however also find and explain a systemic error in the MGP experiment which Michelson would not have known of in 1924. There is an asymmetry of paths, with the anticlockwise path undergoing either an additional reflection or two additional glass transits (subject to mirror configuration). Either would give a fringe shift and confuse main and 'control' beam fringe identification. We have also shown the logical equivalence with GPS, and with CMB anisotropy, where the concept of CMB 'frames last scattered' is confirmed as consistent with the STR postulates. The domain boundaries and the mechanism are identified, with scattering across the full complex plasma frequency range giving continuous spontaneous localisation (= CSL). Modelling may best use 3D Lagrangian Coherent Structures.

Intriguing possibilities arise from the relationship of the quantum mechanisms discussed and resultant effects consistent with the postulates of the STR. All inconsistencies of SR and QM evaporate. We identify and propose possible experiments to falsify the theory (see below). We find that using the quantum mechanisms invoked, the wave equation is co-variant on transformation, but wave-length lambda is not. Two ***classes*** of observer frame are identified and the different results are found as critical. Speed may be *real* (direct interaction) or

apparent (indirect observation). For secondary scattering detections from motion in *another frame* the Proper Time rules do not apply, and the *apparent* delta c and *apparent* c + v are allowed, balanced by *apparent* d/dt and delta f to maintain the constant; $c = f'\lambda$. The Laws of conservation are thus satisfied.

Suggested Experiments;

[Exp.1] Plasma chamber interferometer and re-emitter delta v, to compare optical axis path arrival times. p2.

[Exp.2] A partially evacuated chamber at varying densities to compare n, extinction and birefringence. p2.

[Exp.3] Varying surface transitions for a given glass thickness. We predict the B&B. +0.01 fringe shift. p3.

[Exp.4] B&B vacuum chamber with varying intensity lasers to quantify the kinetic effects on TZ activity. p6.

[Exp.5] Orbiter or probe telemetry to allow analysis of our planetary bow shock for non-linear TZ effects. p8.

References.

Altewischer, E., van Exter, M. P., Woerdman, J. P., 2002. Plasmon-assisted transmission of entangled photons Nature Vol 418,. http://www.molphys.leidenuniv.nl/~exter/articles/nature.pdf

Babcock, G. C.; Bergman, T. G. 1964, "Determination of the Constancy of the Speed of Light", *Journal of the Optical Society of America* 54 (2): 147–150, doi:10.1364/JOSA.54.000147

Baltag A, Smets S. 2010. Quantum Logic as Dynamic Logic. Synthese 179 (2) p. 285-306. http://www.springerlink.com/index/10.1007/s11229-010-9783-6

Bloembergen, N., 1977 (1965) Nonlinear optics. Reading, MA: W.A. Benjamin, Inc., . p229

Brecher, K., 1977. Is the velocity of light independent of the velocity of the source? PRL v39 No.17. http://www.ekkehard-friebe.de/Brecher-K-1977.pdf

Crispino, L. C. B., Higuchi, A., Matsas, G. E. A., Review; "The Unruh effect and its applications," Rev. Mod. Phys. 80, 787-839 (2008).

Czechowski, A., et al., 2006.Estimating the Thickness of the Heliosheath from CELIAS/HSTOF and Voyager 1 Data. AJ., 647:L69-L72, http://iopscience.iop.org/1538-4357/647/1/L69/fulltext/20240.text.html

Davis, R. L. et al. 2001. ApJ 584 L33, SAURON at NGC 4365

Depasse, F. Paesler, M.A. Courjon, D. Vigoureux, J.M. 1995. Huygens-Fresnel principle in the near field. Optics Letters, Vol. 20, Issue 3, pp. 234-236 doi:10.1364/OL.20.000234 http://www.opticsinfobase.org/ol/abstract.cfm?URI=ol-20-3-234

Dialetis, D., 1978. Equivalence of the Ewald-Oseen extinction theorem as a nonlocal boundary-value problem with Maxwells equations and boundary conditions. J. Opt. Soc. Am. 68, 602-610 http://www.opticsinfobase.org/josa/abstract.cfm?uri=josa-68-5-602

Dobbs, C.L. Pringle, J.E. MNRAS 409, 396–404 (2010) and; Dobbs et al. MNRAS 403, 625-645 2010.

Dogariu, A et al., 2001 Delay in light transmission through small apertures. Optics Letters, Vol. 26, Issue 7, pp. 450-452 http://www.opticsinfobase.org/ol/abstract.cfm?uri=ol-26-7-450

Einstein, A. 1952. Relativity. Notes to the 15th edition, (5th Appendix). (English Translation 1954).

Emsellem, E., et al., 2011. Atlas 3D. MNRAS 414 2. 888-912. June,

Enders, P., 2011. The Ewald-Oseen Extinction Theorem in the Light of Huygens' Principle. EJTP 8, 25 127–136.

Fox, J.G., 1965. Evidence against Emission Theories. American Journal of Physics, Volume 33, No. 1. http://adsabs.harvard.edu/abs/1965AmJPh..33....1F

Grzegorczyk, T., M., Kong, J. A., 2006. Electrodynamics of moving media inducing positive and negative refraction. Phys. Rev. B 74, 033102 URL:http://link.aps.org/doi/10.1103/PhysRevB.74.033102

DOI: 10.1103/PhysRevB.74.033102

Hecht, B., Bielefeldt, H., Novotny, L., Inouye, Y., Pohl, D.W., 1996. Local excitation, scattering, and interference of surface plasmons. Phys. Rev. Lett. 77, 1889–1892

Heymens, C., et al, 2005. MNRAS 361.160.

Kaplan, H.G., 2005. The IAU Resolutions on Astronomical Reference Systems, Time Scales, and Earth Rotation Models. USNO. Circ. No. 179. http://aa.usno.navy.mil/publications/docs/Circular_179.pdf

Kantor, W. (Sept. 1962). "Direct First-Order Experiment on the Propagation of Light from a Moving Source," J. Opt. Soc. Am. Vol. 52, No. 8, p. 978.

Kantor, W., 1971. Speed of Gamma Rays Emitted by High Speed Particles. Spectroscopy Letters: An International Journal for Rapid Communication. Volume 4, Issue 7,

Kneipp, K., et al., 1997. Single Molecule Detection Using Surface-Enhanced Raman Scattering. PRL v78. No.9.

Ko, H. C., and C. W. Chuang (1977), On the energy flux and Poynting vector in a moving dispersive dielectric, R Sci., 12(2), 337-340.

Lamothe, É., et al. 2007. Optical forces in coupled plasmonic nanosystems: Near field and far field interaction regimes. NML. http://nam.epfl.ch/pdfs/080.pdf

Lezec. H., Tineke Thio,. 2004. Optics Express, Vol. 12, Issue 16, pp. 3629-3651 http://dx.doi.org/10.1364/OPEX.12.003629

Mackay, T G. Lakhtakia A. 2006. Counterposition and negative refraction due to uniform motion. http://arxiv.org/abs/physics/0610039v1

Michelson, A., Gale, H., Pearson, F., 1925 The Effect of the Earth's Rotation on the Velocity of Light. ApJ 61 140.http://adsabs.harvard.edu/full/1925ApJ....61..140M

Minkowski, H. 'Space and Time'. 1908. Cologne Address. *Jahresberichte der Deutschen Mathematiker-Vereinigung*: 75–88. (Trans. 1920 Space and Time)

Planck, M., 1911. New Radiation Hypothesis. Verh. d. D. Phys. Oes., 13, 138-148; II, 249-259

Quinten, M., 2007 Local fields close to the surface of nanoparticles and aggregates of nanoparticles. APB: Lasers and Optics Vol .73, No. 3, 245-255, DOI: 10.1007/s003400100650 http://www.springerlink.com/content/fhap58g5d0gl8d3m/

Qui, Z.C., Bader S.D., 2000. Surface magneto-optic Kerr effect. Rev. Sci. Instrum. *71*, 1243 *doi:10.1063/1.1150496*

Raman Chandrasekhara. 1922. 'Molecular Diffraction of Light'. (1930 Nobel Prize winning paper).

Scott, D. Smoot, G.F., 2004. (for) 'The Review of Particle Physics', S. Eidelman et al., Phys.Lett., B.592, 1

Cosmic Microwave Background Mini-Review. http://arxiv.org/pdf/astro-ph/0601307v1.pdf

Sukumar, S. 1987. Ionospheric Refraction Effects on Radio Interferometer Phase. J. Astrophys. Astr. 8, 281–294 http://www.ias.ac.in/jarch/jaa/8/281-294.pdf

Tolman, R., 1910 (1912). The Second Postulate of Relativity. Phys. Rev. 31, 26 ibid. 35, 136.

Wang, R. Zeng, A, Yao, A., Langley, D., 2006. Modified Sagnac experiment for measuring travel-time difference between counter-propagating light beams in a uniformly moving fiber. http://cdsweb.cern.ch/record/986047

Wise, J. L., Chhabildas, L. C., APS Conf. Washington. Shock waves in condensed matter, 1985.

Wozniak, H., Michel-Dansac, L., EAS 2007a 24; pp51-56. 2007b Wozniac, H., A&A letters. http://arxiv.org/abs/astro-ph/0701687

THE COSMOLOGICAL IMPLICATIONS OF NONLOCAL GRAVITY

Peter Rowlands
Department of Physics
University of Liverpool
Oliver Lodge Laboratory, Oxford Street
Liverpool, L69 7ZE, UK
p.rowlands@liverpool.ac.uk

Received 1-20-2013

Abstract

Here, we present a review of the possible impact of a theory of nonlocal gravity, proposed by the author,[1] on some aspects of cosmology. The maximal failure of the quantum prediction of the 'cosmological constant' creates difficulties for a quantum theory of gravity, and for gravity as a local force. The attractive nature of the gravitational force and the negative sign of its energy may be indications that it is intrinsically nonlocal and not limited to speed of light transfer. A new set of equations are needed to reconcile the effects with those observed under local measuring conditions. The cosmological redshift, microwave background radiation and arrow of time now become purely physical phenomena suggesting a totally different cosmology from the one currently generally accepted. The 'cosmological constant', as a consequence, was predicted by this method long before it was experimentally discovered. The calculations also provide values for astronomical constants and predictions in particle physics such as the masses of the lightest neutrinos. Cosmology becomes a result of fundamental physical laws and not a merely historical record of arbitrary events that just happened to take place in some inexplicable sequence.

Keywords: Nonlocal gravity, cosmological constant, redshift, microwave background radiation, nilpotent quantum mechanics, holographic principle

Copyright © 2012 by Hadronic Press Inc., Palm Harbor, FL 34682–1577, USA

1 Introduction

Current theories of cosmology have many problematic features. One is that they have developed a culture in which it is considered acceptable to build assumption on assumption as problems arise. Speculation may be considered a necessary evil where solid evidence is lacking, but cosmologists have given their speculations a status as 'mainstream' science which automatically excludes more productive approaches. Also, many of the claims made for matches between theory and experiment are highly suspect and in some cases definitely falsified. However, in my opinion, the worst aspect of cosmology is that it is used as a substitute for physics. Purely physical phenomena such as cosmological redshift, microwave background radiation and the arrow of time are given *ad hoc* cosmological explanations without any attempt to understand them in terms of more general physical principles. The cosmology is 'archaeology', a description of what just happened to take place at different times, rather than physics, or a fundamental explanation of physical phenomena in terms of physical laws. The standard approach to general relativity is part of the problem. The use of the general relativistic field equations to derive a small number of weak field effects has been extended to justify the whole of the physical interpretation that has traditionally been associated with the theory. A key assumption is the belief that gravity is a local interaction like the weak, strong and electromagnetic interactions of particle physics, and that a quantum version of gravity will eventually be found.

In fact, no one could claim quantum gravity has been a success. The most obvious problem is that of nonrenormalizable infinities. Also general relativity and quantum theory cannot be reconciled on the subject of time, which is a classical fourth dimension of space in general relativity but a nonobservable in quantum theory. There is a stupendous mismatch between theory and experiment concerning a quantum gravitational cosmological constant. There is also a failure of quantum gravity to preserve the locality conditions on which it is predicated.

The last two actually give us a clue on how to proceed. First of all, we consider the maximal failure of the quantum prediction of the 'cosmological

constant'. Estimates of the vacuum density required for quantum gravity suggest that there must be one particle in every Compton volume or Compton radius cubed. If we use the Planck mass and the reduced Compton radius, then the vacuum density must be of order

$$m_P^4 c^3 / \hbar^3 = (\hbar c / G)^2 c^3 / \hbar^3 = c^5 / \hbar G^2 = 5.16 \times 10^{96} \text{ kgm}^{-3}.$$

Experimental evidence from supernovae, however, tells us that the measured vacuum density is of order is 0.7×10^{-26} kgm^{-3}, leaving us out from our estimates by a factor 7.37×10^{122}, and even using the non-reduced Compton radius, and geometric factors, would not reduce this number by more than two or three orders of magnitude. Now, using the holographic principle, and considering quantum events as bits of information, Seth Lloyd [2,3] has calculated that the number of 'bit flipping' events that can take place in a 4-D space-time determined by the Hubble event horizon, that is within our universe and within its lifetime as understood in standard cosmology, is of order 10^{123}. If each possible quantum gravity event is a bit-flipping, then our estimate of the vacuum density of space which would make this as wrong as it could possibly be. Such an indicator has to be telling us that one of our starting assumptions is profoundly wrong – 'not even wrong'. This is not a problem, it is a massive opportunity. It requires us to rethink the way we look at locality and nonlocality, and gravity and inertia.

2 The aberration of space

The received wisdom is that gravity is a local force transmitted at c, very likely a quantum force of the same kind as the other three fundamental interactions, and that such time-delayed transmission is a necessary requirement for deriving the equations of general relativity that predict gravitational redshift, light bending, time delay and relativistic perihelion precession. Are these assumptions – based on supposition, rather than evidence – actually correct? Is gravity really 'local'?

Here we come against a significant fact that quantum gravity actually fails to preserve locality. Gravity cannot actually be local (in the general relativistic sense) and quantum. Black holes, as understood in general relativity, are a specific result of assuming locality applies to gravity. Now, according to the rules of locality, the maximum entropy within any space is determined by the

volume of the space, the total entropy being the sum of the entropies of any partitioning within it. In the case of a black hole, however, the maximum entropy, considered in quantum terms, is determined by the area of the event horizon. Quantum gravity is to all appearances irreconcilable with a strict understanding of locality, even though it is necessarily a local theory.

There are several things that are unusual about gravity compared to known local forces: it is universal; we never detect it directly, only through an inertial reaction; in general relativity it is not treated as a force at all; it is incredibly weak; it involves negative energy (attractive force) for identical particles; and its quantum, if it exists, must be spin 2 rather than spin 1. Gravity's incredible weakness makes it possible to derive large dimensionless parameters connecting cosmic and particle events, as observed by authors such as Eddington and Dirac.[4-7] The ratio between the strengths of the gravitational and other forces is very largely the same as the ratios between cosmic and particle times and distances.

Gravity's relative weakness is a considerable problem if it is considered to be a local force, but not if it is really nonlocal. Various indicators suggest that we should expect to find nonlocality at the foundational level. Quantum mechanics demands a mechanism for nonlocal correlation, which is not at present met by any known phenomenon. Nilpotent quantum mechanics requires a duality between local (fermion) and nonlocal (vacuum / rest of the universe), which gravity seems designed to meet.

The duality also makes sense in terms of gauge theory / gravity correspondence, which the nilpotent theory demands as much as string theory. In the nilpotent theory, the sum total of everything in the universe is zero. The 'gravitational vacuum' acts as a conjugate dual to the combined effect of all the other forces, thus providing the gravity-gauge theory correspondence. This is why its energy is negative. It has the same effect as the filled vacuum in the Higgs mechanism, and similarly leads to the 'creation' of inertial mass.

Perhaps even more significantly, mass / energy (the source of gravity) is fundamentally of a continuous nature, as opposed to the discrete and even point-like particle sources of electric, strong and weak interactions. We have the Higgs field, zero point energy, the cosmic microwave background radiation, even ordinary fields, providing a continuous energy source throughout space, suggesting that there is no need for finite time transmission, as all points are immediately connected. In fact, the Higgs field at least implies

that the amount of energy is identical at every point, while the continuity of the distribution is closely connected with the irreversibility of time, as manifested in the second law of thermodynamics.

A continuous mass-energy would appear to require a continuous, and therefore instantaneous, nonlocal type of interaction between elements of energy, rather than a time-delayed local one involving the constant known as velocity of light (c). The equations for the static gravitational interaction have no time or c-related component, and the $U(1)$ symmetry is insensitive to the velocity of transmission.

But how can we observe anything other than discrete observations between discrete objects using discrete interactions? If we imagine gravity as acting irrespective of our observations, we have no space-time structure from observational physics which we can automatically use to describe it. A Lorentzian space-time structure cannot be used for an instantaneous interaction. There is, therefore, an incompatibility between the space-time structure of our observations and the space-time structure we require to set up our gravitational equations. However, this is not uncommon in physics and there is a well-known solution. Newtonian mechanics, for example, requires inertial frames of reference, but there is no such thing as a truly inertial frame.

We get around this by imagining the frame is inertial, and then finding that 'fictitious' effects result from our incorrect assumption. On the rotating Earth, the fictitious effects take the form of two inertial forces: a centrifugal force (mv^2 / r) and a Coriolis force ($2m\boldsymbol{\omega} \times \mathbf{v}$). Suppose that exactly the same thing happens if we apply a Lorentzian space-time to a system subject to nonlocal gravitation.

From a Newtonian point of view, the Lorentzian space-time frame will be non-inertial, and Newton's laws will not apply. Any local coordinate system will have a local rotation from the non-local Euclidean one, exactly as is observed when a light ray passes through a strong gravitational field. The geodesics of such a system will be exactly those of such light rays, and will define the coordinate rotation. The effect is what we might describe as an 'aberration of space' or an 'aberration of space-time'.

So we have a light ray geodesic:

$$\left(\frac{dr}{dt}\right)^2 + r^2\left(\frac{d\phi}{dt}\right)^2 = 0$$

to compare with a light ray geodesic with coordinate rotation:

$$\left(\frac{dr}{dt}\right)^2 + \left(1 - \frac{2GM}{rc^2}\right) r^2 \left(\frac{d\phi}{dt}\right)^2 = 0 .$$

At the same time a system with dynamic energy might be specified by:

$$\left(\frac{dr}{dt}\right)^2 + \left(\frac{d\phi}{dt}\right)^2 = \frac{GM}{r} - E$$

but a system with dynamic energy and coordinate rotation would have an additional term of the same form as a light ray geodesic with coordinate rotation:

$$\left(\frac{dr}{dt}\right)^2 + \left(1 - \frac{2GM}{rc^2}\right) r^2 \left(\frac{d\phi}{dt}\right)^2 = \frac{GM}{r} - E .$$

Daniel Dubois [8] has examined the motion of Mercury's perihelion in terms as an 'anticipatory' system. He asks: does the gravitational interaction travel at the speed of light or instantaneously? He finds that an anticipatory effect converts the radial component to an instantaneous interaction, while the tangential component has a velocity of interaction c which acts effectively to rotate the coordinates of the system.

The inertial force effect becomes exactly that which we would expect to obtain from a relativistic calculation. In a simple extension, we see that we can add a Newtonian potential $-GM / r$ to a light-ray geodesic defined in the absence of a gravitational field to find the degree of rotation of the coordinate system, and hence the inertial force effect to be added to find the new geodesic equation expected under these conditions. The extra terms will now be interpreted as an inertial rotation of the coordinate system, and will appear to be the action of centrifugal and Coriolis forces.

The local coordinate rotation combines two sources: the connection between the space and time coordinates (c), which is needed for local measurement, and

the direct gravitational effect of any source of mass-energy on this speed. Generalising, an inertial rotation of the Lorentzian space-time of measurement will result in the degree of curvature that we would obtain from the field equations of general relativity, or similar. So we conclude that:
(1) the relativistic effects connected with gravity may be considered extrinsic effects of measurement (epistemological) rather than intrinsic (ontological);
(2) as the effects are extrinsic, the gravitational field will remain linear, and so will not be subject to nonrenormalizable infinities;
(3) quantization will be equally extrinsic (fictitious inertial repulsion, rather than real gravitational attraction) and will therefore involve exchange particles of spin 1, rather than spin 2;
(4) the relativistic effects will lead to an extrinsic gravitomagnetism, with Maxwell-type equations, in which rotation will take the place of the magnetic field;
(5) rotation (involving a conserved angular momentum) will be a natural consequence of the observation of gravitating systems, and in fact all gravitating systems have significant intrinsic rotations, which are so far largely unexplained;
(6) the fictitious inertial forces, both centrifugal and Coriolis, may be expected to have directly observable effects in the observation of gravitating systems.

3 Gravitomagnetism

In principle, general relativity is largely a mathematical theory, without significant intrinsic physical content. None of the three physical principles which were the original basis of the theory Einstein was trying to develop – the principle of general covariance, the principle of equivalence and Mach's principle – were preserved in the field equations which defined the final theory. These equations effectively state that a particular energy-momentum distribution produces a particular degree of curvature in space and time, or can be considered equivalent to that curvature. The physical meaning attached to this is not defined by the equations, and requires additional assumptions when we seek particular solutions. As is well known, *any* field of force or momentum distribution can be presented in covariant form, even Newtonian gravity. The success of representing a theory in this way, of course, does not make it necessary to do so, despite the many claims that general relativity

'proves' that space-time is curved, and 'disproves' the existence of a gravitational force. They are simply alternative representations, and both can be accommodated by covariant derivatives. In addition, even if we accept the field equations of general relativity as providing the best mathematical package for explaining the observed effects associated with the theory, we are not obliged to accept any interpretation that requires additional physical input or that goes beyond the mathematical structure. Consequently, rejecting such interpretations is not the same thing as rejecting general relativity as it is *uniquely* represented by the field equations. Nothing in this paper can, therefore, be construed as an attack upon general relativity but there will be definite disagreements with some of the accumulated physical interpretations.

No experimental result so far observed or predicted as observable uses anything other than the Lorentzian 4-vector structure of space-time together with Newtonian gravity. The effects of creating a space-time connection and of acting on it by gravitational fields, of course, occur together and are equivalent to the conventional time dilation and space contraction. The standard results of 'general relativity' – redshift, light deflection, time delay and perihelion precession – are then recovered easily using only classical theory plus the inertial force connection, or, equivalently, 'special relativity' plus the classical Newtonian potential.[9-15]

More esoteric effects attributed to general relativity, such as frame dragging, the Lense-Thirring effect, and 'gravitational waves', are derivable from a set of gravitomagnetic equations entirely analogous to those of Maxwell in electromagnetic theory, and these equations can be derived in the same way. Adapting a procedure put forward by H. Kolbentsvedt,[16] though extending it to include length contraction as well as time dilation, we consider an object of mass M, moving with velocity **u** in the positive x-direction in the frame of the laboratory, and a particle of mass m moving with velocity **v** under its gravitational influence. In the rest frame of mass M, the Lagrangian $\mathcal{L}_0$ of the mass m particle can be found from the variational principle:

$$\delta\int(-mds)=\delta\int\mathcal{L}_0 dt_0=0\,,$$

where

$$ds_0^{\,2}=\gamma^{-2}dt_0^{\,2}-\gamma^2 dr_0^{\,2}$$

is the line element in the rest frame, and

$$\gamma^2 = 1 - \frac{2GM}{rc^2} = 1 - \frac{2\phi}{c^2}.$$

Integrating for the rest frame,

$$\mathcal{L}_0 dt_0 = -m\,(\gamma^{-2}c^2 dt_0^2 - \gamma^2 dr_0^2)^{1/2}.$$

Then, transforming to the laboratory frame, and neglecting higher order terms, we obtain

$$\mathcal{L}dt = -m\,[(c^2 + 2\phi)\,(dt - udx)^2 - (1 - 2\phi)\,(dx - udt)^2 - dy^2 - dz^2]^{1/2}.$$

Once again neglecting the higher order terms, and dividing by dt, we obtain the Lagrangian

$$\mathcal{L} = -\left(c^2 - v^2 + 2\phi - 8\phi\frac{\mathbf{u.v}}{c^2}\right)^{1/2}.$$

When $u \ll v \ll c$, and the rest energy term mc^2 and higher order corrections are neglected, the series expansion approximates to

$$\mathcal{L} = \tfrac{1}{2}mv^2 - m\phi + 4m\phi\frac{\mathbf{u.v}}{c^2}.$$

which is analogous to

$$\mathcal{L} = \tfrac{1}{2}mv^2 - q\phi + q\frac{\mathbf{A.v}}{c}$$

of electromagnetic theory. We should note here the factor of 4 difference, which is effectively due to the combination of 'time dilation' and 'length contraction'. This factor becomes important when it leads to an 'inductive' force associated with gravity equivalent to that derived from the electromagnetic field.

We can now define the rotation term $\boldsymbol{\omega}c$, or 'gravitomagnetic' field, as an analogue of the magnetic field term $\mathbf{B} = \nabla \times \mathbf{A}$, where

$$\boldsymbol{\omega} c = \nabla \times \left(4\phi \frac{\mathbf{u}}{c} \right) = \left(4\phi \frac{\mathbf{u}}{c} \right) \times (\nabla \phi) = 4 \frac{\mathbf{u}}{c} \times \mathbf{g}$$

which leads to a series of Maxwell-type equations.

$$\nabla . \mathbf{g} = 4\pi G\rho$$

$$\nabla . \boldsymbol{\omega} c = 0$$

$$\nabla \times \mathbf{g} = -c \frac{\partial \boldsymbol{\omega}}{\partial t}$$

$$\nabla \times \boldsymbol{\omega} c = 4\pi G\rho \mathbf{v} + c \frac{\partial \mathbf{g}}{\partial t}$$

Here, $G\rho\mathbf{v}$ takes the place of $\mathbf{j}$; and $4\pi G\rho$ that of ρ / ε_0.

From these we can derive gravitomagnetic versions of the Poynting vector, Lorenz force, Larmor precession, energy density of fields, and quadrupole radiation.[14] In all cases, these are fictitious effects, produced by time-dependent inertial forces, rather than instantaneous gravitational ones, and so the 'waves' produced by quadrupole radiation should be seen as fictitious inertial rather than real gravitational. The fictitious or inertial nature of the gravitomagnetic effects is a key component in ensuring that they can be described in a consistent mathematical form, which avoids the problems caused by the nonlinearity which is generally associated with gravitomagnetic formulations.

4 Mach's principle

The true connection between gravity and inertia is one of the most profound questions in physics. Mach's principle suggests that the inertia of a body is determined in some way by an interaction of the rest of the matter in the universe, and the holistic nature of the gravitational interaction suggested by the nilpotent formulation of quantum mechanics seems to indicate that the concept has some fundamental validity. The nilpotent formalism is valid only

over the entire quantum field, and this may relate to the fixing of the rest masses of particles, as well as charges, in renormalization.

Gravity appears to have a 'magnetic' inertial component and so will produce an acceleration-dependent inductive force analogous to that which occurs in electromagnetic theory, say:

$$F = \frac{G}{c^2 r} m_1 m_2 \sin\theta \frac{dv}{dt}$$

by analogy with the electromagnetic expression

$$F = \frac{q_1 q_2 \sin\theta}{4\pi\varepsilon_0 c^2 r} \frac{dv}{dt}.$$

Sciama considered the possibility of explaining Mach's principle using such an inductive force (though in his model it was a real one).[17,18] The inertia of a body of mass $m = m_1$ is attributed to the action of the total mass $m_u = m_2$ within a c-defined event horizon, specified by radius m_u, so making the inductive force equation equivalent to $F = Kma$, with K a constant. Let us also suppose the continuous mass-field required by the nilpotent formalism provides a standard by which we can define a unit inertial mass nonlocally for the entire universe, in the same way as the near-constant gravitational field **g** provides a way of defining a unit mass at the Earth's surface.

We imagine that mass m_u defines a radial inertial field of constant magnitude from the centre of a local coordinate system, and, at the same time, use the principle of equivalence, to equate this to the gravitational field (Gm_u / r_u^2), which, independently of the local coordinate system, defines a unit of gravitational mass within the same event horizon. If we use isotropy to remove the angular dependence, we obtain:

$$\frac{Gm_u}{c^2 r} \frac{dv}{dt} = \frac{Gm_u}{r_u^2}$$

Significantly, we obtain an acceleration

$$a = \frac{dv}{dt} = v\frac{dv}{dr} = \frac{c^2 r}{r_u^2}$$

which can be integrated with respect to r, to give

$$v = \frac{cr}{r_u} = H_0 r$$

where H_0 is Hubble's constant, and the acceleration is now:

$$a = \frac{v^2}{r_u} = H_0^2 r\,.$$

If gravity is nonlocal, then this acceleration is a fictitious one, which describes the effects on the coordinate system produced by using a Lorentzian space-time to model the instantaneous interaction. To calculate the equivalent vacuum density, we combine it with the gravitational force due to total mass m at any distance, to give

$$F = \frac{Gm}{r^2} - H_0^2 r = \left(\frac{4}{3}\pi G\rho - H_0^2\right) r$$

The equivalent Poisson-Laplace equation becomes:

$$\nabla^2\phi = 4\pi G\left(\rho - \frac{3H_0^2}{4\pi G}\right) = 4\pi G\left(\rho + \frac{3P}{c^2}\right) = 4\pi G\left(\rho - 3\rho_{vac}\right),$$

where the vacuum density is

$$\rho_{vac} = \frac{H_0^2}{4\pi G},$$

which is equivalent to a 'dark' energy density or negative pressure

$$-P = \frac{H_0^2 c^2}{4\pi G},$$

and cosmological constant

$$\lambda = 8\pi G \rho_{vac} = 2H_0^2$$

If we define the critical density for a 'flat' universe as

$$\rho_{crit} = \frac{3H_0^2}{8\pi G}$$

we obtain

$$\frac{\rho_{vac}}{\rho_{crit}} = \frac{2}{3},$$

which is within the limits of current observations, though it was obtained twenty years before the first measurements.[9-15,19-20]

This calculation suggests that the so-called 'dark energy' is analogous to a centrifugal force, and a corresponding 'Coriolis' effect might be considered for rotating systems. The argument for a Machian origin for inertia leads to

$$Gm_u = \tfrac{1}{2} c^2 r_u$$

and a universal inertial field equal in magnitude to Gm_u / r_u^2, which defines the unit of inertial mass. The measure of inertia (like centrifugal accelerations of any origin) is valid for all physical objects, whether static or moving. However, for objects that are themselves in motion, there is an additional fictitious (Coriolis) acceleration brought about by rotation of the coordinate system, which is perpendicular to both the real velocity of the object and the axis of rotation of the coordinate system. This effect is, in magnitude, twice that of the centrifugal acceleration, because it incorporates equal components from the change of velocity in space and the change of velocity in time. So the universal or nonlocal inertial Coriolis effect for a rotating or gravitational orbiting system, such as a galaxy, might be considered to be equal in magnitude to $2 \times \tfrac{1}{2} c^2 r_u / r_u^2 = c^2 / r_u$.

The universal Coriolis effect will only be detectable by an observer detecting relative motion with respect to the universal background. There are a

number of possibilities that such observations have already been made. The passages of the spacecraft Pioneer 10 and 11 out of the solar system appear to be retarded by an inward acceleration towards the Sun at ~ (8.74 ± 1.33) × 10^{-10} ms^{-2}, which is close to $H_0 c = c^2 / r_u$. There may also be 'flyby anomaly', or small unexplained increase in speed of satellites passing close to the Earth.[21,22] An entirely different piece of evidence is the flattening of the rotation (v–r) curves of galaxies, which seems to occur at the point where $v^2 / r = c^2 / r_u$, as if the Coriolis acceleration of the coordinate system provided an inertial upper limit to the galactic size. Perhaps, then, the Coriolis effect becomes the ultimate source of galactic rotation. Though neither galactic rotation nor the motions of the Pioneer spacecraft and satellites have been explained in terms of the 'expansion of the universe', it may be significant that each seemingly involves the Hubble constant.

5 The cosmic microwave background radiation

A continuous vacuum can be thought of as being full of virtual fermion-antifermion pairs, with charges, of all types (i.e. electric, strong and weak), of opposite sign. We can consider the 3 types of charge separately. For electric charge, we can consider the vacuum as being approximated by an infinite number of virtual electron-positron pairs. QED and renormalization indicate a fundamental relation between vacuum and observed values of electron mass and charge. The electron seems to be the only particle whose mass is entirely, or almost entirely, electromagnetic in origin.

Dimensional analysis shows that the relation between electron mass and the fundamental unit of charge requires a length scale, though the electron itself seems to be point-like. A so-called 'classical radius' relating the values of electron mass and electric charge is simply a relation between fundamental units:

$$r_c = \frac{e^2}{4\pi\varepsilon_0 m_e c^2}.$$

But if we were to imagine a virtual charge e as being uniformly distributed over some radius, to reflect the nature of vacuum, then we will obtain the relation originally found by Heaviside for electrodynamic mass:

$$\frac{2m_e}{3} = \frac{e^2}{4\pi\varepsilon_0 r_e c^2}.$$

So we could say that a uniform spherical distribution of charge e would produce a mass equivalent m_e over the radius:

$$r_e = \frac{3}{2}\frac{e^2}{4\pi\varepsilon_0 m_e c^2} = 4.2289\times10^{-15}\,\mathrm{m},$$

which is 1.5 the 'classical' radius.

This so-called radius clearly does not indicate the size of real electrons, but it suggests a fundamental relationship between the value of electric charge and the equivalent inertial mass generated by a vacuum process, with the vacuum having the potential to create the mass m_e in association with the charge value e if the radius r_e plays some significant part in the process (e.g. via the holographic principle). However, if we are concerned with a continuous vacuum process, rather than one associated with point-like real particles, we may expect that the 'radius' will have significance in terms of a quantity such as charge or energy density.

Now, the generation of inertial mass is seemingly connected with the simultaneous creation of gravitational properties. Thus, the gravitational energy density associated with these values of r_e, m_e and e may well be a significant quantity in specifying the vacuum state required. This is easily calculated as:

$$\frac{3Gm_e^2}{4\pi r_e^4} = 4.132\times10^{-14}\,\mathrm{Jm^{-3}}.$$

Astonishingly, this is exactly the energy density that would be produced by a uniform distribution of black body radiation at a temperature of 2.72 K, and determined by aT^4, where $a = 7.56 \times 10^{-16}\ \mathrm{Jm^{-3}K^{-4}}$.

Perhaps this is just a remarkable coincidence. Alternatively, the microwave background radiation, which, by being isotropic, appears to provide the universal rest frame desired from the vacuum by the physicists of the nineteenth century, is really a fundamental vacuum property. In this case, we might be able to use the same prediction to derive results for particles whose

masses are determined principally by weak or strong, rather than electric interactions. We should also expect to find a relation between the Machian calculation of inertia and the cosmic microwave background radiation.

There is at least one good reason why we should expect to see a connection between Machian inertia and the microwave background radiation. The whole inertia calculation stems from the idea that the 'relativistic' aspects associated with gravity represent a loss of information due to an inappropriate space-time structure for the observation of this force. Gravity is incapable of the direct observation that we use for the other forces, and information will always be lost in the observing process. This would connect with the background radiation having a black body spectrum, and hence having no discernible characteristics other than temperature. There is also a possible mechanism for generating the radiation, via the acceleration now supposed to be responsible for the 'dark energy'.

The calculation, of course, is a vacuum one, not one connected with real objects – the loss of information comes from the 'aberration' of the coordinate system, not the objects within it. We suppose a vacuum filled with a uniform distribution of virtual particles of charge with numerical value e, but also requiring the equation of gravitational and inertial forces. Let us additionally suppose that the inertial effects are the result of the creation in the vacuum of a noninertial frame of measurement, which occupies the whole of space, with what we will describe as 'component volumes' of radius r_e, irrespective of whether it contains real particles. The noninertial frame will produce an inertial or fictitious acceleration, and the accelerating virtual charges will radiate, according to the Larmor formula, at a rate

$$\frac{dE}{dt} = \frac{2}{3}\frac{e^2}{4\pi\varepsilon_0}\frac{a^2}{c^3}.$$

With a reduced from $c^2 r / r_u$, by the 'general relativistic' factor 4, combining length contraction and time dilation, which is also equivalent to the factor $K = ½$, from the inertial calculation combined with an equal reduction due to the gravitational attraction:

$$\frac{dE}{dt} = \frac{2}{3}\frac{e^2}{4\pi\varepsilon_0 c^3}\frac{c^4 r^2}{16 r_u^4}.$$

On substituting $r = ct$, we obtain

$$\frac{dE}{dt} = \frac{2}{3}\frac{e^2}{4\pi\varepsilon_0}\frac{c^3t^2}{16r_u^4}.$$

Then, integrating between limits 0 and E, and 0 and t,

$$\int_0^E dE = \int_0^t \frac{2}{3}\frac{e^2}{4\pi\varepsilon_0 c^3}\frac{c^3t^2}{16r_u^4}dt$$

from which

$$E = \frac{1}{72}\frac{e^2}{4\pi\varepsilon_0 c^3}\frac{r^3}{r_u^4}.$$

This calculation is for one component volume at distance r. For n_e component volumes at uniform number density ρ, consider an element of volume $dV = 4\pi r^2 dr$:

$$E\rho dV = \frac{12\pi r^2\rho}{4\pi r_e^3}\frac{1}{72}\frac{e^2}{4\pi\varepsilon_0}\frac{r^3}{r_u}d = \frac{1}{24}\frac{r^5}{r_u^4 r_e^3}\frac{e^2}{4\pi\varepsilon_0}dr.$$

But, for a universe filled with virtual particles, the density of volumes of radius r_e becomes

$$\rho = \frac{3n_e}{4\pi r_u^3},$$

where the number of volumes,

$$n_e = \frac{4\pi r_u^3/3}{4\pi r_e^3/3} = \frac{r_u^3}{r_e^3}$$

and so

$$\rho = \frac{3}{4\pi r_e^3}.$$

Hence

$$E\rho dV = \frac{1}{24}\frac{r^5}{r_u^4 r_e^3}\frac{e^2}{4\pi\varepsilon_0}dr\,.$$

Integrating to find the energy radiated over the total volume $4\pi r_u^3/3$:

$$E_{TOT} = \int_0^{r_u}\frac{1}{24}\frac{r^5}{r_u^4 r_e^3}\frac{e^2}{4\pi\varepsilon_0 r}dr = \frac{1}{144}\frac{r_u^6}{r_u^4 r_e^3}\frac{e^2}{4\pi\varepsilon_0} = \frac{1}{144}\frac{r_u^2}{r_e^3}\frac{e^2}{4\pi\varepsilon_0}\,.$$

The corresponding energy density for a uniform continuous distribution of virtual charge is given by

$$\frac{3}{4\pi r_u^3}\frac{1}{144}\frac{r_u^2}{r_e^3}\frac{e^2}{4\pi\varepsilon_0} = \frac{1}{192\pi}\frac{e^2}{4\pi\varepsilon_0 r_e^3 r_u}\,.$$

If we equate this to aT^4, we obtain first-order values for the Hubble radius at 1.22×10^{26} m and the Hubble time at 1.29×10^{10} yr.

If we require, at all times, for Mach's principle, a density r_u close to the 'critical' value, such that

$$\frac{GM}{r} = \tfrac{1}{2}v^2\,,$$

as both classical theory and general relativity require, and

$$\frac{4\pi G\rho_u r^3}{3r} = \frac{c^2 r^2}{2r_u^2}\,,$$

we obtain estimates of:

Hubble mass = 8.23×10^{52} kg
universe density = 1.08×10^{-26} kgm^{-3}
vacuum density = 7.53×10^{-27} kgm^{-3}
and cosmological constant = 1.207×10^{-36} s^{-2} = $5.8 \times 10^{-124}\ 8\pi G\rho_{\text{Planck}}$

6 Other cosmological calculations

The mass density of 1.08×10^{-26} kgm^{-3}, according to current observations, includes only about 4 % baryonic matter. It may be possible to calculate this directly, if we suppose that the vacuum process which creates the inertial masses associated with the electrical charges of the real particles in the universe is equatable, at least in approximate energy density terms, to aT^4. That is, if N_e is the particle density of the real masses produced by the electrical vacuum process, then

$$N_e m_e c^2 \sim aT^4.$$

This leads to a value of 0.504 m^{-3} for the density of particles with charge e. If half of these are electrons and half protons, then the proton density is of order $0.252 \times 100 / 6.47 = 3.9$ % of m_u.

Other, relatively straightforward, calculations fix the neutron / proton ratio and the photon / fermion ratio, without recourse to any cosmological model. The difference in neutron and proton, and proton plus electron, masses are determined experimentally at $\sim$ 2.5 $m_e c^2$ and 1.5 $m_e c^2$. The statistical Boltzmann factor exp ($-2.5\ m_e c^2 / m_e c^2$) or exp ($-1.5\ m_e c^2 / m_e c^2$) then determines the neutron / proton ratio as between 8 and 22 %. The photon / fermion ratio can be fixed at $\sim 2 \times 10^9$ if we take the density of photons N_γ of approximate energy kT and equate $N_e m_e c^2$ and $N_\gamma kT$.

We can also calculate the Fermi constant (G_F) from the weak process of proton-to-neutron conversion in agreement with experimental values. Taking the 'creation' of electron mass as a vacuum process we define the rate at which the energy $m_e c^2$ becomes available to a proton, to convert it to a neutron with a probability between exp (–1.5) and exp (–2.5), as being equivalent to the rate at which the same amount of vacuum energy is converted into thermal energy (in the form kT_p) via redshift, $\sim (8\pi G a T_p^4 / 3c^2)^{1/2}$, and then relate this to the reaction rate for the weak process of proton-to-neutron conversion $\sim (G_F^2 m_e^5 c^2 / m_p^4 \hbar)$, given the same availability of vacuum energy. An order of magnitude calculation then gives $G_F \sim 10^{-5}$ units of mass^{-2} in agreement with experimental values. Since this number is solely determined by the weak coupling and the

mass of the weak interacting boson, and M_W is in turn fixed by the vacuum expectation energy of the Higgs field, the filled vacuum which provides the instantaneous gravitational action assumed in this analysis, it would appear that the classical inertial calculation has the same fundamental meaning as the calculation of the inertial masses of particles through the Higgs mechanism in the Standard Model.

Eddington, Dirac and others[4-7] have pointed to the fact that various dimensionless numbers used to relate orders of magnitude on cosmic and particle scales are of order 10^{40}, 10^{80}, or 10^{120}. Here, using

$$aT^4 = \frac{3Gm_e^2}{4\pi r_e^4} = \frac{1}{192\pi}\frac{e^2}{4\pi\varepsilon_0 r_e^3 r_u}$$

and

$$\frac{e^2}{4\pi\varepsilon_0} = \frac{2}{3}m_e r_e c^2,$$

we obtain

$$\frac{m_e}{r_e^2} = \frac{m_u}{108 r_u^2}, \tag{1}$$

which can also be written as

$$\frac{108Gm_e}{r_e^2} = \frac{Gm_u}{r_u^2}. \tag{2}$$

Here, numbers of the order of 10^{80} are derived ultimately from the ratio m_u / 108 $m_e \sim m_u / m_p$, while numbers of order 10^{40} are derived from r_u / r_e, which equals $(m_u / 108\ m_e)^{1/2}$. Numbers of order 10^{120} to 10^{123} (depending on whether we use m_e or 108 m_e, etc.) come from combinations of these, for example, $m_u r_u / m_e r_e$, or, in more physical terms, the ratio of the gravitational self-energy of the Hubble universe to the electrostatic energy of a unit charge defined over a fermionic 'radius' $(Gm_u^2 / r_u) / (Gm_e^2 / r_e)$. This last scale, in fact, has many interpretations, all of which can be considered equivalent. It appears, for example, as the ratio of maximum available gravitational / inertial energy to the electrostatic self-energy of an elementary charge over some defined radius

($4\pi\varepsilon_0 G m_u^2 / e^2$), whether local or universal, and as the ratio of the maximum energy within the Hubble radius to the energy due to the self-charge of the electron over the same radius ($4\pi\varepsilon_0 m_u c^2 r_u / e^2$). These ratios featured in earlier work by the author, using formulae of the same form as (1) and (2), which relate the 'creation' of mass and charge units through a 'surface boundary' separating the local system from the universal one, through the mediation of the universal gravitational force.[10] In principle, this is analogous to the boundary between fermion and vacuum in nilpotent quantum mechanics, and the ratios also suggest some limit to the number of virtual fermionic states constructible in this way via a vacuum process, with a possible further relation, through QED, to the ratio of the maximum intermediate state energy available to the rest energy of the fermion it can 'create'.

The obvious significance of such dimensionless ratios might suggest that they could, in some way, be obtained using some more fundamental argument and then used to reduce the number of parameters which depend on empirical evidence for their values. A possibility which the early work explored was that a term of order exp ($2\pi / 3\alpha$) m_e, which occurred as a cut-off mass in QED renormalization for the electron,[23,24] might link quantum dimensionless parameters with universal ones; another, reflecting current interest in group theory, and particularly in the so-called 'sporadic groups', might look for an information-theoretical approach for the number of possible units of information or 'bit flips', based on group element combinations (1.226×10^{121} if we use the six sporadic groups which are not subgroups or subquotients of the others). There is not enough information, at present, to decide whether any such approach is likely to succeed. However, a ratio of 1.4 to 2.9×10^{121} emerges if we regard the Hubble constant as a frequency and take the ratio of the Hubble energy ($G m_u^2 / r_u c^2$ or $m_u c^2$) over, say, $H\hbar$. This time, there is no direct input from particle physics, and the inverse ratio of times might indicate that the inertial process, which involves the entire Hubble universe even for a single particle, defines a minimal time interval for the material transition which we define as a 'bit flip'.

Planets, stars, galaxies, etc., have been examined in terms of the fundamental forces involved (gravity, electromagnetism and the weak interaction),[25,26] and it would seem from these analyses that the strengths of the forces determines their optimum masses, radii and lifetimes. Many of these calculations seem to involve the large number ratios. The lifetimes of stars are,

significantly, determined by the product of $\alpha_G^{-3/2} m_p$ and the Compton time for the proton, $h / m_p c^2$; the 'large-number coincidences' (i.e. the gravitational / inertial connection) then makes these of the same order as the Hubble time. The calculations only show that fundamental gravitational / inertial processes are characterized by numbers involving the Hubble scale.

It is clear that the Hubble scale is intrinsic to the physics of the observable universe, irrespective of the cosmological argument used to explain this. The same appears to be true of the microwave background radiation – energy density of starlight in the Milky Way is approximately the same, as are other indicators, such as the galactic magnetic field and cosmic rays; Eddington even used the density of starlight to calculate the temperature of space at 3.2 K many years before the discovery of the cosmic microwave background radiation.[27] It is likely that we will find such 'coincidences' in all systems where gravity plays a major role, reflecting in this way the intimate connection between the gravitational interaction and the vacuum 'creation' of inertial mass, and the scale-independence of the process. There is, indeed, a strong indication that a connection between dark energy and the density of starlight should exist, and, hence, in our terms, explain the apparently observed connection between starlight and the cosmic microwave background radiation, for Leong Ying has produced an argument,[28,29] based on R. M. Santilli's isodual mathematics and theory of antimatter,[30] and appropriate calculations, that stellar nuclear fusion (the cause of the starlight) should be held responsible for the observed dark energy.

The calculations in this section have been largely order of magnitude, but they seem to give an indication that a real, and quantitative, connection between the cosmic microwave background radiation and the cosmological redshift must exist in a purely physical perspective, independent of any cosmological model, and that both radiation and redshift are, in some senses, aspects of the same physical phenomenon – a fact which purely cosmological models have never really established. There seems to be every reason to suggest that the inertial and gravitational energies associated with generating the mass m_e from vacuum could be equal to that associated with a microwave background at $T = 2.72$ K, and that the inertial process could be responsible for generating the background energy.

7 Application to strong and weak interactions

If the process described in the previous section is universal, then we should expect that the cosmic microwave background radiation will generate particles with the appropriate minimal masses for the strong and weak, as well as electric charges. For the electric force we have

$$\frac{1}{192\pi}\frac{e^2}{4\pi\varepsilon_0 r_e^3 r_u} = \frac{3Gm_e^2}{4\pi r_e^4} = aT^4$$

and

$$\frac{2m_e}{3} = \frac{e^2}{4\pi\varepsilon_0 r_e c^2} = \frac{\alpha\hbar}{r_e c}.$$

What happens if we replace electric with strong or weak charges? If the fine structure constant for a coupling is α', corresponding to a mass m and length scale r, then we can derive comparative relations for the different interactions:

$$mr \propto \alpha'$$

$$m \propto r^2$$

from which, also,

$$m^3 \propto \alpha'^2.$$

The strong coupling at the proton mass (1 GeV) is about 0.29, which leads to

$$m = 11.7\ m_e = 5.96\ \text{MeV} \qquad r = 1.4 \times 10^{-14}\ \text{m}$$

The mass is typical of those projected for u and d quarks, and the length scale is associated with nuclei held together by the strong interaction. Applying this to the Coulombic part of the combined electroweak interaction (for example, in beta decay), where the weak coupling is about 4 times the electric, the mass becomes about 2.5 m_e, and the length scale about 6.7×10^{-15} m. The mass scale, here, is equal to the mass difference between neutron and proton (~

2.5 m_e) and the length scale is not too far from the order of nucleon / nuclear size.

The effective strength and range of the pure weak coupling, however, is significantly reduced by the fact that it requires a massive intermediate boson (W or Z), and is determined by the Fermi constant, which incorporates the W or Z mass. The range (r) of the interaction can be calculated from $\hbar$ / $M_Z c^2$, as of order 2.166×10^{-18} m, which, using $m \propto r^2$, leads to a mass equivalent to 2.6×10^{-5} m_e, or 0.13 eV. Here we can use this to predict the mass value for the lightest neutrino. This very probably has a Dirac origin, but we may suspect that there may be a Majorana process involved in the mass differences between the neutrino generations.

8 The holographic principle

The equations we have obtained relating to inertia are information-based. The fictitious inertial and Coriolis forces and the cosmic background temperature are indicators of information loss, which can be treated on a digital basis if space (or vacuum) is regarded as composed of entangled virtual particle-antiparticle pairs created by any of the three fundamental interactions for which we have calculated characteristic masses and distance scales. Only the electric interaction, however, can be imagined as operating on a universal scale.

Equation (1) can be seen as a version of the holographic principle, relating the information about the number of virtual particles or antiparticle pairs filling the observable universe, which may be derived from m_u / m_e, to the ratio of the universal to fermionic bounding areas ${r_u}^2$ / ${r_e}^2$, and the connecting mechanism is ultimately the nonlocal gravitation. From the basic equations, others may be derived, for example,

$$324\alpha \frac{G\hbar}{c^3} r_u = r_e^3,$$

and

$$\frac{r_u^3}{r_e^3} = 324\alpha \frac{r_u^2}{r_P^2} = 2.36 \frac{r_u^2}{r_P^2},$$

where r_P is the Planck length. This means that the number of virtual fermion–antifermion states of characteristic length r_e in the Hubble universe relates also to the total number of bits of information available according to the holographic principle, which relates to r_u^2 / r_P^2. Lloyd calculates this,[1,2] using this ratio, at order 10^{123}. As stated in section 5, we have previously found ratios of order 10^{123} to have a number of meanings which are essentially identical to this one, if the vacuum fermion is taken to be the smallest unit of physical 'information', and it is conceivable, as we have suggested in section 5, that this dimensionless number may have its origin in some more fundamental mathematical or physical principle.

Also, in equation (2), r_u and r_e can be thought to represent times (r_u / c and r_e / c) as well as distances, so r_u / r_e can be thought of as a measure of the number of times 'information' can be transmitted across a system of length r_e during the Hubble time t_u. With $m_u / 108\ m_e$ as an approximate measure of the number of real systems transmitting such information, then the total number of transmissions during time r_u / c will be $\sim r_u^3 / r_e^3$. Lloyd describes this as the quantum geometric limit, the number of 'bit flipping' events that can take place in a 4-D space-time determined by the Hubble event horizon. Again, it is of order 10^{123}. In fact, if the number of 'flips' or transmissions available to one 'material' bit, of length r_e, in time t_u is defined by $t_u / t_e = r_u / r_e$, then the number of 'material' bits (or real particles) in the universe will necessarily of order r_u^2 / r_e^2 or $m_u / 108\ m_e$. In the present theory, the minimum unit of 'information' is the fermionic state (or the unit charge), and the ratio of the total number of possible fermionic states to the number of realised fermionic states is of order 10^{40}.

The 'holographic principle' equation (2) provides a direct connection between mass and the bounding area of the fermionic system to that of its Hubble universe through gravity and inertia, in exactly the same way as happens with the nilpotent fermion and its vacuum. The role of gravity as carrier of this information, and as the agent of the connection between the fermion and vacuum or the rest of the universe, is established as the 'cause' of the holographic principle.

9 Gravity and nilpotent quantum mechanics

The holographic principle for the fermion, which was effectively predicted in earlier work leading to an equation analogous to (1),[8,9] is also a consequence of nilpotent quantum mechanics. In the nilpotent formalism,[14,31-43] we define a fermionic operator of the form ($\pm ikE \pm \mathbf{i}\mathbf{p} + jm$), where i, j, k are unit quaternions, the momentum operator $\mathbf{p}$ is a multivariate (or quaternion-like) vector (with basis units $\mathbf{i}$, $\mathbf{j}$, $\mathbf{k}$), and the four $\pm$ options represent an abbreviated way of describing a 4-part row or column vector or spinor. The algebraic structure underlying this description is a commutative combination of the quaternion and vector units, (i, j, k, 1) and ($\mathbf{i}$, $\mathbf{j}$, $\mathbf{k}$, 1), which results in a group structure with 64 elements. This can also be seen as a combination of two vector spaces, which, through the way in which they manifest themselves, can be called real space and vacuum space. They are totally dual, but are mathematically asymmetric because the generators needed to produce the group structure involve a 5-fold asymmetric combination of the basic units (typically as ik, $i\mathbf{i}$, $i\mathbf{j}$, $i\mathbf{k}$, j), which is isomorphic to the matrices of the conventional γ algebra of the Dirac equation.

The nilpotent structure incorporates quantum mechanics but also goes well beyond it. The energy and momentum operators E and $\mathbf{p}$ in the nilpotent operator need not represent just $i\partial / \partial t$ and $-i\nabla$, but can also incorporate field terms or covariant derivatives. Once specified, the operator defines the entire quantum system, as it automatically and uniquely generates a phase factor on which it acts to create a nilpotent amplitude, whose argument can also be written in the form ($\pm ikE \pm \mathbf{i}\mathbf{p} + jm$), with E and $\mathbf{p}$ now representing eigenvalues, which then squares to zero. In principle, this incorporates QED and other quantum field theories, as the E and $\mathbf{p}$ terms can be redefined at every stage in the interaction process, so yielding, for example, Lamb-shifted versions of these operators.

In addition, the *mathematical* structure of the operator also includes (ultimately through the mathematical distinctness of the three terms $\pm ikE$, $\pm \mathbf{i}\mathbf{p}$, and $+ jm$) the characteristic weak, strong and electric interactions, with their respective $SU(2)$, $SU(3)$ and $U(1)$ symmetries. The respective sources of these interactions are seen to be charges, specified by the quaternion units k, i and j, and the three idempotent expressions $k(\pm ikE \pm \mathbf{i}\mathbf{p} + jm)$, $i(\pm ikE \pm \mathbf{i}\mathbf{p} + jm)$, and $j(\pm ikE \pm \mathbf{i}\mathbf{p} + jm)$ are identified as weak, strong and electric vacuum

operators which effectively partition the continuous vacuum, equivalent to the 'rest of the universe' as seen by the fermion, into discrete components which respond to the three discrete charges. (They can also be seen to be the carriers of the three conserved components of angular momentum – handedness, direction and pure magnitude – with the entire nilpotent structure representing an angular momentum operator.) In addition, when we examine the ($\pm ikE \pm \mathbf{i}\mathbf{p} + jm$) as a 4-part structure, we see that, while the lead term represents the fermion itself, the other three terms represent 'reflections' of the lead term in each of these three vacua, which physically manifest themselves as respective T, P and C transformations of the original fermionic state.

The 5-fold structure can be seen as being a duplicate one, created out of the charges represented by $\boldsymbol{k}$, $\boldsymbol{i}$ and $\boldsymbol{j}$ being superposed on the original time, space and mass to produce energy, momentum and rest mass. Because the middle term in each case is also 3-dimensional, this means that we have 5 units representing energy, momentum and mass (or time, space and mass), and another 5 representing weak charge, strong charge (with 3 units), and electric charge. This structure has all the symmetry groups required of string theory, with self-duality in phase space determining vacuum selection, as required. Nilpotency, however, makes the fifth term in each case redundant, and so the 10 dimensions become, in nilpotent combination, equivalent to 8, as in the original set of base units used for the fundamental parameters, space, time, charge and mass (**i**, **j**, **k**, i, $\boldsymbol{i}$, $\boldsymbol{j}$, $\boldsymbol{k}$, 1). This set of units acts like a 'broken octonion' and can also be mapped onto a regular octonion. As a double 4-vector, with the signature of a complexified single 4-vector, it can also be related to Penrose's twisters, [44] which similarly have 4 real and 4 imaginary parts, though they lack a crucial element of structure which this group of units needs to represent fundamental physics. It is interesting, in addition, that Baez and Huerta have related 10-dimensional string theory to the need for representing the 2-dimensional space-time string of the particle within an octonionic 'space'.[45] If the particle is actually a nilpotent point, then we necessarily reduce this again to 8 dimensions. (Since octonions require 1 real and 7 imaginary parts, then at least one of the dimensions must be timelike if the others are spacelike.)

Now, the whole point of nilpotency is that it is an indication of the fact that nature is structured on a zero totality. The creation of a fermion of the form ($\pm ikE \pm \mathbf{i}\mathbf{p} + jm$) requires the simultaneous creation of the 'rest of the universe' as

a total (continuous) 'vacuum' specified by $-(\pm ikE \pm \mathbf{i}\mathbf{p} + jm)$. The Pauli exclusion principle is then a consequence of the fact that the combination state of fermion and vacuum is zero, as well as the superposition, because nilpotency determines that

$$-(\pm ikE \pm \mathbf{i}\mathbf{p} + jm)(\pm ikE \pm \mathbf{i}\mathbf{p} + jm) = 0.$$

The zero totality is between real (observed) space and unobserved (vacuum) space. The four terms in the nilpotent operator allow a cancellation, over the two spaces, of energy, momentum, angular momentum, space and time coordinates, and all charges; even the mass term can be removed by replacing the conventional differential operators with commutators. Antimatter exists in this universe to the same extent as matter, but the built-in mathematical asymmetry means that it is mostly situated in the (unobserved) vacuum space, rather than the (observed) real space.

Here we have points of contact with the theory of Ying,[28,29] and the isodual mathematics of Santilli.[30] Over many publications, Santilli has developed a new structure in mathematics, based on a new definition of -1, and has used it to incorporate antimatter on the same basis as matter in physical theory, with many predicted effects. Ying has used Santilli's isoduality to create a 'twin universe' theory in which 'all contents and processes of each universe have equal magnitude but opposite polarity, including energy-mass that in the anti-parallel universe will have negative quantities producing the necessary gravitational repulsion to drive the cosmic expansion'.[29] In Ying's twin universe, 'the complete cosmos exists as a ten-dimensional entity with two identical but anti-parallel four-dimensional space-time (energy-entropy) universes residing on the opposing surfaces of a two-dimensional common membrane'[29] Here, we have complete contact (in mathematical terms) if the membrane in one theory becomes the nilpotent condition in the other.

Santilli's theory has two spaces (positive and negative) and two times (forward and backward) to account for matter and antimatter, and antimatter is assumed to exist in the observable universe on the same basis as matter. Ying, however, has matter and antimatter in the observed universe, with anti-matter and anti-antimatter in the dual or twin universe. There is no 'missing' antimatter because it is in the dual universe. The theory assumed in this paper is that physics requires dual spaces – real (observable) space and vacuum

(unobservable) space – and the so-called 'missing' antimatter is in vacuum space. Real space has real fermions and antifermions, while vacuum space has virtual fermions and antifermions, in total agreement with Ying's viewpoint. In the language of the current paper, the isodual predictions of Santilli concerning antimatter would be accommodated as vacuum effects, rather than observable ones.

Now, while Ying's theory uses the twin universes as the driver of cosmic expansion, and to produce stellar nucleosynthesis, my own position is that we have a redshift, equivalent mathematically to a velocity of expansion, and an acceleration term equivalent to centrifugal force, and these (like Ying's) are derived from purely physical principles. This means that it becomes a matter of interpretation whether we regard these effects as 'real' ones. We are not compelled to answer physical questions by assuming cosmological conditions. The cosmological conditions should rather be determined on the basis of physical principles. If we assume the effects are 'real' (whatever that may mean), then we will unravel the cosmological history of the universe; if we assume that they are not, then we will have an abstract theory based on zero totality which doesn't require a cosmological history, with 'creation' from nothing an event that is happening 'now'. (I have looked at both explanations and am not yet convinced that an absolute decision can be made, but my inclination is towards the pure abstraction.) It may be that the question is meaningless, like choosing between different 'interpretations' of quantum mechanics. Ultimately, however, the physical processes in the universe can be seen to result from physical explanations and not from unexplained accidents of history.

Each fermion state is defined as unique because its total (continuous) vacuum state is unique, and each fermion can adopt a unique energy-momentum state with respect to all others because the continuous vacuum states are automatically and instantaneously correlated, as the vacua, unlike the fermions, are universal and nonlocal. The instantaneous correlation process is what we call 'gravity', and the unit associated with it and its source, mass(-energy), is the real number 1 (or –1), thus completing the quaternion system with the three imaginary units associated with charge, $\boldsymbol{k}$, $\boldsymbol{i}$ and $\boldsymbol{j}$. The vacuum associated with gravity is specified by the nilpotent operator $-(\pm i\boldsymbol{k}E \pm \boldsymbol{i}\mathbf{p} + \boldsymbol{j}m)$, meaning that gravitational energy is negative, and that the universal gravitational interaction is the only one which can maintain zero totality by

allowing the complete annihilation of the fermion with its vacuum. The nilpotency, with $(\pm ikE \pm \mathbf{i}\mathbf{p} + jm)(\pm ikE \pm \mathbf{i}\mathbf{p} + jm) = 0$, also automatically defines a boundary between the fermion and the gravitational vacuum, separating locality (inside the bracket) from nonlocality (outside it). The fundamental dualities responsible for the zero totality condition ensure that a physical state cannot be defined without a simultaneous definition of everything that negates it.

The nilpotent structure also corresponds to a version of the first and second laws of thermodynamics, which, in effect, define the local and nonlocal properties of $(\pm ikE \pm \mathbf{i}\mathbf{p} + jm)$. The first law says that we cannot define a fermionic system unless $(\pm ikE \pm \mathbf{i}\mathbf{p} + jm)$ squares to zero, and so conserves energy. The second law says that we can only define the conservation over the entire universe, and that this conservation is unique for each nilpotent state. If the nilpotent states are unique in time as well as space – within the relativistic covariance and causality required by the operator – then a condition for irreversibility is defined, and we have an arrow of time which has nothing to do with a particular cosmological history of the universe.

On the basis of the work presented in the previous sections, we can specify for a discrete fermion a fictitious *inertial* vacuum of the form $(\pm ikE \pm \mathbf{i}\mathbf{p} + jm)$, which is a kind of totality of the three discrete vacua, but which is actually equivalent to the fermion itself. This is a direct expression of the kind of gravity / gauge theory correspondence which has emerged (for different reasons) in string theory, but which has been a component of the nilpotent quantum mechanics from the beginning, and of the quaternionic fundamental particle structures which preceded it in earlier versions of the theory. The nilpotent structure shows that continuous gravity is *necessary* to quantum theory, just as much as Heisenberg uncertainty (which itself ensures that we cannot avoid a continuous zero-point vacuum), not that it is contradicted by it. 'Quantum gravity' is a meaningless idea, though we can of course quantize gravitational *inertia*, which is a description of the quantized fermionic state itself.[14]

In addition to all its other advantages, the nilpotent formulation of the fermionic state immediately incorporates both quantum holography and the holographic principle. In the case of quantum holography, the nilpotent $(\pm ikE \pm \mathbf{i}\mathbf{p} + jm)$ can be thought of as a quantum hologram in which the phase is encoded in the first term, the amplitude in the second, and the reference phase

in the third. Significantly, the nilpotency effectively makes one of the terms redundant, and so we can, for example, reconstruct the information using only phase and reference phase, or E and m. In the case of the holographic principle, where the entire information about a system is encoded in a bounding area (either as distance × distance or distance × time), we see that the terms E and $\mathbf{p}$, in effect, represent the equivalent of a time and a single dimension in space (the spatial direction being fixed with the spin and orthogonal to the time), and so code the entire information about the fermionic system in the equivalent of a bounding area. The phase and amplitude can be represented either by two coordinates of space, or one coordinate of space and one of time constructing a 'world sheet', since a fundamental duality allows switching between the representations. (It is significant, here, that, using anticommutative differentiation, the nilpotent operator itself can be reduced to just E and $\mathbf{p}$ terms.) In both quantum holography and the holographic principle, it is nilpotency, and hence *gravity*, which determines the holographic nature.

10 Conclusion

The original starting point for this research was a long-held belief that the intrinsically nonlocal nature of gravity would lead to extrinsic effects related to the velocity of light in the observation of gravitating system. A significant result of this was that rotation / angular momentum (the 'aberration of space') emerged as a necessary consequence of the actions of gravity, and not as an unexplained add-on assumption. Many predictions have resulted from this. Thus, the theory has always required an infinite, flat, Euclidean universe, at the critical density, exactly as now established by experimental data, but totally against majority opinion in the preceding decades. Again, and this is one of the most significant results, the acceleration effect in the cosmological redshift, with the correct order of magnitude, was a prediction made two decades before the experimental discovery, not a *post hoc* explanation.[9-15] In addition, a connection with the cosmic background radiation suggested that the temperature was 2.72 K, well before exact values were established.[46] The results have been derived independently of any cosmological model, so, in principle, they could be compatible with the 'Standard' cosmological model currently accepted (if we make the additional assumption that that theory does not self-contradict in other respects), but the fact that cosmological phenomena

can be explained purely as *physics*, without assuming any particular history of the universe, might remove some of the imperative for assuming the model to be true.

Among other anticipations or partial anticipations of significant results are versions of gravity / gauge theory correspondence, and an approach to a holographic principle, based on gravity and the inverse square law, in which the information unit is identifiable from the beginning as the minimum charge structure or fermionic state, and which, as in the versions based on black holes and string theory, is structured on a vacuum constructed from virtual fermion / antifermion pairs. Here, also, is an anticipation of the significance of the 10^{120} scale in many contexts linking universal and local conditions. In fact, a number of calculations allow us to link cosmological and fundamental particle scales in a way which enables specific values for the significant numbers in both areas to be evaluated with a minimum of (and, possibly, eventually zero) free parameters, and for further predictions to be made, in particular, of the mass scale for neutrinos. The holographic principle, or the gravitational linking of universal and individual particle scales, shows further that the 'large number' relations between cosmic and particle scales are a consequence of the gravitational / inertial connection between the local and the nonlocal. Though in its earliest form,[9,10] this would have appeared highly speculative, subsequent calculations, considered 'mainstream', seem to provide an almost exact parallel in all significant respects.

The theory has, of course, been able to generate a number of interesting numerical results, but arguments of this kind should always be treated with a greater degree of caution than more abstract ones leading to general principles, as it is certainly possible to generate numerical results that are nothing more than interesting coincidences. In addition, the status of some of the relevant data (for example, that concerning the Pioneer and other gravitational anomalies, and even quark and neutrino masses) is by no means established and is still under extensive review. However, the successful predictions already made (especially of the 'dark energy' effect), the very strong connection made with nilpotent quantum mechanics, the good area of agreement with the work of Santilli and Ying, the successful incorporation of Mach's principle and the explanation of the origin of gravitational rotation, together with the anticipation of the holographic principle and its consequences, in addition to gravity / gauge correspondence, seem to suggest that the outcome of this particular research

programme has justified the seemingly speculative assumptions on which it was originally based. It suggests that it may be well worth exploring further to see if further predictions, explanations and calculations might result from its many-faceted structure.

References

[1] P. Rowlands, The cosmological implications of nonlocal gravity, in press in *JCMSE*, volume 13 (2013), 1.

[2] S. Lloyd, Computational Capacity of the Universe. Phys. Rev. Lett., 88 (23) (2002), 237901.

[3] V. Giovannetti, S. Lloyd and L. Maccone, Quantum-Enhanced Measurements: Beating the Standard Quantum Limit, Science, 306 (2004), 1330-6.

[4] A. S. Eddington Proc. Cam. Phil. Soc., 2 (1931), 15.

[5] A. S. Eddington, *Relativity Theory of Protons and Electrons*, Cambridge University Press, 1936.

[6] P. A. M. Dirac, The Cosmological Constants, Nature, 139 (1937), 323.

[7] P. A. M. Dirac, A New Basis for Cosmology, Proc. Roy. Soc. 165 A (1938), no. 921, 199-208.

[8] D. M. Dubois, Anticipative effect in relativistic physical systems, exemplified by the perihelion of the Mercury planet, The Noetic Journal, 6 (2005), 99-115 (R. L. Amoroso, B. Lehnert and J.-P. Vigier (eds.), Special issue: The Search for Unity in Physics: Extending the Standard Model, Proceedings of the IVth Vigier Symposium in Paris, France, September 15th-19th, 2003, Celebrating the 83rd Birthday of Jean-Pierre Vigier).

[9] P. Rowlands, *The laws of physics and fundamental particles*, NVA Ltd, Liverpool, 1979.

[10] P. Rowlands, The fundamental parameters of physics, ASIS/NAPS microfiche 04068, 1982.

[11] P. Rowlands, Is the gravitational field really nonlinear?, Proceedings of Conference on Physical Interpretations of Relativity Theory III, 311-318, British Society for Philosophy of Science, London, September 1992.

[12] P. Rowlands, *A Revolution Too Far: The Establishment of General Relativity*, PD Publications, Liverpool, 1994.

[13] P. Rowlands, An algebra for relativistic quantum mechanics, in M. C. Duffy and M. Wegener (eds.), *Recent Advances in Relativity Theory*, Volume

2: Material Interpretations, Hadronic Press, Palm Harbor, Florida, 2001, 249-266.
[14] P. Rowlands, *Zero to Infinity The Foundations of Physics*, World Scientific, 2007.
[15] P Rowlands, Non-Local Gravity and Dark Energy, Galilean Electrodynamics, 20, no. 3 (2009), 42, 48, 53, 60.
[16] H. Kolbentsvedt, Amer. J. Phys., 56 (1988), 523-4.
[17] D. W. Sciama, Monthly Notices RAS, 113 (1953), 34.
[18] D. W. Sciama, The Physical Foundations of General Relativity, London, 1972, pp. 36 ff.
[19] B. P. Schmidt et al, Astrophys. J., 507 (1998), 46.
[20] S. Perlmutter et al, Astrophys. J., 517 (1999), 565.
[21] J. D. Anderson, P. A. Laing, E. L. Lau, A. S. Liu, M. M. Nieto, S. G. Turyshev, Indication, from Pioneer 10/11, Galileo, and Ulysses Data, of an Apparent Anomalous, Weak, Long-Range Acceleration, Phys. Rev. Lett., 81 (1998), 2858–2861.
[22] J. D. Anderson, J. K. Campbell, J. E. Ekelund, J. Ellis, and J. F. Jordan, Anomalous Orbital-Energy Changes Observed during Spacecraft Flybys of Earth, Phys. Rev. Lett., 100 (2008), 091102.
[23] P. F. Browne, Int. J. Theor. Phys., 15 (1976), 73.
[24] P. F. Browne, Found. Phys., 7 (1977), 165.
[25] B. J. Carr and M. J. Rees, Nature, 278 (1979), 605.
[26] J. Silk, Nature, 265 (1977), 71.
[27] A. S. Eddington, The temperature of space, chapter 13 in *Internal constitution of the stars*, Cambridge University Press, 1926.
[28] L. Ying, Nuclear fusion drives present-day accelerated cosmic expansion, Hadronic J., 32 (2009), 573-88.
[29] L. Ying, Dark Energy is Stellar Nuclear Fusion Replicated in a Mirrored Universe, The Open Astronomy Journal, 4 (2011), 54-56.
[30] R. M. Santilli, Isodual theory of antimatter, Dordrecht: Springer, 2006.
[31] P. Rowlands, An algebra combining vectors and quaternions: A comment on James D. Edmonds' paper, Speculat. Sci. Tech., 17 (1994), 279-282.
[32] P. Rowlands, Some interpretations of the Dirac algebra, Speculat. Sci. Tech., 19 (1996), 243-51.
[33] P. Rowlands, The physical consequences of a new version of the Dirac equation, in G. Hunter, S. Jeffers, and J-P. Vigier (eds.), *Causality and Locality*

in Modern Physics and Astronomy: Open Questions and Possible Solutions (Fundamental Theories of Physics, vol. 97, Kluwer Academic Publishers, Dordrecht, 1998, 397-402.
[34] P. Rowlands and J. P. Cullerne, The connection between the Han-Nambu quark theory, the Dirac equation and fundamental symmetries, Nuclear Physics A 684 (2001), 713-5.
[35] P. Rowlands, The nilpotent Dirac equation and its applications in particle physics, arXiv:quant-ph/0301071.
[36] P. Rowlands, Symmetry breaking and the nilpotent Dirac equation, AIP Conference Proceedings, 718 (2004), 102-115.
[37] P. Rowlands, The nilpotent vacuum, Hypercomplex Numbers in Geometry and Physics, 2 (2004), 97-111.
[38] P. Rowlands, Removing redundancy in relativistic quantum mechanics, arXiv.org:physics/0507188.
[39] P. Rowlands, A mathematical description of the fermionic state, Hypercomplex Numbers in Geometry and Physics, 4, 1(7) (2007), 141-153.
[40] P. Rowlands, Relativistic quantum mechanics from a single operator, International Journal of Computing Anticipatory Systems, 22 (2008), 206-1.
[41] P. Rowlands, What is vacuum?, arXiv:0810.0224.
[42] P. Rowlands, Physical Interpretations of Nilpotent Quantum Mechanics, arXiv: 1004.1523.
[43] P. Rowlands, Dual Vector Spaces and Physical Singularities, AIP Conference Proceedings, 1316 (2010), 102-111.
[44] R. Penrose, Twistor Quantization and the Curvature of Spacetime., Int. J. Theor. Phys. 1, 61-99, 1968.
[45] J. C. Baez and J. Huerta, The strangest numbers in string theory, Scientific American, May 2011, 18.
[46] P. Rowlands, *Oliver Lodge and the Liverpool Physical Society*, Liverpool University Press, 1990.